UNIVERSITY OF IOANNINA

SCHOOL OF HEALTH SCIENCES-DEPARTMENT OF MEDICINE and

BIOMEDICAL RESEARCH INSTITUTE (BRI), FOUNDATION FOR RESEARCH AND

TECHNOLOGY-HELLAS (FORTH), IOANNINA ,GREECE

Interdisciplinary Postgraduate Program "Molecular-Cellular Biology and Biotechnology"

Master's thesis:

The role of ARF6 in human embryonic stem cell pluripotency and differentiation

By Rakovoliou Elena,

Biologist, Bsc, Msc

Supervisors:

Theodore Fotsis, Emeritus Professor of Biological Chemistry, Medical School, University of Ioannina

Carol Murphy, Researcher B', BRI, FORTH, Ioannina

Ioannina, 2022

To the memory of my grandma Stella

Acknowledgements

The present Thesis was carried out at the Biomedical Research Institute of Ioannina, Greece (BRI) in the Murphy-Fotsis laboratory, during the period 2021-2022, under the supervision of Professor Theodore Fotsis and Dr. Carol Murphy. This Thesis completes my master graduate studies in the Interdisciplinary Postgraduate Program "Molecular-Cellular Biology and Biotechnology" in the Medical School of University of Ioannina.

First and foremost, I would like to offer my special thanks and gratitude to my primary supervisor Dr. Carol Murphy, Researcher B' of BRI, Ioannina for her mentorship at every stage of the research project. It 's a great privilege and honour to work and study under her guidance, as her knowledge, constructive criticism, motivation and insightful suggestions benefited me throughout these years. I would like to extend my sincere acknowledgement to my research supervisor Prof. Theodore Fotsis, Emeritus Professor of Biological Chemistry, Medical School, University Ioannina, for giving me the opportunity to join his team. I am extremely thankful for his unwavering support, belief in me and advice. His intelligence, immense knowledge and plentiful experience have inspired me during my academic studies.

Besides my mentors, I would like to thank the rest of my thesis committee: Prof. Frillingos Stathis, Professor of Biological Chemistry, Medical School, University of Ioannina, Prof. Papamarcaki Thomais, Professor of Biological Chemistry, Medical School, University of Ioannina and Dr. Gkogkas Christos, BRI Group Leader-Division of Biomedical Research, Ioannina for reading my thesis and evaluating my effort.

Allow me to show my heartful thanks to Dr. Markou Maria for her invaluable support, guidance, close collaboration, as well as friendship throughout this year on this project. She taught me the way to deal with stem cell biology experiments, and overall she spent hours for stimulating discussions, advising and motivating for the best result. My sincere thanks also goes to Dr. Bellou Sofia, for her unparallel support and useful advice. I learned from her experience how to face stressful situations and do the best for the success. Furthermore, I would like to show my great thanks to Dr. Bagli Eleni for her valuable help for my investigation during my thesis, her innovative ideas and especially sharing with me her statistical analysis knowledge.

I also had great pleasure of working and collaborating with all the team members in Fotsis-Murphy lab these two years, Katerina Apostolidi, Manolis Iakovidis and Athanasia-Zoi Pappa.

Last but not least, I owe a huge debt of thanks to my parents, Petros and Katerina, for their pure love and support in all of my decisions.

Best poster Award in the 72th Annual Conference of the Hellenic Society of Biochemistry & Molecular Biology (HSBMB)

POSTER 56: **The role of ARF6 in human embryonic stem cell pluripotency and differentiation**

Elena Rakovoliou[1*], Angelos Papadopoulos[2], Maria Markou[1], Sofia Bellou[1,3], Nikoleta Kostopoulou[1], Eleni Bagli[1], Theodore Fotsis[1,4], Carol Murphy[1]

[1]Foundation of Research and Technology-Hellas, Biomedical Research Institute, University Campus, 45110 Ioannina, Greece

[2]School of Biosciences, College of Life and Environmental Sciences, University of Birmingham, UK [3]Confocal Laser Scanning Microscopy Unit, Network of Research Supporting Laboratories, University of Ioannina, Ioannina, 45110, Greece

[4]Laboratory of Biological Chemistry, Medical School, University of Ioannina, 45110 Ioannina, Greece [*]Presenting author

Abstract

ADP-Ribosylation Factor 6 (ARF6) is a low molecular weight GTPase localised to the plasma membrane and endosomal compartments. As ARF6 cycles through its active (GTP-bound) and inactive (GDP-bound) form, it regulates cell surface ligand internalisation, post internalisation trafficking along the endocytic pathway (1), endosomal recycling (2) and fusion of recycling vesicles with the plasma membrane (3). Through its regulator proteins, ARF6 affects many cellular functions including receptor signalling, cell motility, adhesion (4), abscission (5) and lipid homeostasis (6). ARF6 is indispensable during embryonic development, as Arf6 knock-out leads to a lethal phenotype in mice (10.1128/mcb.00298-06 7). We are interested in the membrane receptor trafficking and signalling output of the TGF-β superfamily members (TGF-β, Activin A and BMP4) in the pluripotency and differentiation of human Embryonic Stem Cells (hESCs). The ActivinA/TGF-β family ligands, maintain the pluripotent profile of hESCs (7,8), and signal through heteromeric complexes of type I and type II transmembrane serine/threonine kinase receptors which phosphorylate SMAD2/3 proteins (9). The phosphorylated SMAD2/3 proteins oligomerise with SMAD4, translocate to the nucleus and regulate transcription using a large network of interactions with transcription factors, co-activators and co-repressors (10). On the other hand, the BMP4 family ligand, which signals through SMAD1/5/8, promotes differentiation of hESCs through a similar mechanism (11). Previous results from our lab indicate that ARF6 is implicated in Activin A / TGFβ signalling. Using hESCs that over-express ARF6 or CRISPR-KO lines, we addressed the role of ARF6 in the phosphorylation of SMADs upon ligand induction. We found significant alterations in SMAD phosphorylation upon activation or inactivation of ARF6, suggesting that ARF6 is an important factor in the responses of hESCs to Activin A / TGFβ family ligands. Here we extend these studies and address the role of ARF6 in differentiation of the above genome edited hESCs to 3 germ layers, mesoderm, endoderm and ectoderm (12–14). Our results are consistent with an effect of ARF6 in the differentiation to all germ layers. KO ARF6 hESCs exhibit enhanced expression of key markers of mesendoderm/ mesoderm (BRACHYURY, MIXL1, WNT3), extra-embryonic endoderm (AFP2, GATA6) and trophoectoderm (CDX2) following induction by BMP4 (14). In the case of ectoderm, PAX6, a marker of neuroectoderm differentiation was enhanced in the absence of ARF6 (12). Finally, markers of endodermal differentiation (SOX17, FOXA2) were reduced by ARF6 KO (13). We present our findings and discuss their significance.

Περίληψη

Η ADP-Ribosylation Factor 6 (ARF6) είναι μια GTPάση χαμηλού μοριακού βάρους που εντοπίζεται στην πλασματική μεμβράνη και στα ενδοσωμικά διαμερίσματα. Καθώς η ARF6 εναλλάσσεται μεταξύ της ενεργού (συνδεδεμένης με GTP) και της ανενεργού (συνδεδεμένης με GDP) μορφής της, ρυθμίζει την ενδοκυττάρωση του προσδέτη της κυτταρικής επιφάνειας, την μετά την εσωτερικοποίηση διακίνηση κατά μήκος της ενδοκυτταρικής οδού (1), την ανακύκληση των ενδοσωμάτων (2) και τη σύντηξη των κυστιδίων ανακύκλησης με την πλασματική μεμβράνη (3). Μέσω των πρωτεϊνών-τελεστών της, η ARF6 επηρεάζει πολλές κυτταρικές λειτουργίες, συμπεριλαμβανομένης της σηματοδότησης των υποδοχέων, της μετανάστευσης των κυττάρων, της προσκόλλησης (4), της απόσπασης (5) και της ομοιόστασης των λιπιδίων (6). Η ARF6 είναι απαραίτητη κατά τη διάρκεια της εμβρυϊκής ανάπτυξης, καθώς η αποσιώπηση της ARF6 οδηγεί σε θανατηφόρο φαινότυπο στα ποντίκια (7).

Μας ενδιαφέρει η διακίνηση των μεμβρανικών υποδοχέων και ο αντίκτυπος της σηματοδότησης των μελών της υπεροικογένειας TGF-β (TGF-β, Activin A και BMP4) στην πολυδυναμία και τη διαφοροποίηση των ανθρώπινων εμβρυϊκών βλαστικών κυττάρων (hESCs). Οι συνδέτες της οικογένειας ActivinA/TGF-β, διατηρούν το προφίλ πολυδυναμίας των ανθρώπινων εμβρυϊκών βλαστικών κυττάρων (7,15), και μετάγουν το σήμα μέσω των ετερομερών συμπλεγμάτων των υποδοχέων διαμεμβρανικής κινάσης σερίνης / θρεονίνης τύπου I και τύπου II, οι οποίοι φωσφορυλιώνουν τις πρωτεΐνες SMAD2/3 (9). Οι φωσφορυλιωμένες πρωτεΐνες SMAD2/3 ολιγομερίζονται με τη SMAD4, μετατοπίζονται στον πυρήνα και ρυθμίζουν τη μεταγραφική δραστηριότητα μέσω ενός μεγάλου δικτύου αλληλεπιδράσεων μεταγραφικών παραγόντων, συν-ενεργοποιητών και συν-καταστολέων (10). Από την άλλη πλευρά, ο προσδέτης της οικογένειας BMP4, ο οποίος επάγει τη σηματοδότηση μέσω των SMAD1/5/8, προωθεί τη διαφοροποίηση των ανθρώπινων εμβρυϊκών βλαστικών κυττάρων μέσω παρόμοιου μηχανισμού (11). Προηγούμενα αποτελέσματα από το εργαστήριό μας δείχνουν ότι η ARF6 εμπλέκεται στη σηματοδότηση της Ακτιβίνης A / TGFβ. Χρησιμοποιώντας ανθρώπινα εμβρυϊκά βλαστικά κύτταρα που υπερεκφράζουν την ARF6 ή σειρές CRISPR-KO, εξετάσαμε τον ρόλο της ARF6 στη φωσφορυλίωση των SMADs κατά την επαγωγή του προσδέτη. Βρήκαμε σημαντικές

μεταβολές στη φωσφορυλίωση των SMAD κατά την ενεργοποίηση ή την απενεργοποίηση της ARF6, γεγονός που υποδηλώνει ότι η ARF6 αποτελεί βασικό παράγοντα στις αποκρίσεις των ανθρώπινων εμβρυϊκών βλαστικών κυττάρων στους προσδέτες της οικογένειας Ακτιβίνης Α / TGFβ.

Εδώ διερευνούμε και εξετάζουμε τον ρόλο της ARF6 στη διαφοροποίηση των παραπάνω γονιδιωματικά επεξεργασμένων ανθρώπινων εμβρυϊκών βλαστικών κυττάρων σε 3 βλαστικά στρώματα, το μεσενδόδερμα, το ενδόδερμα και το νευροεκτόδερμα (12–14). Τα αποτελέσματά μας συμφωνούν με την επίδραση της ARF6 στη διαφοροποίηση σε όλα τα βλαστικά στρώματα. Τα ανθρώπινα εμβρυϊκά βλαστικά κύτταρα με ΚΟ της ARF6 παρουσιάζουν ενισχυμένη έκφραση βασικών δεικτών του μεσενδοδέρματος/ μεσοδέρματος (BRACHYURY, MIXL1, WNT3), του εξωεμβρυϊκού ενδοδέρματος (AFP2, GATA6) και τροφοεκτοδέρματος (CDX2) μετά από επαγωγή από BMP4 (14). Επιπλέον, ο PAX6, ένας δείκτης διαφοροποίησης του νευροεκτοδέρματος που επάγεται υπό χημικά καθορισμένες συνθήκες (12), ενισχύθηκε επίσης απουσία της ARF6. Εν τω μεταξύ, οι δείκτες της ενδοδερμικής διαφοροποίησης (SOX17, FOXA2) που επάγονται από την Ακτιβίνη Α μειώθηκαν κατά την απαλοιφή της ARF6 με CRISPR (13). Παρουσιάζουμε τα ευρήματά μας και συζητάμε τη σημασία τους.

Table of Contents

Abbreviations

A

ACAP	Arf GAP with Coiled-Coil, Ankyrin Repeat and PH domains
ADAP	Arf GAP with dual PH domains
AGAP	Arf GAP with GTPase domain, Ankyrin Repeat and PH domain
Akt	Protein Kinase B
AP-2	Adaptor Protein 2
APC	Adenomatous Polyposis Coli
ARAP	Arf GAP with Rho GAP domain, Ankyrin Repeats and PH domain
ARF	ADP Ribosylation Factor
ARNO	ADP-ribosylation Factor Nucleotide-binding site Opener
AS	Adult Stem
ASAP	Arf GAP with SH3 domain, Ankyrin Repeat and PH domain

B

BCA	Bicinchoninic Acid Assay
bFGF	Basic Fibroblast Growth Factor
BMP	Bone Morphogenetic Protein
BMPR	Bone Morphogenetic Protein Receptor
BRAG	Brefeldin A-resistant ARF GEF
BSA	Bovine Serum Albumin

C

CAS9	CRISPR Associated Protein 9
CAV1	Caveolin-1
CC	Coiled-Coil
CCPs	Clathrin Coated Pits
CDX2	Caudal type Homeobox 2

CIE	Clathrin Independent Endocytosis
CME	Clathrin Mediated Endocytosis
CRISPR	Clustered Regulatory Interspaced Short Palindromic Repeats

D

DMEM	Dublecco's Modified Eagle Medium
DNA	Deoxyribonucleic Acid

E

EBs	Embryoid Bodies
EDTA	Ethylenediaminetetraacetic Acid
EEs	Early Endosomes
EFA6	Exchange Factor for ARF6
EMT	Epithilial to Mesenchymal Transition
ER	Endoplasmic Reticulum
ERC	Endocytic Recycling Compartment
ERK	Extracellular Signal Regulated Kinase
ES	Embryonic Stem
ExEn	Extraembryonic Endoderm

F

FAs	Focal Adhesions
FBS	Fetal Bovine Serum
FGF	Fibroblast Growth Factor
FGFR	Fibroblast Growth Factor Receptor

G

GAP	GTPase Activating Protein
GDP	Guanosine Diphosphate
GEF	Guanine Nucleotide Exchange Factor

GEP100 Guanine Nucleotide Exchange Protein 100

GFP Green Fluorescence Protein

GIT G Protein Receptor Kinase (GRK)

GSK3 Glycogen Synthase Kinase

GTP Guanosine Triphosphate

H

hESCs Human Embryonic Stem Cells

HGF Hepatocyte Growth Factor

hiPSCs Human induced Pluripotent Stem Cells

HMG High Mobility Group

hPSCs Human Pluripotent Stem Cells

HRP Horseradish Peroxidase

HSCs Hematopoietic Stem Cells

I

ICM Inner Cell Mass

iPS Induced Pluripotent Stem

K

KOSR Knockout Serum Replacement

L

LEF Lymphoid Enhancer Binding Factor

LIF Leukaemia Inhibitor Factor

LRP6 Lipoprotein Receptor-Related Protein 6

M

MAPK Mitogen Activated Protein Kinase

MDCK cells Madin Darby Canine Kidney cells

mEpiSCs Mouse Epiblast Stem Cells

mESCs Mouse Embryonic Stem Cells

MHC	Major Histocompatibility Complex
MSCs	Muscle Stem Cells
MSCs	Mesenchymal Stem Cells
N	
NEEAs	Non Essential Aminoacids
O	
OCT-4	Octamer Binding Transcription Factor-4
P	
PAGE	Polyacrylamide Gel Electrophoresis
PAX6	Paired Box Protein 6
PBS	Phosphate Buffer Saline
PH	Pleckstrin Homology
PI(4,5)P2	Phosphatidylinositol 4,5-biphosphate
PI3K	Phosphatidilinositol 3-Kinase
PI4P	Phosphatidylinositol 4-Phosphate
PIP3	Phosphatidylinositol 3,4,5-triphosphate
PIP5K	Phosphotidylinositol-4-Phosphate-5 Kinase
PIPs	Phosphatidyl Inositol Phosphates
PIs	Phosphoinositides
PLCγ	Phospholipase Cγ
PLD	Phospholipase D
PLD2	Phospholipase D2
plgR	Polymeric Immunoglobin Receptor
PMP22	Peripheral Myelin Membrane Protein 22
PMSF	Phenylmethylsulfonyl Fluoride
POU	Pit-Oct-Unc
PP2A	Protein Phosphatase 2A

PtdIns	Phosphatidylinositols
Q	
qRT-PCR	Quantitative Reverse Transcription-Polymerase Chain Reaction
R	
RHOA	Ras Homology Family Member A
RAC	Ras-Related C3 Botulinum Toxic Substrate
REs	Recycling Endosomes
RNA	Ribonucleic Acid
ROCK	Rho-Asspciated Protein Kinase
S	
SC	Stem Cells
SDS	Sodium Dodecyl Sulfate
SFM	Serum-Free Minimal
SMAD	Mothers Against Decapentaplegic Homolog
SMAP	Small ARFGAP
SOX	Sex Determining Region Y-Box
T	
TE	Trophectoderm
TGF-β	Transforming Growth Factor β
V	
VEGF	Vascular Endothelilal Growth Factor
VEGFR	Vascular Endothelilal Growth Factor Receptor
W	
WNT	Wingless-related integration site

List of Figures

List of Tables

Convention

The level of statistical significance in all the figures included is depicted by the use of Significance stars.

* P<0.05

** P<0.01

*** P<0.001

**** P<0.0001

Chapter 1

Introduction

ADP-Ribosylation Factor 6 - ARF6

In higher eukaryotes, ADP-ribosylation factors (ARFs) comprise a group of six small (20kDa) ubiquitous Ras-related GTPases that are required for maintaining the integrity of organelle structure and intracellular transport. ARF proteins are regulated through a cycle of GTP binding and hydrolysis, which activate and inactivate, respectively, the G protein (1–3). In vitro, ARF proteins function as cofactors in the cholera toxin-catalyzed ADP-ribosylation of the a-subunit of heterotrimeric Gs, hence the name, (4–6) and have also been shown to stimulate the activity of phospholipase-D (22–26). A plethora of cellular processes require ARF proteins, including the recruitment of coat proteins promoting cargo sorting in vesicles, the recruitment and activation of enzymes such as the phosphatidylinositol (PtdIns) kinases that alter membrane lipid composition, and interaction with cytoskeletal factors (27).

There are six mammalian ARFs that can be subdivided into three separate classes based on sequence homology: class I (ARF1/2/3), class II (ARF4/5) and class III (ARF6) (28). Class I and II ARFs regulate vesicular trafficking between the Golgi appartus and Endoplasmic Reticulum (ER) (29). The only member of class III is ARF6, the least-conserved ARF protein that shares 66% amino acid homology with ARF1. So, ARF6 is the outcast of the family, both in sequence and function, and regulates both clathrin-mediated endocytosis (CME) and clathrin-independent endocytosis (CIE) and endosomal recycling, **Figure 1.1** (2).

ARF6 is localized to the plasma membrane, cytosol, and endosomal membranes depending on its nucleotide status and has been shown to regulate endocytic trafficking at the cell periphery (16,19,30), adhesion (31), abscission (3) and lipid homeostasis (6). Also, ARFs are myristoylated at their N-terminus. Cytosolic ARF6 associates with membranes in a GTP-dependent manner, while the dissociation from the plasma membrane requires a magnesium sensitive GTP hydrolysis (32). Subsequently, as all GTPases, ARF6 cycles between an active (GTP-bound) and an inactive (GDP-bound) state through the action of regulator proteins. The activation of ARF6 is regulated by guanine nucleotide exchange factors (GEFs), which catalyze

the exchange of GDP for GTP. Conversely, GTPase-activating proteins (GAPs) hydrolyze GTP to GDP, therefore inactivating the molecule (22,23).
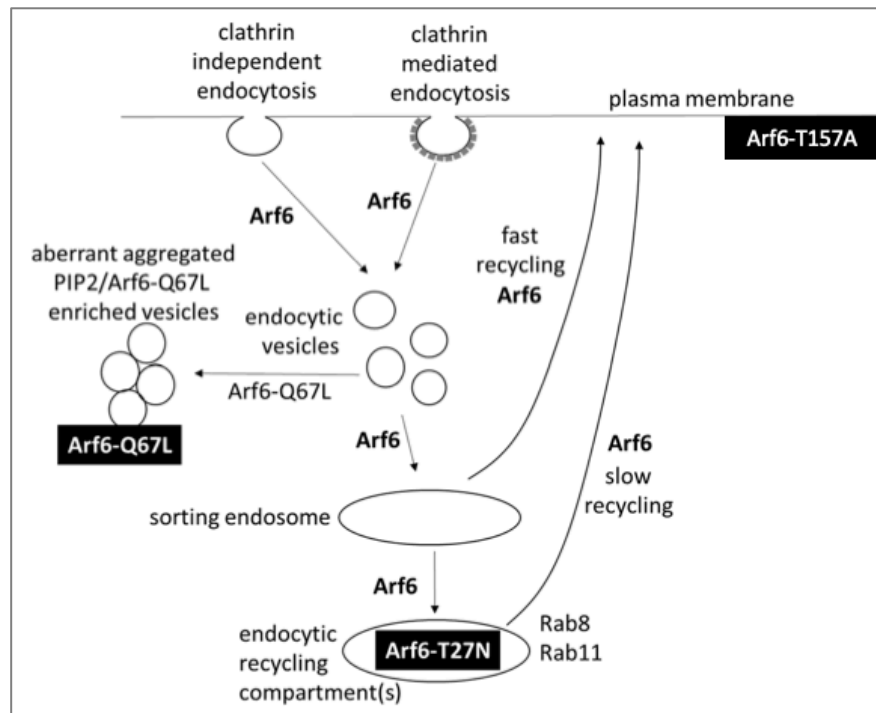
Figure 1.1: *The role of Arf6 in intracellular trafficking upon clathrin-mediated and clathrin-independent endocytosis*. The location of Arf6 mutants in the cell is indicated as the white text on a black background. (33)

Perturbing the expression or cycling of ARF6 has a detrimental phenotype *in vivo* in various species. In *Drosophila*, overexpression of a dominant negative mutant resulted in neural malformations and inhibited myoblast fusion (35,36). In mice, knockout of ARF6 has a mid-gestation lethal phenotype, attributed to impaired liver and fetal hepatic cord development (7). Interestingly, conditional ablation of ARF6 in endothelial cells of mice *in vivo* did not exhibit a lethal phenotype, suggesting that its expression is dispensable in endothelial tissues during development (37).

1.1.   ARF6 Structure and Mutants

ARF6 consists of four distinct regions that are responsible for its functionality and subcellular localization. ARF6-GTP associates tightly with membranes, an interaction mediated by an amphipathic helix along with a myristoylated N-terminal helix, which flips open upon binding GTP and inserts into the lipid bilayer. The N-terminal helix interacts with the nucleotide binding

site through the Interswitch, comprised of two β-strands and a β-hairpin loop, connecting the Switch I and Switch II regions. These two domains are located centrally in the protein and are responsible for the interaction of ARF6 with its cellular partners, specific GAPs and GEFs (38,39). Switch I, Switch II and its binding Interswitch regions undergo conformational changes upon ARF6 activation and displace the amphipathic helix from a hydrophobic pocket, allowing it to bind with membranes. In addition, the hydrophobic residues that are exposed further strengthen the association of ARF6 with phospholipids, **Figure 1.2** (40).
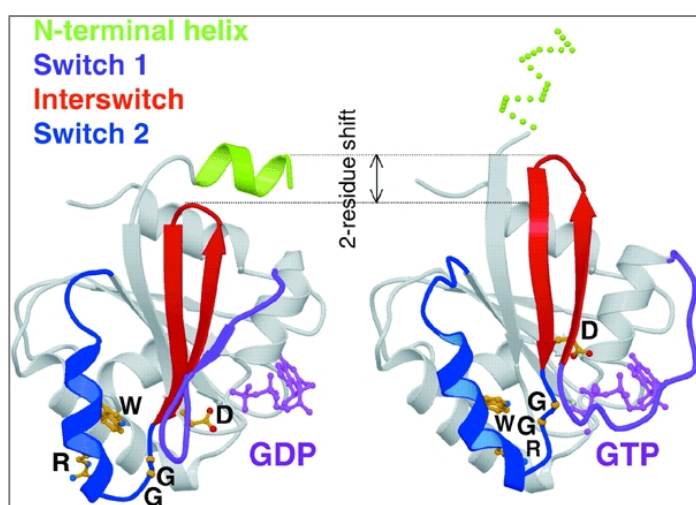
Figure 1.2: *ARF6 Structure in GDP/GTP Forms*. In the GDP form of ARF6 (Left) Switch I (Purple), Switch II (Blue) and the Interswitch (Red) regions form a hydrophobic pocket that harbours the N-terminal amphipathic helix (Green). In that state, a conserved aspartic acid residue protrudes from the Switch II domain and along with GDP stabilises the structure. Exchange of GDP for GTP causes a conformational shift on the Interswitch region by exactly two residues. This shift displaces switch I and II regions and allows the protein to bind to GTP, which is available in the cytoplasm. In addition, the movement of the Interswitch dislodges the helix from the pocket with the latter being now able to associate with membranes. Adapted from (41).

Crystallization of ARF6 in both the GTP- and GDP- bound forms allowed for the generation of constitutively active (ARF6Q67L), dominant negative (ARF6T27N) and fast cycling (ARF6T157A) mutants that are indispensable for studying ARF6 function, **Figure 1.3.** ARF6Q67L cannot hydrolyse the bound GTP, whereas ARF6T27N cannot bind GTP and therefore exhibits limited activation. Both of these mutations are part of the effector domain of ARF6 and thus interfere with the GTP-GDP cycle. Moreover, affecting the activation state of ARF6 also interferes with its localization (42). ARF6T157A is an activated mutant of ARF6 that rapidly exchanges GTP for GDP more quickly than the wild-type ARF6 suggesting that it is a fast cycling mutant, while still being able to undergo hydrolysis by GAPs. This mutant has also enhanced ARF6 activity in vivo and induces cortical actin rearrangements in HeLa cells (Lack's cervical cancer cells) and enhanced motility in MDCK cells (Mardin-Darby canine kidney cells). The function of ARF6T157A is attributed to the limited ability of the alanine residue, located in the Interswitch, to form van der Waals bonds with the guanosine ring (41,43).
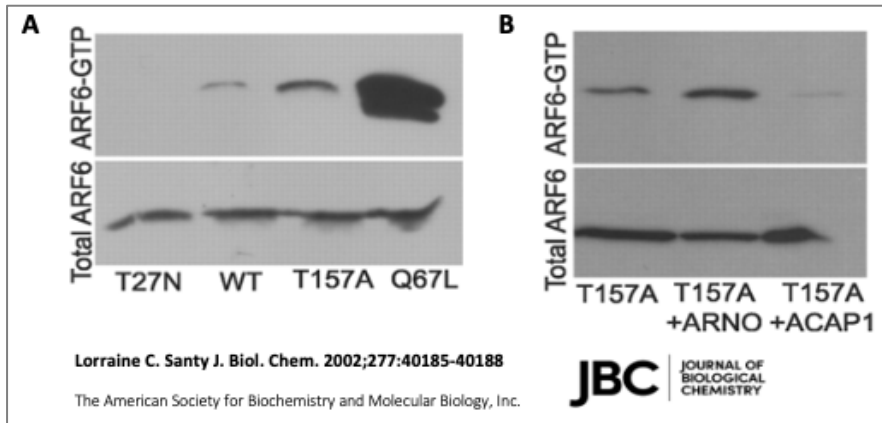
Figure 1.3: *ARF6 T157A is more active than wild-type ARF6 and is still subject to normal regulation*. A) MDCK cells were infected with adenovirus encoding HA-tagged WT, dominant negative (T27N), constitutively active (Q67L), or T157A ARF6 for 4 hours. Cells were lysed and GTP-ARF6 isolated by incubation with glutathione S-transferase-GGA3. ARF6 levels were quantitated by Western blotting with monoclonal anti-HA antibody. B) MDCK cells were transfected with plasmids encoding ARF6 T157A either alone or in combination with the GEF ARNO or the GAP ACAP1. ARF6-GTP was isolated and quantitated as described above. Gels are representative of at least 4 separate experiments (44).

1.2. Activation Machinery of ARF6 through GEFs

In the resting cell, ARF6 binds GDP and in response to cell stimulation by several agonists such as hormones, neurotransmitters and growth factors, ARF6 exchanges bound GDP for GTP, thus is activated. This exchange is facilitated by guanine nucleotide-exchange factors (GEFs), which activate small G proteins, **Figure 1.4** (45). So far, 15 ARF GEFs have been identified in the human genome, 8 of the above act specifically on ARF6 and are classified into 3 separate GEF families. The Cytohesin family comprises of Cytohesin 1, Cytohesin 2/ARNO and Cytohesin 3/ GRP1. The EFA6 family (Exhange factors for ARF6) includes the EFA6A/B/C and D. And the BRAG family (Brefeldin A-resistant ARF GEF) consists of the BRAG1, BRAG 2/GEP 100, and BRAG3 (46). Unlike the last two families, Cytohesins promote GDP/GTP exchange not only on ARF6, but also on other ARF GTPases in a similar manner (46).
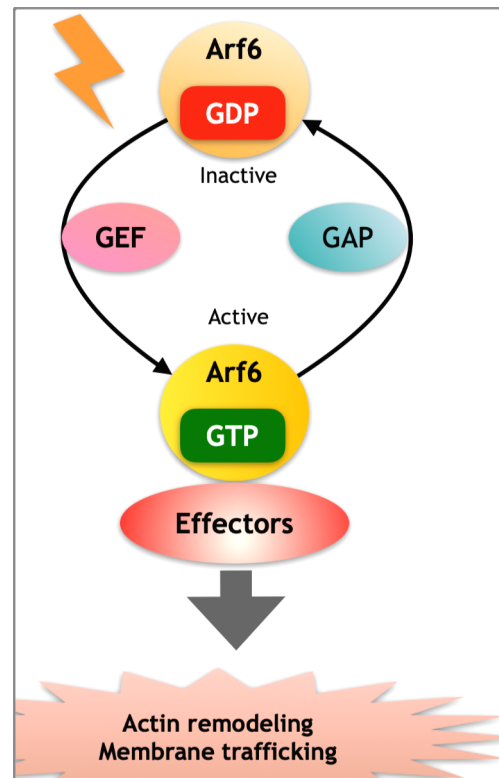
Figure 1.4: *GTP- and GDP-bound state are regulated by GEFs and GAPs.* GEFs stimulate the exchange of GDP for GTP, resulting activation of ARF5 ("ON"). GAPs promote GTP hydrolysis, and return ARF6 to GDP-bound state ("OFF") (202).

The structure of ARF6 GEFs are characterized by a central catalytic domain of approximately 200 amino acid referred to as the Sec7 domain, based on its homology to yeast Sec7p, **Figure 1.5** (37,38) , and also contain a Pleckstrin Homology (PH) domain. The Sec7 domain includes a conserved glutamate residue that competes with GDP and promotes its dissociation, allowing ARF6 to bind cytosolic GTP in it's nucleotide binding pocket, and resulting in the activation of ARF6. On the other hand, the PH domain associates with PIPs, and other effectors, guiding the GEFs to appropriate subcellular compartments (46). In addition, in response to G protein signalling a Coiled-Coil (CC) domain which is present in the structure of all the above GEFs has been implicated in ARF6 activation (47).
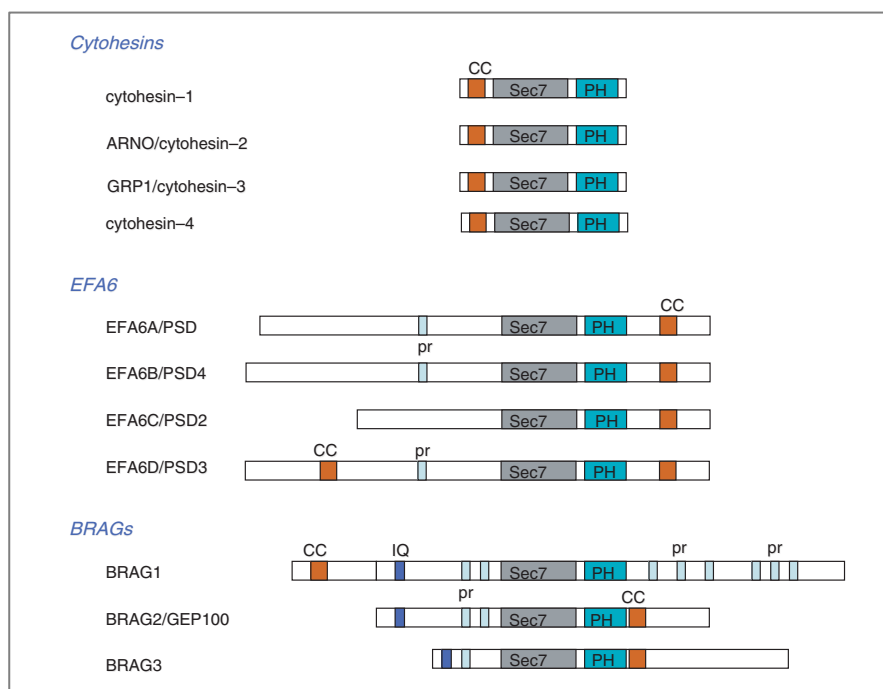
Figure 1.5: *Structures of Arf6 GEFs*. Arf GEFs are characterized by the catalytic Sec7 domain composed of approximately 200 amino acid residues, which are located in the central region of GEFs. All Arf6 GEFs possess a PH domain that serves as a binding site for specific phosphoinositides and/or partner proteins. GEFs of cytohesin family shows relatively wide selectivity in their substrate specificity. On the other hand, GEFs of EFA6 family and GEP100/BRAG2 of BRAG family are specific for Arf6. CC: coiled-coil domain, PR: proline rich domain, IQ: IQ domain, PH: pleckstrin homology (48).

The translocation of ARF6 GEFs has been found to be directly regulated by cell surface receptors in an agonist dependent manner. GEFs translocate to membranes in order to activate their substrates by interaction of their PH domain with phosphoinositides (PIs). Interestingly, association of GEFs with PIs does not increase their catalytic activity but is indispensable for the precise regulation of ARF6, in response to agonist stimulation of cells, in appropriate subcellular compartments (49,50). Cytohesins interact with PIP3 which is

generated by PI3K in response to membrane receptor signalling (51). This interaction recruits cytohesins to the plasma membrane, which allows cytohesins to interact with ARF6, thereby stimulating GDP/GTP exchange on ARF6 without stimulation of GEF activity. In addition to PIP3 binding, ARNO is recruited to the membrane in response to insulin stimulation. However, it is still unclear whether ARNO-dependent ARF6 activation is related to PIP3 or insulin receptor binding (50,52). Furthermore, EFA6 family members preferably interact with PI(4,5)P2 and GEP100 with PI4P, PI(4,5)P2 and PIP3 scribed, which function directly on ARF6, regulating different processes (46,53). ARF GAPs are subdivided into subfamilies according to overall domain structure. The classification has two major groups, those with the ARF GAP domain at the immediate N terminus (ARF GAP1 type) and those with a pleckstrin homology (PH) domain N-terminal of the ARF GAP domain and ankyrin (ARK) repeats immediately C-terminal (ASAP, ACAP, AGAP and ARAP) (48–50). GAP activity has been confirmed in at least one of the eight subtypes. However, two subtypes lack detectable GAP activity and other ARF GAPs, the GAP activity is dispensable for some cellular functions, leading to the hypothesis that the ARF GAPs perform other functions in addition to negatively regulating ARF proteins. ARF effectors might serve one purpose, **Figure 1.6** (2,12,50,51).
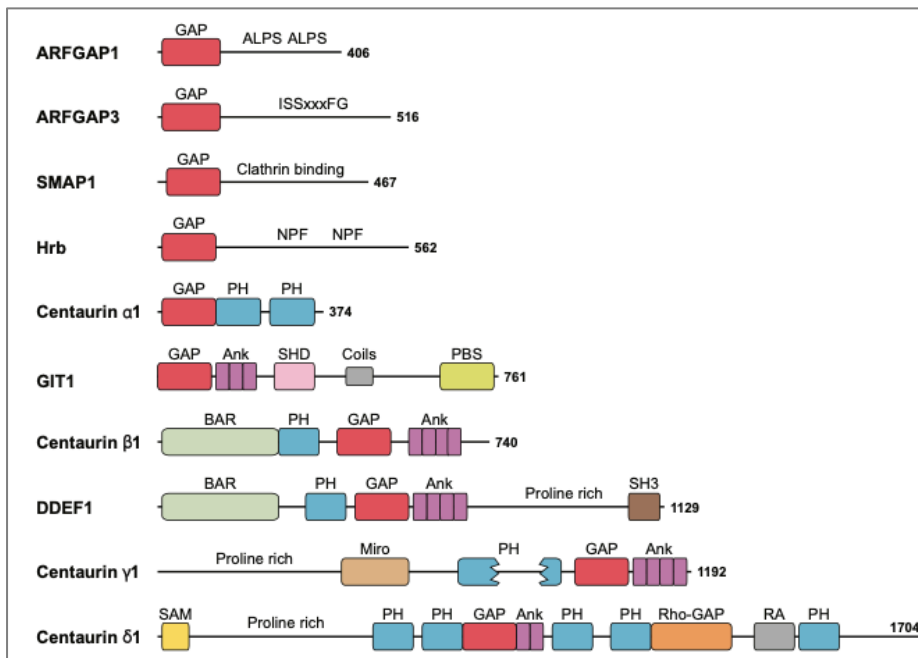
Figure 1.6: *Domain structures of ARF GAPs*. The human GTPase-activating proteins (GAPs) for ADP-ribosylation factor (Arf) family G proteins. Shown are the domain structures of a single representative of each of the ten families of Arf-GAP domain proteins found in humans. The other domains are as follows: Ank, ankyrin repeats; BAR, Bin/Amphiphysin/Rvs; coils, coiled-coil; Miro, Miro GTPase like; PBS, paxillin-binding site; PH, pleckstrin homology; RA, Ras association; SAM, sterile alpha motif; SH3, Src-homology 3; SHD, Spa2 homology domain. Also shown are motifs or sequence features: ALPS (ArfGAP1 lipid packing sensor), proline rich, clathrin binding, NPF, and ISSxxxFG are motifs comprised of the indicated amino acids .

ARF GAP1 was the first ARF GAP to be cloned and implicated as a regulator of membrane trafficking (53). Specifically, ARFGAP1 has been found to inactivate ARF6 in a clathrin Adaptor Protein-2 (AP-2) dependent manner, thus connecting ARF6 to CME (59). ADAP1 and ADAP2 associate with phosphatidylinositol 3,4,5-trisphosphate (PIP3) via their PH domains and regulate ARF6 in specific compartments. ADAP1 binds to PIP3 and arrests ARF6 in endosomes, prohibiting its distribution to the plasma membrane (60). ADAP2 has been associated with the ARF6-dependent endocytosis of RNA viruses (61). Unlike ARFGAP1, GIT1 and GIT2, GAPs have been found to promote hydrolysis of GTP bound to ARF6, as well to all mammalian ARFs (62). The specific inactivation of ARF6 by GIT1 causes the highly expression of GIT1 in several types of cancers, including breast, cervical, colon and liver (63–67). In addition, GIT1 overexpression leads to reduced internalisation of the β2-adrenergic receptor and increased receptor phosphorylation, a process in which ARF6 is directly implicated (68). ACAP1 and ACAP2 proteins preferentially inactivate ARF6 over other ARFs. In HeLa cells, their overexpression inhibits the creation of cellular protrusions, a process in which ARF6 is implicated i(69). ARAP2 and ARAP3 are also involved in ARF6-dependent adhesion processes. ARAP2 promotes focal adhesion growth by inactivating ARF6 and RAC1 (Ras related C3 botulinum toxin substrate 1). Focal adhesions (FAs) are dynamic structures that connect the actin cytoskeleton with the extracellular matrix (70). ARAP3 binds to PIP3 and abrogates RHOA and ARF6 cycling, thus stimulating the formation of lamellipodia, **Figure 1.7** (71).
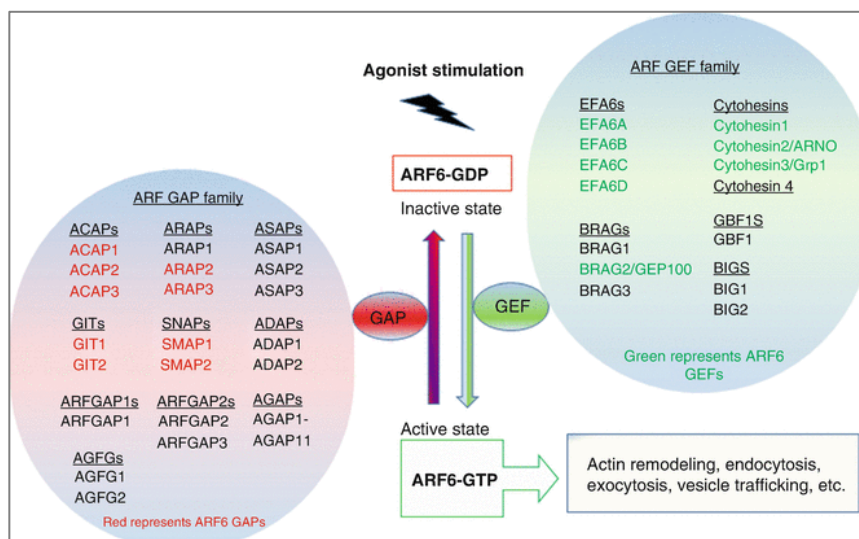
Figure 1.7: *Cycling of Arf6 between inactive and active forms and its modulators*. Upon agonist stimulation of the cell, GDP on Arf6 is exchanged for GTP by the action of Arf6-specific GEFs, resulting in the activation of Arf6. Arf6 is thus activated and transduces the signal downstream to regulate actin cytoskeleton remodeling and membrane trafficking at the plasma membrane and endosomes. Thereafter, Arf6 is inactivated by the support of GAPs. To date, 8 members of Arf6 GEFs, which belong to BRAG, cytohesin, and EFA6 families, and 9 members of Arf6 GAPs, which belong to GIT, ARAP, ACAP, and SMAP families, have been identified (64).

1.3. ARF6 in Endocytosis and Trafficking

ARF6 that localizes to the plasma membrane and endosomal compartments regulates a wide range of cellular processes including endocytosis, endocytic membrane trafficking, actin remodeling and endocytic recycling in concert with various effector molecules and other small GTPases (72). It facilitates membrane ruffling at the cell surface during endocytic processes recruiting membrane lipids and effector molecules, in addition to promoting peripheral actin rearrangements . Specifically, ARF6 is involved in the regulation of endocytosis in Clathrin – dependent (CME) and –independent (CIE) manners. It has been demonstrated that ARF6 acts like a key activator for Phosphatidylinositol-4-Phosphate-5-Kinase (PIP5K) and Phospholipase D (PLD). Activating these two factors leads to an increase in the levels of PI(4,5)P2 with the latter functioning cooperatively with activated ARF6 to recruit AP-2, thus promoting CME (70,71). This process is tightly regulated by SMAP1, an ARF6GAP that has been shown to interact with Clathrin heavy chains. ARF6 also interacts with and recruits the nucleoside diphosphate kinase Nm23-H1 (73). The latter controls Dynamin activity by regulating thesupply of GTP and is therefore involved in the Dynamin dependent vesicle fission process during endocytosis endocytosis (73). ARF6 has found to be an upstream regulator of canonical Wnt/β-catenin signalling. Relying on that, in MDCK cells, Wnt stimulation has been shown to promote ARF6 activation which leads to E-Cadherin internalisation. Therefore, E-Cadherin is characterized as cargo using the ARF6 and Clathrin – dependent endocytosis pathway (74). In the same cell line, ARF6 was shown to modulate the apical CME of the polymeric immunoglobulin receptor (pIgR), as overexpression of the hydrolysis resistant mutant of the GTPase abolished its internalization. Consequently, active ARF6 recruits the actin from the cell cortex to the clathrin-coated pit to enable dynamin-dependent endocytosis, **Figure 1.8** (75).
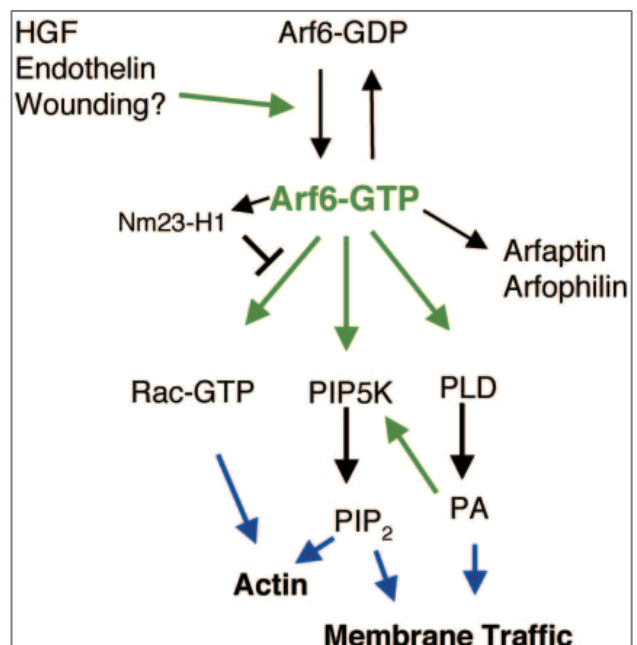
Figure 1.8: *Proteins and pathways affected by Arf6.* Green arrows denote stimulation. Blue arrows denote an influence of Rac-GTP, PIP$_2$, and PA on actin structures and membrane traffic (79).

Apart from CME, ARF6 also regulates the internalisation of cargo independently of Clathrin. This process involves membrane ruffling through activation of RAC and rearrangements in the lipid composition of the plasma membrane. RAC is activated in response to ARF6 activation, an event catalyzed by EFA6, **Figure 1.9** (76). The latter, similar to CME, involves increase of PI(4,5)P2 by sequential activation of ARF6, PLD and PIP5K. PI(4,5)P2-enriched membrane domains act as scaffolds, recruiting ACTIN remodeling enzymes that aid in ruffling (75). In addition, the forming vesicles which are distinct due to their enrichment in cholesterol, fuse with early endosomes (EEs) that also contain CME cargo (78). Cargo that enter cells in this manner includes the Major Histocompatibility Complex (MHC) Class I, the M2-muscaranic Acetylcholine receptors, β1 Integrins, the Peripheral Myelin- membrane Protein 22 (PMP22) and others (79).

Cycling of ARF6 is implicated in vesicular trafficking. More specifically, hydrolysis allows for internalization and vesicle sorting, while subsequent reactivation leads to endosomal recycling (78). This is also supported by the fact that hydrolysis resistant mutants of ARF6 lead to the formation of intracellular vacuoles that are enriched for PI(4,5)P2 and F-ACTIN (80). ARF6-dependent recycling is associated with tubular endosomes that emanate from the Endocytic Recycling Compartment (ERC) and carry cargo to the cell surface. This is highlighted by the fact that perturbing ARF6 activation by inhibiting ERK leads to recycling endodomes (Res) arrest in the ERC (81). In this process, ARF6 activates Phospholipase D2 (PLD2) and PIP5K. PLD2 catalyzes the formation of phosphatidic acid and diacylglycerol,
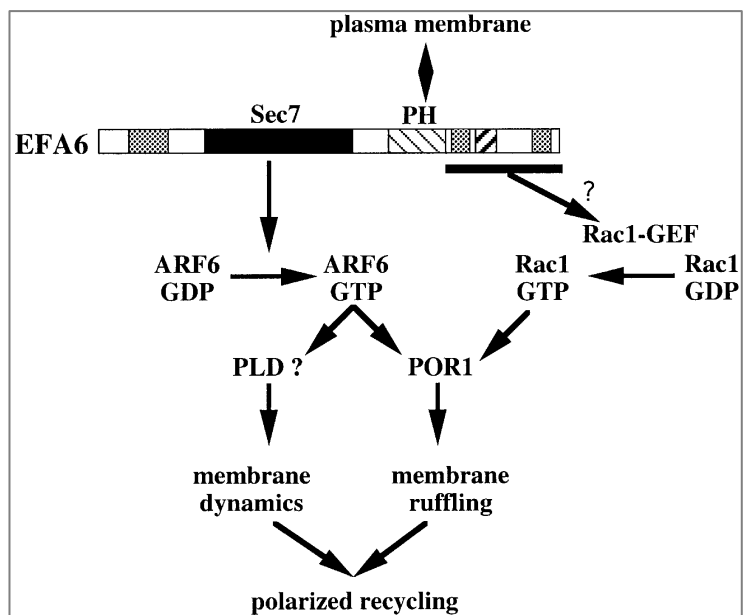
Figure 1.9: *Model of EFA6-regulated actin reorganization.* Targeting of the PH domain of EFA6 to the plasma membrane allows Sec7 domain-catalyzed nucleotide exchange on ARF6. GTP-bound ARF6 interacts with and activates specific downstream effectors at the plasma membrane. Activation of PLD leads to the generation of fusogenic lipids involved in the fusion of recycling membranes with the plasma membrane. In parallel, EFA6 allows Rac1 activation by recruiting a Rac1-specific GEF. The ARF6 and Rac1 pathways converge at the level of POR1 that interacts with both GTP-bound ARF6 and Rac1 to control membrane ruffling. Recycling of membrane occurs at discrete sites of the plasma membrane that coincide with areas of membrane ruffling (76).

two molecules essential for the fusion of REs with the plasma membrane (82). Similar to its role in CME and CIE, PIP5K generates PI(4,5)P2 which acts by recruiting enzymes important in membrane fusion and ACTIN polymerization (80). Fibroblast Growth Factor Receptor (FGFR) has been shown to follow this recycling route, as limited PI(4,5)P2 causes its endosomal accumulation which leads to impaired cell proliferation (83). In addition, Hepatocyte Growth Factor (HGF)- stimulated β1 integrin recycling is also controlled by ARF6 activation, as pharmacological inhibition of ARF6GEFs perturbs integrin trafficking. This is important in cancer drug development, as suppression of ARF6 activation leads to impaired tumor angiogenesis and growth (37).

2. Stem Cells: An overview

"Nothing in Biology Makes Sense Except in the Light of Evolution" is a 1973 essay by the evolutionary biologist Theodosius Dobzhansky (84). The question however is, how the evolution of stem cells started? The answer may be hidden behind the ability of stem cells, as a population of undifferentiated cells to extensively proliferate (self-renewal), usually arise from a single cell (clonal), and differentiate into different types of cells and tissue (potent) (83). The appearance of stem cells could be considered fundamental in the length of evolutionary saga, as their existence could be dated back million of years and their development seems to be the result of natural selection (84).

The term "stem cell" can be traced back to the late 19th century (85). Stem cells are undifferentiated cells that are present in the embryonic, fetal, and adult stages of life, being indispensable to human physiology, both during development driving tissue formation, and throughout adulthood maintaining tissue homeostasis. So, stemness is the property of stem cells to self-renew and differentiate into other cell types, that are building blocks of tissue and organs (86).

2.1. Stem Cell Classification Based on Differentiation Potential

Depending upon their differentiation potential, stem cells can be classified as totipotent, pluripotent, multipotent, oligopotent or unipotent (83,87). Totipotent cells can give rise to a fully functioning , fertile organism (88). In the case of mammalian embryogenesis only the

fertilised oocyte and the two identical cells arising from the first mitotic division have the capacity to differentiate into embryonic and extra-embryonic cells (89,90). Pluripotent stem cells have the ability to differentiate into specialized cell types derived from one of three primary germ layers: ectoderm, endoderm, or mesoderm (89). Multipotent cells reside in most adult tissues and are able to give rise to several limited in number cell types, which are generally referred to by their tissue or germ layer origin (mesenchymal stem cell, adipose-derived stem cell, endothelial stem cell, etc.) (83,90). Mesenchymal stem cells (MSCs) are the most well studied multipotent cells (91,92). These can be derived from a variety of tissue including bone marrow, adipose tissue, bone, Wharton's jelly, umbilical cord blood, and peripheral blood (93,94). Oligopotent cells are able to self-renew and form two or more mature cell types within a tissue. Hematopoietic stem cells (HSCs) are the most typical example of oligopotent stem cells, as they can differentiate into both myeloid and lymphoid lineages. Being able to produce only T and B cells, lymphoid cells are known as bipotent (95). Ultimately, unipotent cells have the capacity to differentiate into only one cell type. A typical example of unipotent cells are muscle stem cells (MSCs) (96). The stem cell hierarchy based on their differentiation potential is depicted in **Figure 2.1**.
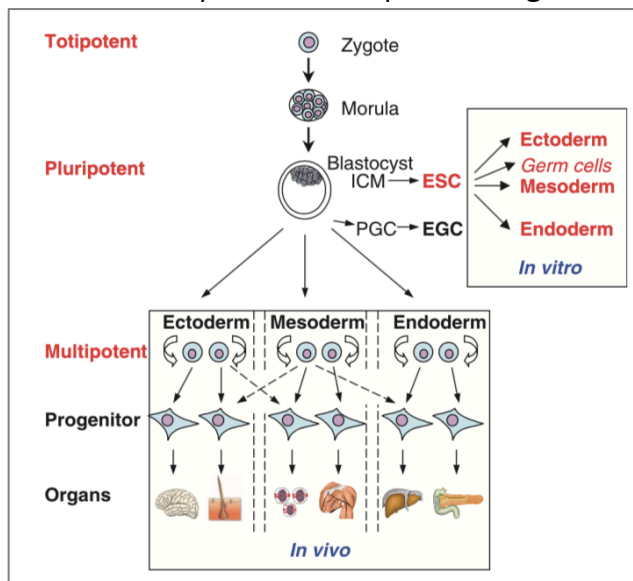
Figure 1.10: *Stem cell hierarchy*. Zygote and early cell division stages (blastomeres) to the morula stage are defined as totipotent, because they can generate a complex organism. At the blastocyst stage, only the cells of the inner cell mass (ICM) retain the capacity to build up all three primary germ layers, the endoderm, mesoderm, and neuroectoderm as well as the primordial germ cells (PGC), the founder cells of male and female gametes. In adult tissues, multipotent stem and progenitor cells exist in tissues and organs to replace lost or injured cells. At present, it is not known to what extent adult stem cells may also develop (transdifferentiate) into cells of other lineages or what factors could enhance their differentiation capability (dashed lines). Embryonic stem (ES) cells, derived from the ICM, have the developmental capacity to differentiate in vitro into cells of all somatic cell lineages as well as into male and female germ cells (89).

Based on their origin stem cells can be classified into five broad types: embryonic, fetal, perinatal, adult (resident or tissue-specific) and iPS cells (induced pluripotent stem cells). In general embryonic and iPS cells are pluripotent, whereas fetal and perinatal are multipotent, and adult stem cells are usually oligo- or unipotent (97).

2.1.1. Embryonic stem cells

In adult mammals, only the germ cells undergo meiosis to produce oocytes and spermatozoans, which fuse to form the first diploid cell, the zygote, which is totipotent. In fact, the zygote is at the top of the hierarchical stem cell tree being the most primitive and producing the first two cells by cleavage (86). Approximately 96 hours after insemination, several successive mitotic cell divisions generate the morula, with 16-64 totipotent cells. Following cleavage, the newly formed blastomeres or ''morula'' enter the phase of compaction (blastula stage). The blastocyst comes into being through compaction of the cells and the accumulation of intercellular fluid, leading to the formation of the blastocyst cavity (blastocoel). The embryoblast differentiates into the hypoblast, adjacent to the blastocyst cavity, and the epiblast. The two to four innermost cells of the preceding morula develop into the so-called inner cell mass of the blastocyst expresses the characteristic transcription factors OCT4 and NANOG (98)(99), and develops into the fetus. Whereas the outer cell mass of blastocyst, the trophoblast, is positive for CDX2, and generate the embryonic membranes and placenta, **Figure 2.2, 2.3** (100,101).
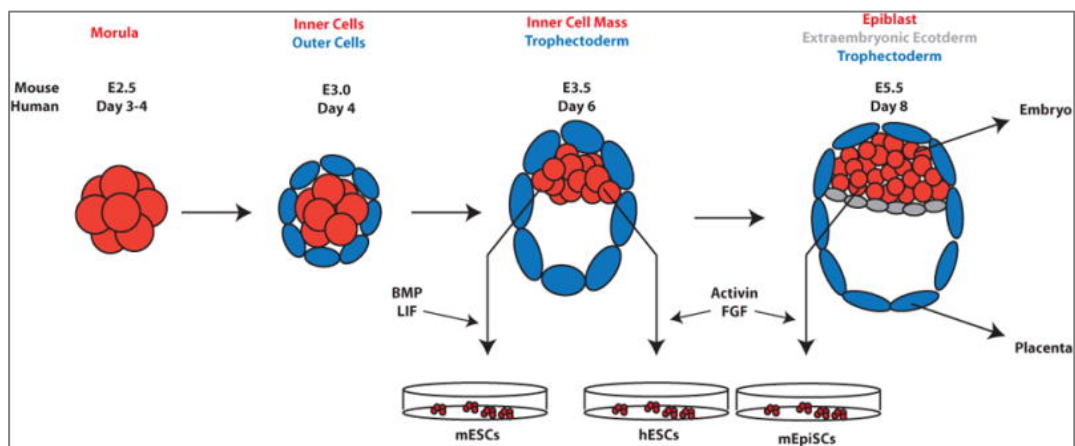
Figure 1.11: *Early Mammalian Embryonic Development*. After morula stages, the first cell fate decisions take place, and cells sort to outer and inner populations. Outer cells give rise to the extraembryonic trophectoderm (TE), while inner cells form the inner cell mass (ICM). The ICM is located asymmetrically at one side of the blastocoel cavity within the TE. Subsequently, the ICM further differentiates to the extraembryonic endoderm (ExEn) and the epiblast, which gives rise to the embryonic ectoderm, mesoderm, and endoderm. Mouse and human embryonic stem cells are derived in vitro by explanting the ICM (203).

The embryonic stem cells are pluripotent, derived from the inner cell mass (ICM) of the blastocyst, 5-6 days post fertilization (102,103). These cells are able to produce all the cell types of the adult organism, and are used for stem cell cultures, as they can be maintained in an undifferentiated state for a prolong period in culture, **Figure 2.4** (95).

The next developmental stage is gastrulation, which leads to the formation of the gastrula, composed of the three germ layers (ectoderm, mesoderm, and endoderm), which give rise to tissues and organ rudiments during subsequent development (104). All three germ layers originate from the epiblast, with formation of a thickening of the epithelium on the surface of the epiblast (86,94).
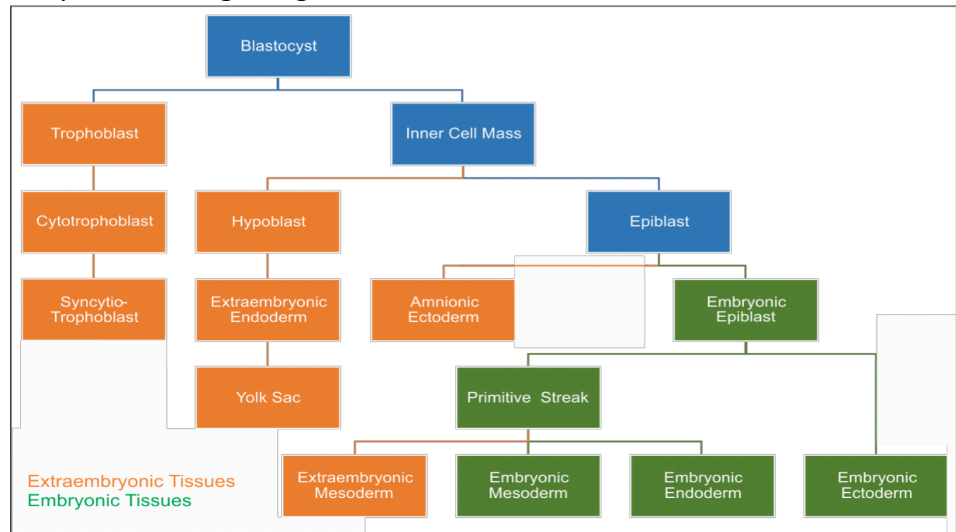
Figure 1.12: *Human Developmental Ontology Tree*. Graphical representation of tissue development during early embryogenesis in the human embryo. The information of the differentiation events spans from day 4 and the segregation of the blastocyst till day 15 and the generation of the trilaminar germ disk (https://discovery.lifemapsc.com/library/images/developmental-ontology-tree) .
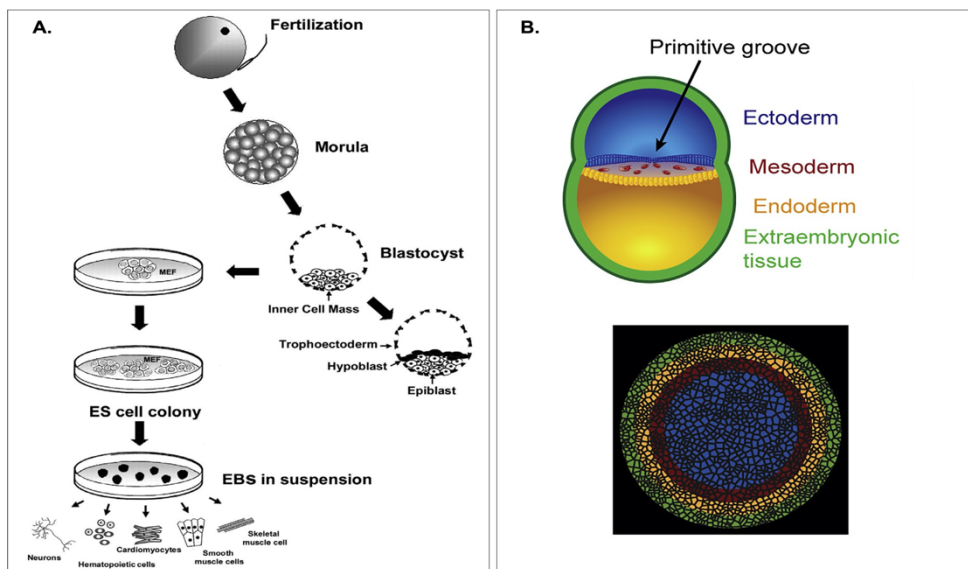
Figure 1.13: *Early embryogenesis and derivation of ES cell line*. A) Five days after fertilization, during the blastocyst stage, the embryo is made up mostly of trophectoderm and the ICM, which will eventually give rise to all of the embryonic tissues. The ES cell lines were generated from the ICM. Immunosurgery was used to isolate these cells, which were then plated on the MEF feeder layer. While being cultivated on top of the MEF feeder layer, ES cells can be expanded in the undifferentiated condition. The ES cells develop into specialized cells, such as neuronal, hematopoietic, skeletal muscle, smooth muscle, and cardiac tissue, when they are taken out of the feeder layer and grown in suspension as 3D cell aggregates (EBs) (105). B) Diagram of a human embryo at the gastrulation stage, illustrating how the embryo corresponds to a micropatterned 2D colony of hESCs that give rise to extra embryonic (CDX2-positive, green), endodermal (SOX17-positive, yellow), mesodermal (BRA-positive, red), and ectodermal (SOX2-positive, blue) fate layers (106).

The first ESC lines were generated in 1981 from mouse blastocysts (107,108), while the first human embryonic stem cell lines (hESCs) were established 17 years later isolated from the inner cell mass (ICM) of donated frozen preimplantation embryos (103). Since then, around 250 human ESC lines have been generated in different laboratories in the world by placing the isolated cells of the inner cell mass on human or mouse feeder layers of fibroblasts, **Figure 2.5** (103,104). Meanwhile, on registries like the International Stem Cell
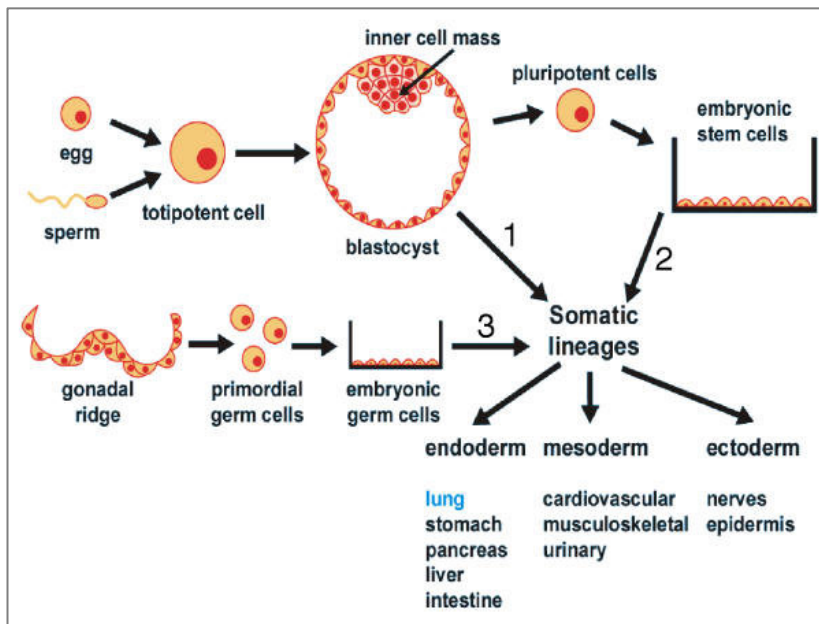
Figure 1.14: *Cell lineage determination during embryogenesis and generation of pluripotent embryonic cells*. The three primary germ layers form during normal development (path 1). Embryonic stem cells from the inner cell mass (path 2) or embryonic germ cells from the gonadal ridge (path 3) can be cultured and manipulated to generate cells of all three lineages (117,204).

Registry (www.umassmed.edu), more than 1000 hESC lines are currently listed. The majority of hESC lines, but not all of them, are derived from embryos that are still in the blastocyst stage (109). These embryos typically come from blastocysts that have been cryopreserved and are given to hESC research because they are no longer needed for reproduction (110).

Embryonic stem cells from mice exhibit two distinct pluripotent states, naïve or primed, which represent the earlier human blastocyst stage and the more advanced epiblast-like stage respectively (111). Specifically, mESCs that are derived from the inner cell mass (ICM) of preimplantation embryos represent naïve pluripotent stem cells, whereas mEpiSCs that are derived from the epiblast of the post-implantation embryo typify the primed state. The signalling profile of human ES cells resembles closely that of mEpiSCs, even though they are isolated from preimplantation embryos (112). Recently, multiple groups have modified culture conditions to revert and maintain hPSCs closer to a naïve-like pluripotency state. However, although global transcriptome analysis shows similarities between naïve-like hPSCs and mouse ES cells, there are still distinct differences in gene expression patterns and different culture requirements (113). Primed pluripotent hES cells exhibit high levels of DNA methylation, low

cloning efficiency and cannot chimerise with pre-implantation blastocysts. In addition, they favour glycolysis over oxidative phosphorylation, and female primed pluripotent hES cells rely on FGF2 and NODAL signalling for pluripotency maintenance, and exhibit post-X-chromosome-inactivation status (114). Also hES cells rely on FGF2 and NODAL signalling for pluripotency maintenance, in contrast with ''naïve'' mES cells that depend on LIF, **Table 1** (115). To overcome the differentiation barrier between naive and primed PS cells, a specific cocktail of transcription factors (TFs) and pathway inhibitors is introduced into primed PS cells to initiate resetting (116).

	Naïve	**Primed**
Origin	ICM of early blastocyst	Post impantation epiblast (Egg cylinder) or embryonic disc
Representative examples	mESCs, miPSCs	mEpiSCs, hESCs, hiPSCs
Colony morphology	Compact and domed	Compact and flat
Differentiation bias	None	Variable
Transcriptome	Similar to mouse ES cells	Similar to mouse epiblast stem cells
Cytokines	LIF	bFGF/TGF-β
Pluripotency factors	OCT4, NANOG, SOX2, KLF2, KLF4	OCT4, SOX2, NANOG
Clonagenicity	High	Low
Metabolic activity	Oxidative phosphorylation, glycolysis	Glycolysis
X-inactivation	Xaxa	Xaxi or xaxe naïve

Table 1: *Characteristics of Naïve and primed hPSCs*. A comparison of Naïve and primed hPSCs and the characteristics that are shared and distinct between these two stem cells states (117).

2.1.2. Adult Stem Cells

As mentioned previously, in addition to the ESCs, there are sources rich in non-embryonic stem cells, or adult stem cells. Adult stem cells also known as somatic stem cells, resident stem cells

or tissue-restricted stem cells, are undifferentiated cells residing in differentiated tissues and possess fundamental properties of stem cells, that is, self-renewal capacity and the ability to differentiate into multiple lineages (98). The most common source of adult stem cells is the bone marrow, a mesoderm derived tissue, which contains 2 types of stem cells: hematopoietic stem cells (HSCs) which further differentiate into mature blood cells, and the less differentiated stromal mesenchymal cells (118). In addition, adult stem cells can be isolated from several other organs such as the brain (neuronal stem cells), skin (epidermal stem cells), eye (retinal stem cells) and gut (intestinal stem cells) (119). So, these primitive cells are generally stored in a specialized environment called the niche, which consists of a combination of extracellular matrix signalling and soluble factors that regulate stem cell proliferation, migration, differentiation, and apoptosis (98,116). In their niche, adult stem cells are connected to supporting cells, protected from external harmful stimuli, and kept quiescent until the arrival of an appropriate activating signal. Tissue-specific adult stem cells proliferate, migrate to leave the niche, and differentiate to replace senescent or deteriorated cells, maintaining the organ structure and function. Also, they are able to repair mild injuries in various organs including the skin, liver, intestine, kidney, and bone marrow (98). However, such endogenous regenerative mechanisms appear insufficient to cope with severe damage, as in the case of myocardial infarction (120,121) or cerebral ischemia (122,123).

2.2. Human Embryonic Stem Cells
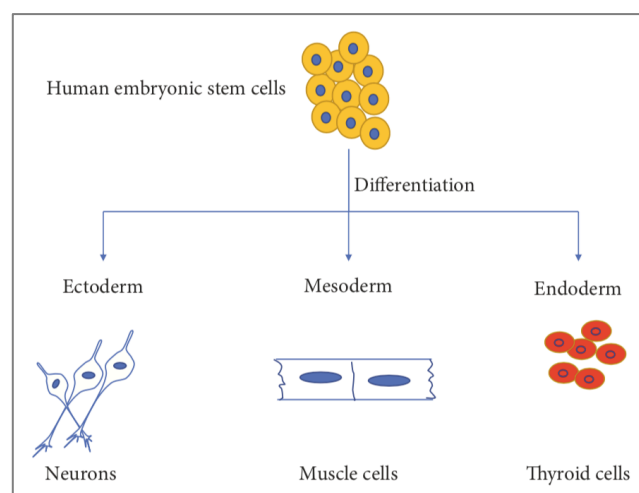
Figure 1.15: *Multilineage potential of human embryonic stem cells*. Human embryonic stem cells can be differentiated into three germ-layers such as ectoderm, mesoderm, and endoderm (124).

2.2.1. Core Transcriptional Regulatory Circuitry in Human Embryonic Stem Cells

Self-renewal of ESCs relies on maintaining the unique transcriptional profile of ESCs, while differentiation requires a flexible transcriptional profile which can be altered in differentiating cell types, **Figure 2.6** (125). In this section, the function of the homeodomain transcription factor OCT4 (126,127), the variant homeodomain transcription factor NANOG (128,129), and the high mobility group (HMG)-box transcription factor SOX2 (130) will be summarized, as these have proven indispensable for the maintenance of pluripotency regardless of the culture system (131). These key transcription factors have been identified as a core-regulatory circuit maintaining ES cells in the pluripotent state in vitro, **Figure 2.7** (132).
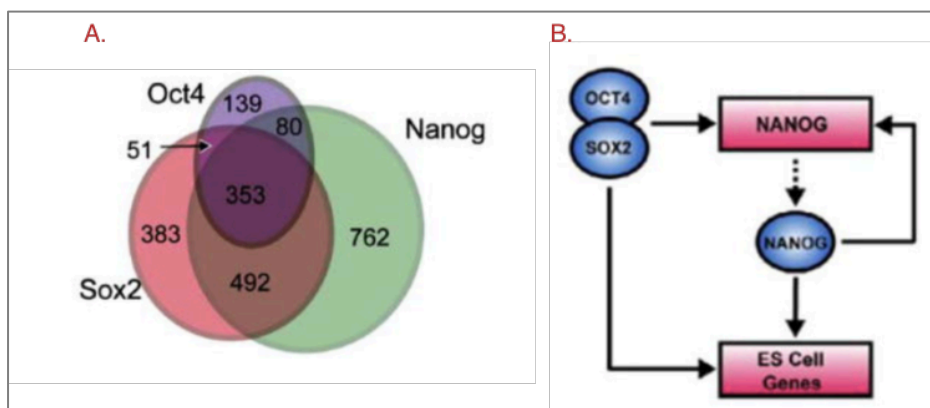
Figure 1.16: *OCT4, NANOG and SOX2 in hES Cell Pluripotency.* A) OCT4, NANOG and SOX2 are responsible for the regulation of 2360 genes. Interestingly, all three factors form a complex that influences the transcription of 353 genes. B) OCT4 and SOX2 complex to upregulate the transcription of *NANOG* and other ES cell genes. NANOG will subsequently promote ES cell gene expression resulting in a feed forward loop. Data presented above data have been obtained via mapping of genome-wide binding sites of the respective transcription factors. Adapted from (133).

Octamer-binding transcription factor 4 (OCT4), is a member of the class 5 POU (Pit-Oct-Unc) family of homeodomain transcription factors, and in humans is encoded by the POU5F1 gene (129,134). The POU family of transcription factors can activate the expression of their target genes through binding an octameric sequence motif of an AGTCAAAT consensus sequence (135–138). Both the N- and C-terminal tails of OCT4 are important for gene transactivation (132). Oct4 plays a critical role in the establishment and maintenance of pluripotency, OCT4 knock-out has an embryonic lethal phenotype in mice, due to the inability to form a pluripotent ICM at the blastocyst stage (126). Oct-4 expression in embryos begins at the 4–8-cell stage and is accompanied by widespread expression in all blastomere nuclei (139). Upon blastocyst formation, Oct4 expression becomes restricted to the ICM, and is downregulated in the TE and primitive endoderm, **Figure 2.8** (135). Niwa et al measured the

levels of OCT4 expression at various ES cell states, and the results indicated that OCT4 controls the pluripotency of stem cells in a quantitative fashion (140). Specifically, they determined that high levels of Oct4 expression drives ES cells to endoderm and mesoderm lineages, while stem cells with low level of Oct4 differentiate into TE (137,138). OCT4 has also been found to be essential for somatic cell reprogramming (141).
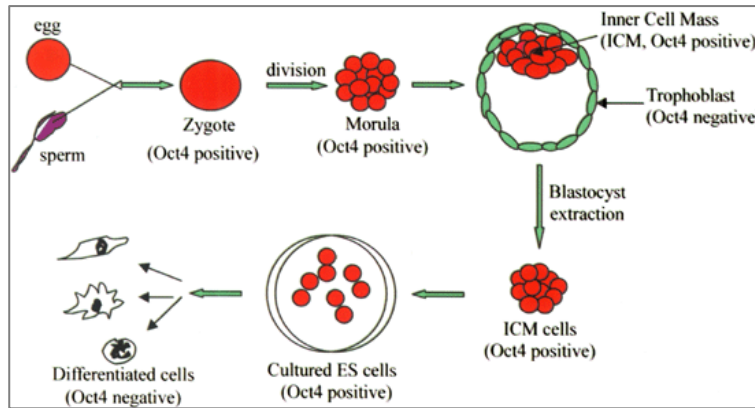
Figure 1.17: *ES cells and Oct4 expression.* The isolation and differentiation of ES cells in vitro are illustrated schematically starting with the fertilization of an egg by a sperm to form a zygote. At the blastocyst stage, inner cell mass (ICM) becomes visible and can be extracted and cultured in vitro to form embryonic stem (ES) cells. Cultured ES cells can be induced to differentiate into various cell types that are negative for Oct4. The stages of Oct4 expression are noted and the cells with Oct4 expression are marked in red colour. There is a general correlation between Oct4 expression and totipotency (135).

NANOG is another homeobox-containing transcription factor with a critical role in regulating the cell fate of the pluripotent ICM during embryonic development, maintaining the pluripotent epiblast and preventing differentiation to primitive endoderm (128). Structurally, Nanog can be considered simply as a three-domain protein – N-terminal domain, homeodomain, and C-terminal domain (142). The homeodomain structure of NANOG that promotes DNA binding, involves three α-helices close to the N-terminal tail which are connected by loops (143,144). NANOG knock-out has an embryonic lethal phenotype in mice (145). Based on the differences in gene expression between wild-type and Nanog null cells, it has been proposed that Nanog regulates pluripotency mainly as a transcriptional repressor for downstream genes that are important for cell differentiation such as Gata4 and Gata6 (132). During early embryogenesis, after the first segregation event, when trophoectoderm is separated from the ICM, the expression of NANOG is restricted to the human inner cell mass (ICM) at varying levels. Whereas the trophoblastic layer is positive for the homeobox transcription factor caudal type homeobox 2 (CDX2) (101). The second differentiation event, namely the segregation of epiblast and hypoblast from the cells of the ICM is suggested to involve NANOG and GATA6. Specifically, NANOG expression is confined to the epiblast on the blastocoelic surface, and GATA6 is characterized as a hypoblastic marker (146). Interestingly, cells with a high expression of NANOG demonstrate low expression of GATA6 and vice versa

(147). Therefore during embryogenesis NANOG is implicated in cell fate decisions. In culture, NANOG expression levels of both hES and mES cells fluctuate significantly. This fluctuation appears to be stochastic and creates a highly heterogenic population within the same colony of NANOG high and low cells. The former appear to be less and the latter more prone to differentiation signals.

One of the critical factors that control both pluripotency and neural differentiation of hPSCs is the sex determining region Y-box 2 (Sox2). It is a member of the Sox (SRY-related HMG box) gene family that encode transcription factors with a highly conserved high-mobility-group (HMG) DNA binding domain (148). Sox2 heterodimerizes with Oct4 and other nuclear factors to activate pluripotent gene expression or to regulate their downstream target genes (149–151). The heterodimers bind via their POU and HMG domains specific motifs within the DNA with the conserved sequences ATGAAAT (OCT4) and CATTGTC (SOX2) (152). Additionally, Sox2 is a robust interacting partner of NANOG forming a heterodimeric complex. The sequence of Sox2 responsible for interaction between Sox2 and NANOG is a triple-repeat motif of S X S/T Y. In Sox2, tyrosine to alanine mutations within this motif, in mES cells, leads to increased differentiation, thus highlighting the importance of this interaction for the preservation of pluripotency (153). During early embryogenesis, Sox2 expression is initially detected in cells at the morula stage, becoming more specifically located in the ICM of blastocyst and epiblast during the latter stages (130). In mice, Sox2 knock-out has a lethal phenotype due to the failure of ICM to form the epiblastic layer (154). In hES cells, knockdown of Sox2 has been shown to favour differentiation to trophoectoderm, while compromising pluripotency. In addition, reduction of Sox2 expression resulted in reduced expression of several key stem cell factors, including OCT4 and NANOG, linking these three factors together in a pluripotent regulatory network, **Figure 2.9, 2.10** (155). Therefore, Sox2 plays an essential role in regulation of pluripotency and
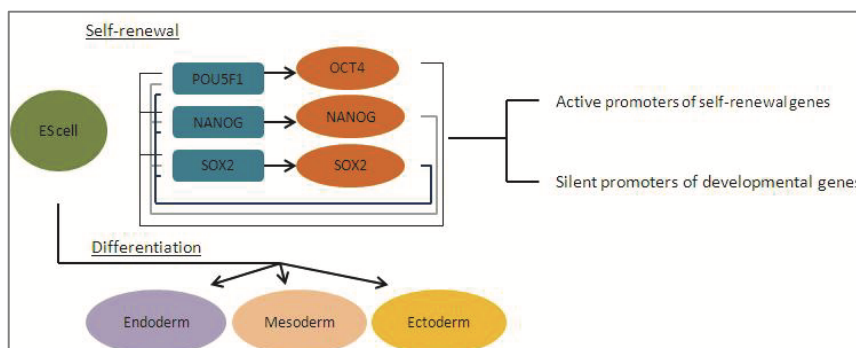
Figure 1.18: *The key transcription factors of hESC pluripotency*. OCT4, SOX2, and NANOG form the core transcriptional network and autoregulatory loop regulating stem cell self-renewal. OCT4, SOX2, and NANOG promote the expression of self-renewal genes and suppress the expression of developmental genes (160).

embryonic development. Later in development SOX2 is a critical factor for directing the differentiation of PSCs to neural progenitors and the development of the central nervous system. Specifically, in neural progenitor cells, Sox2 interacts with neural transcription factors, such as Pax6 (Paired-box protein 6) to activate neural progenitor gene expression (148,156).
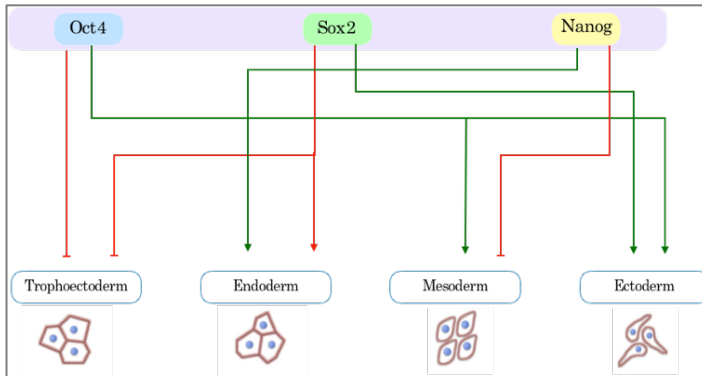
Figure 1.19: *Core pluripotency transcription factors as lineage specifiers.* Pluripotency transcription factors exert lineage-specific blockades on differentiation to particular lineages (hatched red lines) while often concomitantly directing differentiation to an alternative lineage (green arrows). Hence, pluripotency factors function as classical lineage specifiers, and provide ESCs the ability to differentiate to specific fetal lineages (133).

2.2.2. Major Signalling Pathways in hESCs
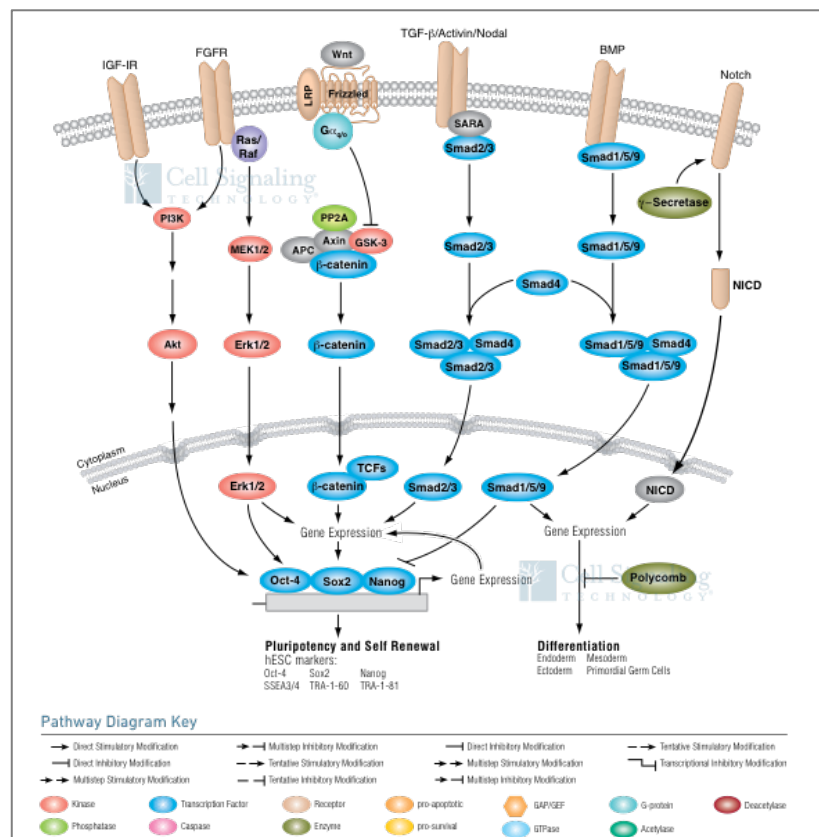
Figure 1.20: *Signalling pathways in hESCs. In human ESCs (hESCs),* the predominant signalling pathways involved in pluripotency and self-renewal are TGF-β, which signals through Smad2/3/4, and FGFR, which activates the MAPK and Akt pathways. The Wnt pathway also promotes pluripotency, although this may occur through a non-canonical mechanism involving a balance between the transcriptional activator, TCF1, and the repressor, TCF3. The BMP pathway, which uses Smad1/5/9 to promote differentiation by both inhibiting expression of Nanog, as well as activating the expression of differentiation-specific genes. Notch also plays a role in differentiation through the notch intracellular domain (NICD). (From Cell Signalling TECHNOLOGY, https://www.cellsignal.com/contents/science-cst-pathways-developmental-biology/pluripotency-and-differentiation/pathways-pluripotency)

Several kinase signal transduction pathways modulate the core pluripotency transcription factors in response to both intrinsic and extrinsic stimuli, preserving stem cell self-renewal and differentiation potential. Synergy between these pathways ensures the maintenance of pluripotency, **Figure 2.11**.

2.2.2.1. TGF-β/Activin/Nodal signalling pathway

It should come as no surprise that members of the TGF superfamily can contribute to both pluripotency and differentiation given their numerous pleiotropic roles in embryonic development, **Figure 2.12**. Activin was isolated from swine gonads in 1986 as a protein that stimulates FSH release, as opposed to Inhibin, which suppresses FSH secretion. Four inhibin subunits (βa, βb, βc, and βe) merge to generate a variety of activins, either as homodimers or heterodimers (157). Both activin A and Nodal signal through the same cell surface receptors (ALK4 or ALK7 and ACTRIIA or ACTRIIB) and activate the same intracellular mediators (SMAD2 or 3) (158)(155).
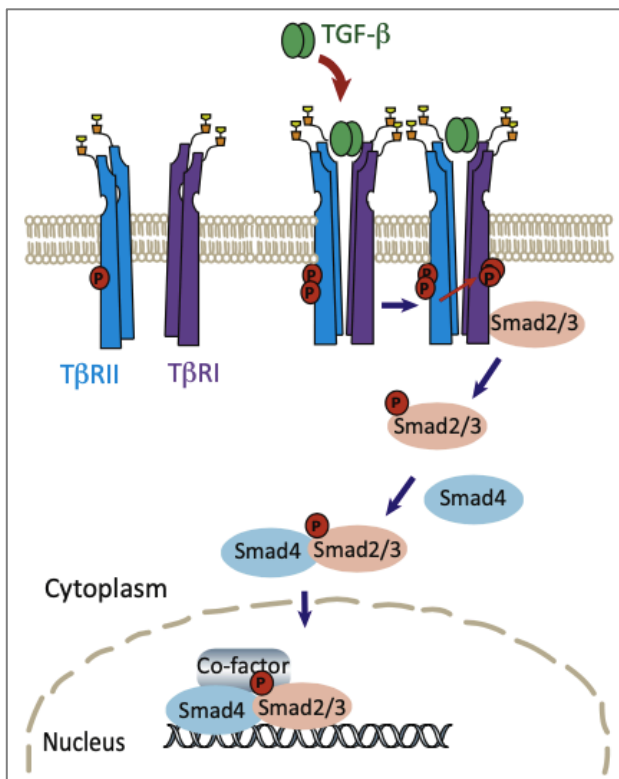
Figure 1.21: *Model of SMAD activation induced by TGF-β resultinh in SMAD mediated gene expression*. The TGF-β dimer binds to the the type II TGF-β receptor (TbRII), which promotes recruitment of type I TGF-β receptor (TbRI) into a heteromeric receptor complex, enabling TbRII to transphosphorylate the GS domain of TbRI. The subsequently activated TbRI then phosphorylates the C-terminal serines of Smad2 and Smad3 to activate them. These receptor-activated R-Smads next link up with a co-Smad (Smad4), and the Smad trimers then penetrate the nucleus where they link up with additional transcription cofactors at Smad-binding regulatory DNA sequences of target genes, directly activating or suppressing target gene expression (174).

The use of hESCs provides a useful tool to elucidate the relationship between this pathway and pluripotency. Numerous studies have demonstrated that TGFβ/activin A/Nodal play a crucial role in the biology of hESCs. In previous findings, Nodal was shown to protect

hESCs against spontaneous NE differentiation (159). Research into MEFs' capacity to sustain hESCs revealed that they release activin A precursor, suggesting that activin A maintains pluripotency (160). In fact, activin A (160,161), or combination of activin A with FGF2 (8) allows the undifferentiated proliferation of hESCs without the necessity for MEFs and MEF released factors. Stronger proof of the pathway's significance comes from a comparison of chromosomally normal hESCs with chromosomally abnormal hESCs with higher self-renewal capability (161). The studies demonstrate that the latter cell line expresses activin A and Nodal at greater levels whereas Follistatin, an activin inhibitor, is expressed at lower levels (161). Accordingly, two important pluripotency transcription factors are perturbed by Follistatin treatment (161).

It appears logical to assume that pluripotency may be SMAD dependent given that SMAD2,3 are active in undifferentiated hESCs and SMAD2/3 signalling decreases upon differentiation (162). More precisely, TGFβ or activin A ligands maintain hES cells' pluripotency in vitro by moderately activating the SMAD2/3 pathway in conjunction with PI3K-AKT signalling (163). The SMAD2/3/4 complex that is created moves into the nucleus and physically engages the Nanog gene promoter, boosting the transcriptional activity of the gene (164). Nanog is regarded as a crucial defender of pluripotency since it inhibits both FGF-induced NE differentiation and activin A-induced progression from ME to definite endoderm (15). Consequently, Nanog overexpression sustains hES cell pluripotency intact, suggesting that activin A/TGFβ sustains Nanog expression at high levels to achieve the same outcome. In that case, SMAD2/3 and Nanog physically interact, SMAD2/3's transcriptional activity is decreased, and the drive for endodermal differentiation is suspended (15). As mentioned above, Nanog also interacts with the promoters of the transcription factors Sox2 and Oct4. These elements work together to create an autoregulatory network that protects the pluripotency of hES cells (133).

Finally, it should be highlighted that although SMAD2 and SMAD3 are generally acknowledged together in literature, it's possible that hESCs might not regard them as equally important. Indeed, only SMAD2 is essential for pluripotency because of its dual capacity to retain Nanog and inhibit BMP (165). This is demonstrated when SMAD2 levels decrease and

hESCs become susceptible to autocrine BMP signals that direct them toward the ME, TE, and germ cell lineages (165).

2.2.2.2.   BMP signalling pathway

Bone Morphogenetic Protein (BMP) was first identified in 1965. It is a unique extracellular multifunctional signalling cytokine belonging to the large transforming growth factor-beta (TGF-β) superfamily (166). BMP is a key factor in determining the non-osteogenic embryological development of animals in addition to being a regulator of bone induction, maintenance, and repair (167). BMP4 knock out can be lethal for mouse embryos since majority of them die early, and the reported defects are related to gastrulation and ME differentiation (168).

BMPRs are composed of three parts: a short extracellular domain, a single membrane-spanning domain, and an intracellular domain with the active serine/threonine kinase region (169) BMP is reported to be bind to three BMPRI (BMPRIA or ALK3, BMPRIB or ALK6, and ALK2 or ActR-1A activin receptor) and three BMPRII (BMPRIIB, ACTRIIA, and ACTRIIB) (170). The cytoplasmic portion of BMPRI has a highly conserved TTSGSGSG motif that is distinctive and crucial for kinase activity (171). The kinase domain of BMPRII is followed by a characteristic, long C-terminal tail containing 530 amino acids (172). While BMPRI contains inactive and inducible kinases, BMPRII has constitutively active kinases.

BMP signalling pathways are initiated by the BMPRs located in a particular membrane domain of caveolin-1 (CAV1) and clathrin-coated pits (CCPs) at the cell surface (173,174). Similar to activin signalling, BMP signalling works in a similar manner. BMPs frequently bind primarily to type I receptors in the absence of type II receptors, but most require the combination of type II and type I receptors for higher affinity binding and signal transduction. This is in contrast to TGF- and activins, which bind primarily to the type II receptors and encourage the recruitment of type I receptors (174). The type I receptor, which transmits certain intracellular signals, is trans phosphorylated by the type II receptor kinase. BMPRIA signals are thereby promoted to downstream substrates.

The expression of genes that are directly related to hES cell plyripotency appears to be

suppressed by the BMP4 pathway effector proteins SMAD1/5/9. SMAD1 has been shown to bind to the Nanog promoter, which results in downregulation of Nanog (164).

The expression of genes that are directly related to hES cell pluripotency appears to be suppressed by the BMP4 pathway effector proteins SMAD1/5/9. SMAD1 has been shown to bind to the Nanog promoter, which results in downregulation of Nanog (164). The degree of ERK activation determines how differentiated cells respond to BMP4 stimulation. As previously mentioned, activation of ERK causes cells to produce Nanog continuously during the early stages of differentiation, which encourages them to take on a mesodermal fate. When ERK is not present, BMP4 signalling causes cells to form extraembryonic lineages (175). Recent work in mES cells reveals that BMP4 protects pluripotency by acting through ERK, then KLF2, and other pathways. In addition, SMAD1 physically interacts with KLF4, and the resulting complex suppresses SMAD1 activity (176,177).

BMP4 induces both extra-embryonic and embryonic hESCs differentiation. Shorter exposures (24 hours) of hESCs to BMP4 result in mesodermal populations that express Brachyury (14), whereas longer exposures (seven days) result in trophoblastic cells (11), or a combination of populations that express markers for both trophoblasts (hCG alpha and beta) and extra-embryonic endoderm (AFP, SOX7), **Figure 2.13** (14).
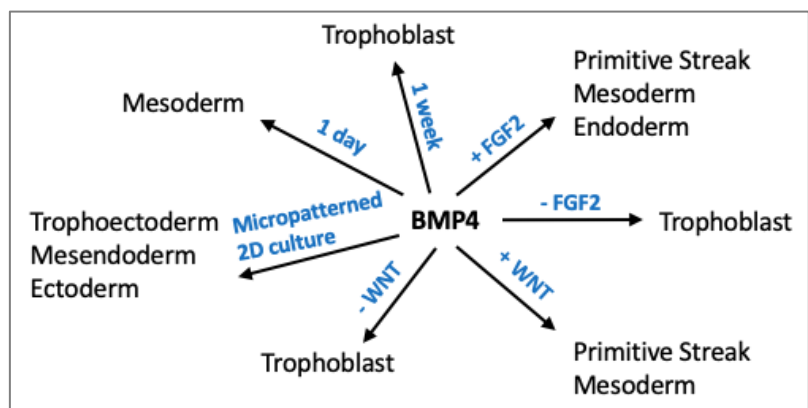
Figure 1.22: *hESCs' BMP4-induced destiny*. BMP4 is linked to a variety of fates, and ongoing research is examining the underlying mechanisms behind the observed diversity (14).

BMP4 interacts with various signalling pathways to coordinate fate acquisition. WNT activity and MEK/ERK activity both influence the outcome of BMP4 induction. In further detail, BMP promotes trophoblastic differentiation in the absence of FGF2, but ME differentiation is enabled when FGF2 is present and MEK/ERK is activated (175). Moreover, endogenous WNT signals in culture are accountable for the variety observed following BMP4 induction, WNT3

orchestrates PS and mesodermal differentiation once BMP4 triggers it (178). However, BMP4 controls the production of genes related to trophoblasts when WNT is inhibited (178).

It is interesting to note that BMP4 induction has also been associated with a rise in the EMT marker MSX2 and the EMT regulator SLUG. The promoters of the aforementioned factors have been shown to directly bind to activated SMAD1/5/9 proteins, which increases the production of those factors. This implies that BMP4 signalling has a direct role in EMT, a process crucial for the development of the primitive streak that indicates the start of gastrulation (179)

2.2.2.3.   FGF and the MAPK pathway

FGF2 (or basic FGF) is the first growth factor identified as being crucial for hESC pluripotency maintenance and self renewal (162). It is widely accepted that hES cells have most commonly been cultured in the presence of basic fibroblast growth factor (bFGF) either on fibroblast feeder layers or in fibroblast-conditioned medium (175,181). The ligand binds to tyrosine kinase FGF receptors on the plasma membrane and promotes autophosphorylation of its intracellular domain tyrosine residues. In hES cells, the activation of FGFR kinase leads to phosphorylation of FGFR substrate 2a (FRS2a), recruitment of phospholipase Cγ (PLCγ), and thus activation of two signalling cascades (PI3K-AKT and MEK-ERK) that promote cell proliferation and self-renewal (165–167). Interestingly, these two pathways cross-talk, with PI3K maintaining ERK activation to pluripotency-compatible levels. This fact explains how both low (<10ng/mL) and high (>50ng/mL) levels of FGF2 have the same effect on hES cells, preserving pluripotency. In brief, low doses of the FGF2 moderately activate ERK1/2, while high doses also activate PI3K-AKT, which in turn suppresses ERK1/2 activity (163). Recent research has shown that FGF2 signalling leads to mesoderm differentiation, as it switches the outcome of BMP4 induced differentiation of human ES cells by maintaining NANOG levels through the MEK-ERK pathway. In the absence of FGF2, NANOG expression level declines rapidly and BMP4 drives hES cells to extraembryonic lineages (175). In addition, activation of the FGF pathway regulates the ability of activin A/Smad2,3 to control the balance between pluripotency and endodermal differentiation, as the latter pathway is context dependent. Under self-renewing conditions, FGF2 and PI3K-AKT suppresses ERK and Wnt signalling, allowing SMAD2,3 to activate a specific group of target genes implicated in pluripotency. On

the other hand, inactivation of PI3K-AKT signalling leads to activation of Wnt pathways and its effectors such as β-catenin and SNAIL, which cooperate with SMAD2/3 to induce genes involved in early differentiation, **Figure 2.11** (163).

2.2.2.4. Wnt signalling pathway

Activation of the Wnt pathway controls a wide variety of processes in embryonic development and adult homeostasis (169). It consists of over 30 extracellular ligands that initiate signalling by binding to Frizzled (FZD) and low-density lipoprotein receptor-related protein 6 (LRP6) on the plasma membrane (186). The Wnt/β-catenin pathway, also known as canonical Wnt pathway is responsible for the regulation of cytoplasmic β-catenin protein stability. In the presence of Wnt molecules, β-catenin accumulates in the cytosol, translocates into the nucleus and regulates gene expression together with TCF/LEF (T-cell factor / lymphoid enhancer-binding factor) transcription factors. In the absence of Wnt, the transcriptional coactivator β-catenin is degraded by a multiprotein "destruction complex" that includes the tumor suppressors Axin and adenomatous polyposis coli (APC), the Ser/Thr kinases GSK-3 and CK1, protein phosphatase 2A (PP2A), and the E3-ubiquitin ligase β-TrCP (171). So, β-catenin is phosphorylated by GSK3β and then marked by polyubiquitination for degradation by the proteasome. (172). Multiple conflicting studies suggested a role of Wnt/β-catenin signalling in the regulation of hES cells (161,189–193). Apart from different culture conditions, growth media, substrates and cell lines, which are factors that indeed contribute to variations in the results, recent research argues that different pools of GSK3β complexes exist in separate cellular compartments, exerting different signals. When all GSK3β pools are chemically inhibited, β-catenin is activated and acts in concert with SMAD2/3 to initiate hES cell differentiation (191). On the other hand, low doses of GSK3β inhibitors sustain pluripotency through stabilization of the pluripotency gene c-MYC (163). The core pluripotency factor OCT4 has also been implicated in Wnt signalling, as it has been found to mitigate β-catenin-related differentiation cues, **Figure 2.11** (194).

Aims of the Thesis

Pluripotency and the capacity for self-renewal are two traits that set embryonic stem cells (ESCs) apart from other cell types. Numerous cell signalling pathways control these features, which enable ESCs to develop into any type of cell in the adult body and divide continuously in the undifferentiated state. Members of the TGF superfamily play a key role in the pluripotency and differentiation of hESCs. Previous results from our lab implicated the ARF6 GTPase in the signalling of activin A and BMP4, both key members of the TGF superfamily involved in human embryonic stem cell pluripotency and differentiation. In this thesis we expand on these earlier findings and address the role of ARF6 to the 3 germ layers, mesoderm, endoderm and ectoderm. To achieve this goal we undertook the following:

- Determine the role of ARF6 in mesoderm induction by BMP4
- Establish protocols for endoderm and ectoderm induction and standardise detection of representative markers of both lineages
- Elucidate the role of ARF6 in endoderm formation
- Investigate the role of ARF6 in ectoderm formation

Chapter 2

Experimental procedures

2. Cell Culture

2.1. Human Embryonic Stem Cells (hESCs) culture

The maintenance and propagation of human embryonic stem cells (hESCs) requires the use of specific nutrients combined with careful handling to maintain pluripotency. The medium used for this purpose was mTeSR™Plus (Stem Cell Technologies, #100-0276), a fully chemically defined nutrient, xenobiotic agent and animal serum free medium.

All experiments were performed using 4 cell lines. H1 hESC line was purchased from Wicell Research Institute, WB0113, Madison, USA and is the control line for H1 CRISPR knock-out ARF6 (H1-ARF6KO) cell line. H1-ARF6T157A-GFP stable cell line and the vector control cell line H1-GFP, were both derived from the parental H1 line by transfection and selection of the relevant hESC optimised expession plasmids. All genome edited H1 cell lines were constructed by Dr Angelos Papadopoulos in our lab.

Six-well tissue culture plates (Corning, 3506) were coated with 83ng/ml hESC-qualified Matrigel (Corning, 354277) diluted in DMEM/F12 (ThermoFisher Scientific – 10770245) medium and incubated for 1h at room temperature, the Matrigel solution was then removed, wells washed x 1 with DMEM/F12 and cells plated into the well. Spontaneously differentiating cells were manually removed from the cultures. The percentage of these cells was always less than 10% and is an indicator of a healthy culture. Only cultures meeting this criterion were used in the experiments.

The hESCs were passaged when most colonies were large, compact with dense centers and their borders were beginning to fuse (approximately 5 days). Cells were washed with 1ml of DMEM/F12 and passaged enzymatically using 1ml of dispase (1mg/ml) (ThermoFisher Scientific, 1710541) for 1min at 37°C until the edges of the colonies started to shrink but without the colonies detaching from the dish. At the end of the incubation, the dispase was removed and 2 washes of the well with 2ml DMEM/F12 were performed to remove all enzyme

residues. To harvest the hESCs colonies, 1ml of mTeSR™Plus was added and using a scraper (Corning, 3010) the cells were detached from the surface of the dish and transferred to a 15ml falcon tube. To be sure that all cells were transferred, and that no selection for less adherent colonies occurred, this procedure was performed twice. Namely, another 1ml of mTeSR™Plus was added to the well and using a scraper, all remaining cells were scraped off and transferred to the falcon tube. The colonies were then dissociated into small clumps by gentle agitation to obtain the appropriate size required and replated onto Matrigel-coated six well plates in a 1:7 ratio. Finally, the dish was very gently shaken and placed in the 37°C incubator.

H1 cells were also passaged using Versene-EDTA 0.02% (Lonza – BE17-711E) instead of dispase. In short, cells were incubated with Versene-EDTA for 3min at room temperature until the colony boarders began to detach from the well, and were subsequently dissociated into small clumps (3-5 cells). The cell aggregates were transferred into new 6-well dishes and allowed to attach and proliferate for 24 hours in fresh media supplemented with 5μM ROCK inhibitor (Fasudil) (LC Laboratories) to increase cell adhesion. The day after, the medium was changed without ROCK inhibitor.

Prior to freezing, H1 cells were passaged from 6-well plates as described above, and collected in 15mL falcon tubes. They were centrifuged at 800rpm for 5min at room temperature and resuspended in 1mL of mFreSR reagent (Stem Cell Technologies – 05855). Next, they were transferred into cryovials and stored for 24 hours at -80° C before being transferred to liquid nitrogen. Many vials were frozen from the same passage in order to decrease variability between experiments.

During thawing, cryovials containing H1 cells were thawed in a 37°C waterbath for approximately 30sec, and transferred to a 15mL falcon tube containing 4mL of fresh medium containing 5μM ROCK inhibitor. Next, cells were centrifuged at 800rpm for 5min at room temperature, collected with fresh medium and plated in 6-well dishes in the presence of 5μM ROCK inhibitor, which was removed the day after plating by refreshing with fresh medium without the inhibitor.

2.1.1. Cell Differentiation Protocols.

2.1.1.1. Differentiation of hESCs to mesoderm

Prior to differentiation, H1 wt, H1-ARF6KO, H1-GFP and H1-ARF6T157A-GFP lines were first passaged with Versene-EDTA 0.02% onto 6-well plates coated with matrigel and cultured in mTeSR™Plus medium. The medium was exchanged every two days.

When cells reached approximately 50% confluency, mesoderm differentiation was induced by substituting mTeSR™Plus medium with mTeSR™Plus medium supplemented with 50ng/ml human bone morphogenetic protein-4 (BMP4) (ThermoFischer Scientific-PHC9354) for 1-2-4 and 7 days. On day 4 of differentiation, the culture medium (mTeSR™Plus) was half changed until day 7 to remove the dead cells. Subsequently, after 1, 2, 4 and 7 days cells were lysed using lysis buffer (containing PBS pH=7.0, 1% SDS (Sigma-75746) and 100μM phenyl methane sulphonyl fluoride PMSF protease inhibitor), protein was quantitated using Pierce™ BCA® Protein Assay Kits and Reagents (Thermo Scientific-23225). RNA was also extracted at this stage, **Figure 2.1** (14).
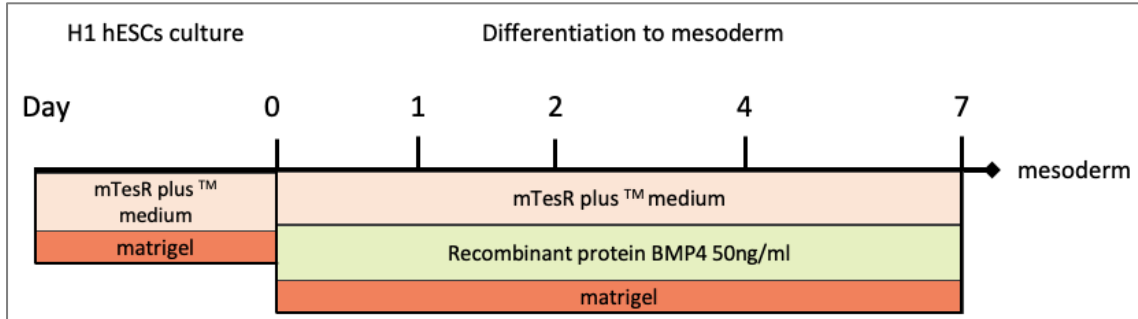
Figure 2.1: *Differentiation protocol to mesoderm*

2.1.1.2. Differentiation of hESCS to neuroectoderm

The hESCs were cultured in six-well tissue culture plates coated with matrigel and mTeSR™Plus medium. Briefly, H1 colonies were detached with 1 mg/ml dispase (ThermoFisher Scientific, 1710541) and dissociated into small clumps. Neuroectodermal differentiation was initiated by growing the H1 clumps in suspension in non-adherent plates with the ESC growth medium consisting of Dulbecco's modified eagles medium (DMEM/F12) (ThermoFisher Scientific-10770245), 20% Knockout replacement serum (KOSR), 0.1mM Non-Essential Aminoacids

(ThermoFisher Scientific-11140-050), 2mM glutamine (Thermo Fisher Scientific, 25030-024) and 100μM β- mercaptoethanol (ThermoFisher Scientific, 21985-023) to form embryoid bodies for 4 days. On day 4 of differentiation, the embryoid bodies were transferred to a serum-free minimal (SFM) medium consisting of DMEM/F12, 0.1mM Non Essential Aminoacids and 2 μg/ml heparin (Sigma-Aldrich, H3149-100KU), and grown in suspension. After 3 days in suspension, on day 7, they were attached to laminin-coated (Sigma-Aldrich, 114956-81-9) ibidi dishes (μ-Dish, 35mm, 81156) for immunostaining and laminin coated twenty four-well tissue culture plates for western blotting. On day-10 cells were harvested and used for further analysis by western blot and immunofluorescence, **Figure 2.2** (12).
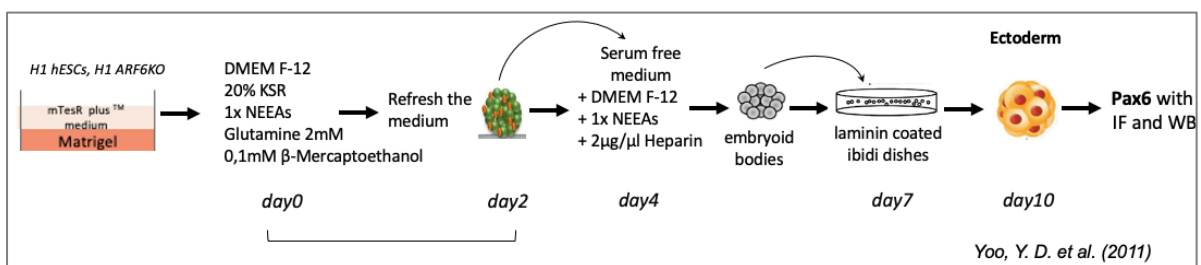
Figure 2.2: *Differentiation protocol to neuroectoderm*

2.1.1.3.   Differentiation of hESCs to definitive endoderm

The hESCs were cultured in six-well tissue culture plates coated with matrigel and cultured in mTeSR™Plus medium. For endodermal differentiation, eighty percent confluent cells were placed in RPMI 1640 (ThermoFisher Scientific-21875034) medium containing 1% GlutaMax (ThermoFisherScientific-35050061), 0.5% defined fetal bovine serum (FBS; HyClone) supplemented with 100 ng/ml activin A. Three days postinduction, the medium was refreshed using the same RPMI-based medium with 1% GlutaMax, 100 ng/ml activin A and 2% FBS. Differentiation was continued for another 2 days, and on day 5 total RNA was extracted for RT-PCR, **Figure 2.3** (13).
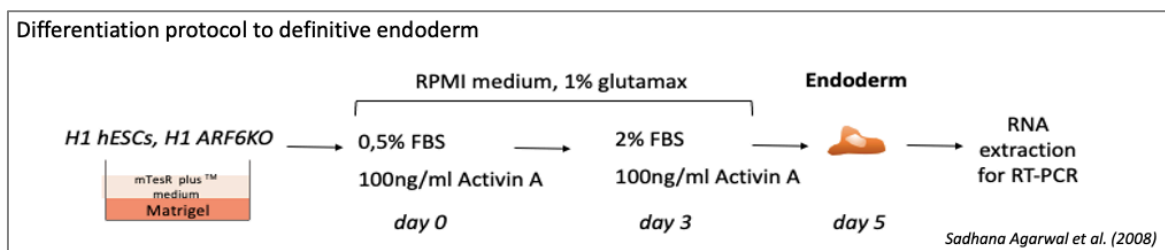
Figure 2.3: *Differentiation protocol to definitive endoderm*

2.2. Biochemical Methods

2.2.1. Immunofluorescence

Cells were plated on ibidi dishes (μ-Dish, 35mm, 81156). For cell fixation, cells were washed with PBS and a 3.7% paraformaldehyde solution (Sigma-Aldrich-P6148) was added for 15min at room temperature. This was followed by a second wash with PBS and incubation with 50mM NH4Cl (Sigma-Aldrich-A4514) (in PBS) for 15min. Then, incubation with Triton-X 0.1% (ThermoFisher Scientific – 10254583) (in PBS) for 4min was performed to increase cell membrane permeability. Subsequently, a wash with PBS and incubation with 10% FCS for 20min was performed to block the non-specific antigenic sites. The cells were then incubated with the primary antibody in 10% FCS for 1 hour, **Table 2**. At the end of the incubation, three 5-minute washings with PBS were performed, shaking, in order to remove excess primary antibody. Next, the secondary antibody diluted in 10% FCS was added to the ibidi dishes for 1 hour (Table 3). They were washed again with PBS thrice for 5minutes while shaking. Then, for nuclear staining the cells were stained with Draq5 (Abcam, ab108410) at 5μM for 5 minutes. Afterwards, they were washed once with PBS and they were observed using a LeicaSP5 Confocal Microscope equipped with Argon, HeNe, 561 lasers.

2.2.2. SDS-PAGE Electrophoresis and Western Blotting

Tissue culture cells were washed twice with PBS and lysed with lysis buffer as described in section *3.1.2.1.*. Samples were then sonicated (Branson Digital Sonifier), thrice for 10 seconds at 13% amplitude and then boiled for 10 minutes. This was followed by centrifugation at 13.200rpm for 20 minutes and collection of the supernatant. Protein concentration of each sample was determined using the BCA Protein Assay Kit and a photometer set at 562nm. After processing these values with Microsoft Excel, the total protein content of each sample was calculated, and so the suitable amount of each lysate was transferred to a 1.5ml tubes, with sample buffer (SDS) 4x Laemmli (say what is inside the buffer) enriched with 0,025% β-mercaptoethanol (Gibco, 21985). Subsequently, these cell extracts were electrophoresed on 8-12% SDS-polyacrylamide gels according to their molecular weight and transferred to nitrocellulose membranes (Whatman). To check the efficiency of the protein transfer, the nitrocellulose membrane was stained with 0.1% PonceauS (Sigma Aldrich, P3504-100G) for 5 min and excess pigment was removed with Western Buffer 1x.

After blocking for 20 minutes in 5% milk in Western buffer (10 mM Tris-HCl pH 7.2, 0.1% Tween-20, and 150mM NaCl) or in 5% Bovine Serum Albumin, BSA (A9647-10G) in western buffer to block non-specific antigenic sites, membranes were incubated overnight at 4°C with the primary antibodies, **Table 2**. Subsequently, membranes were washed 3 times for 10min in western solution under agitation. Finally, the membranes were incubated with secondary antibodies conjugated to Horse Radish Peroxidase (HRP) dissolved in 5 % skimmed milk or IRDye Fluor antibodies in western solution for 1 hour at room temperature followed by the same washes as above. For protein visualization membranes were incubated for 2 minutes with Amersham ECL Western Blotting Detection Reagent (Amersham, RPN2209) and chemiluminescence was detected using the Azurec600 system. In the case of Fluor antibodies, membranes were analyzed using the same Azurec600 system.

Antibody	Clone	Host species	Company	Catalogue Number	Working Concentration
a-actin	JLA20	Mouse	DSHB, USA	AB_528068	30ng/ml
a-ARF6	D12G6	Rabbit	Cell Signalling, USA	#5740	Used at 1:1000 dilution
a-Brachyury	Polyclonal	Goat	R&D Systems, USA	AF2085	200ng/ml
a-hGAPDH	2G7-S	Mouse	DSHB, USA	AB_2617426	102µg/ml
a-HSC70	B-6	Mouse	Santa Cruz Biotechnologies	SC-7298	200ng/ml
a-Pax6	N-terminal region, aa 1-223	Mouse	DSHB, USA	AB_528427	WB: 100ng/ml IF: 200ng/ml
a-Tubulin	E7	Mouse	DSHB, USA	AB_2315513	170ng/mL
Peroxidase AffiniPure a-mouse HRP	Polyclonal	Goat	Jackson Immunoresearch Laboratories, USA	115-035-062	100ng/mL

Peroxidase-AffiniPure Goat a-Rabbit (H+L)	Polyclonal	Goat	Jackson Immunoresearch Laboratories, USA	111-035-144	100ng/mL
Peroxidase Rabbit anti-goat IgG	Polyclonal	Rabbit	Sigma Aldrich, USA	A8919	100ng/mL
IRDye® 800CW anti-mouse	Polyclonal	Goat	LICOR, USA	926-32210	200ng/ml
IRDye® 800CW anti-rabbit	Polyclonal	Goat	LICOR, USA	926-32211	200ng/ml
IRDye® 680RD anti-rabbit	Polyclonal	Goat	LICOR, USA	926-68071	200ng/ml
IRDye® 680RD anti-mouse	Polyclonal	Goat	LICOR, USA	926-68070	200ng/ml
Alexa Fluor® 594 donkey α-mouse	Polyclonal	Donkey	Jackson ImmunoResearch	715-585-151	2,5µg/ml

Table 2: *Table lists of antibodies*. The name of the antibodies used in this report, accompanied by information regarding clone, species, company name, catalogue number and dilution factor.

2.3. RNA isolation and qRT-PCR

2.3.1. RNA extraction

For the extraction of RNA, cells were cultured in six-well tissue culture plates. When cells were confluent as indicated, they were washed once with PBS (Pan-Biotech, P04-36500) and incubated with 200µl of trypsin (ThermoFisher Scientific – 25200056) for 1min at 37°C. Subsequently, they were dissociated and were collected with PBS containing 2% fetal bovine serum (FBS; HyClone FCS). The cell suspension was then centrifuged at 1200rpm for 5 minutes, the supernatant was discarded and the cell pellet was washed with PBS, and was again centrifuged at 1200 rpm for 5 minutes. Finally, the cell pellet was collected and kept at -20°C.

Total cell RNA was isolated using the commercial kit NucleoSpin RNA (MACHEREY-NAGEL GmbH & Co KG). The concentration of RNA in each sample was measured using a

NanoDrop OneC (Thermo Fisher Scientific, Waltham, MA, USA) and in parallel its quality was checked by the ratio of sample absorbance at 260 nm to the absorbance at 280 nm. Samples for which the 260/280 ratio was between 1.8-2 were considered high purity and were further analyzed.

2.3.2. Quantitative Reverse Transcription-Polymerase Chain Reaction (qRT-PCR)

The quantitative Reverse Transcription-Polymerase Chain Reaction (qRT-PCR) method was used to determine the expression of the genes studied. The qRT-PCR was performed using the standard one-step QuantiTect SYBR Green RT-PCR Kit (Qiagen, 204243) and the AriaMx Real-Time PCR machine (Agilent Technologies, G8830A). The PCR amplification reaction mix for each sample consisted of 5µl SYBR Green PCR Master Mix, 4µM forward and reverse primers, 0,1µl of RT-mix and 1,4µl distilled water in a total volume of 10µl. Because of the small amount of volumes needed for the PCR amplification reaction, a mastermix of SYBR Green PCR Master Mix, distilled water and RT mix was first prepared for the total number of samples per reaction. Then samples for the reaction were prepared using the appropriate pairs of primers (Table 2) to a final concentration of 4µM. The reaction was performed in an AriaMx RealTime PCR System, The data were analysed using AriaMx software and CT values were normalised against GAPDH using the equation: $2^{-\Delta Ct}$. All primers were synthesized by MWG Eurofins.

Conditions of the qRT-PCR reaction	
Reverse transcription	50°C for 20min
Activation of DNA polymerase	95°C for 15min
Double helix opening (denaturation)	95°C for 15sec
Annealing of primers	52-60°C for 20sec
Extension of the product	72°C for 30sec
45 cycles in total	

Table 3: *Protocol for qRT-PCR*

Primer Description	Primer Sequence	Tm
GAPDH FW	5'-GGTCGGAGTCAACGGATTTGGTCG-3'	57°C
GAPDH RV	5'-CCTCCGACGCCTGCTTCACCAC-3'	57°C
GATA6 FW	5'-ACGCCGCCTTCCCCCATCTCT-3'	58°C
GATA6 RV	5'-CCCCAGGCGCCGAAGGTC-3'	58°C
MIXL1 FW	5'-GAACAGGCGTGCCAAGTCTCG-3'	58°C
MIXL1 RV	5'-TTCGGGCAGGCAGTTCACATCTAC-3'	58°C
WNT3 FW	5'-CTGGCGAAGGCTGGAAGTGG-3'	55°C
WNT3 RV	5'-CGGCCCGCCTCGTTGTTG-3'	55°C
CDX2 FW	5'-CACGCAGCCCCGCAGACTACCATC-3'	58°C
CDX2 RV	5'-CTTCCGCATCCACTCGCACAGG-3'	58°C
SOX17 FW	5'-TCCCATGCACCCCCGACTC-3'	55°C
SOX17 RV	5'-TGCTGGTGCTGGTGCTGGTGTTG-3'	55°C
GATA4 FW	5'-GTCGCCGCGCTTCTCCTTCC-3'	57°C
GATA4 RV	5'-GCTCCGCCGCCACTGCTGT-3'	57°C
FOXA2 FW	5'-CCCGCGACCCCAAGACCTACAG-3'	57°C
FOXA2 RV	5'-GAGCGAGTGGCGGATGGAGTTCT-3'	57°C
GAPDH FW	5'-GGTGTGAACCATGAGAAGTATGA-3'	57°C
GAPDH RV	5'-GAGTCCTTCCACGATACCAAAG-3'	57°C
AFP2 FW	5'-ACACAAAAAGCCCACTCCAGCATC-3'	55°C
AFP2 RV	5'-GTCATAGCGAGCAGCCCAAAGAAG-3'	55°C

Table 4: *Table lists the name and sequence of primers used in this report*, FW: Frward, RV: Reverse.

2.3.3. Statistics

Data were analyzed with SPSS 22.0 (SPSS, Inc). Variables with continuous data were expressed as means ± standard deviation values. A normality test was performed to apply the T-test or Mann-Whitney test for comparison between means of two conditions and ANOVA for comparison of means between more than two conditions. In the case of multiple comparisons, Bonferroni correction was applied to calculate the final statistical significance value p. For qualitative variables, categorical data were assigned a value and the x^2 (chi-square) test was applied. The values of *statistical error P* calculated in the two-sided (2-tailed) test were considered statistically significant when they were less than 0.05.

Chapter 3

3. Results

3.1.   Induction of mesodermal and extra-embryonic markers in ARF6KO H1 cells by BMP4

3.1.1.   ARF6 KO increases the expression of BRACHYURY upon induction with BMP4

Previous experiments in our lab, conducted by Dr. Angelos Papadopoulos (AP), demonstrated that ARF6 is implicated in Activin A and BMP4 signalling in H1 cells. Expression of ARF6T157A, the fast cycling mutant of ARF6, in H1 cells resulted in enhanced phosphorylation of SMAD2/3 and SMAD1/5/9 upon Activin A or BMP4 induction, respectively, compared to the induction in H1 wt cells (data not shown). In agreement, CRISPR KO of ARF6 in H1 cells resulted in decreased phosphorylation of SMAD2/3 and SMAD1/5/9 upon Activin A or BMP4 induction (data not shown). As BMP4 induces mesoderm differentiation, AP investigated whether the alteration of SMAD phosphorylation by ARF6 led to alterations during differentiation downstream of BMP4 induction. This was achieved by addressing a time course of induction of Brachyury downstream of BMP4 induction in the ARF6 and control H1 cell lines. He found that indeed Brachyury induction was altered in the cell lines. In 2 independent clones expressing ARF6T157A, Brachyury was induced by BMP4 but at lower levels than in the control H1 cell line, **Figure 3.1**. In 3 independent ARF6 KO clones Brachyury was very strongly induced by BMP4 at much higher levels than control H1 cells, **Figure 3.2**. The timing of Brachyury was not altered in either case, **Figure 3.1 and 3.2.**
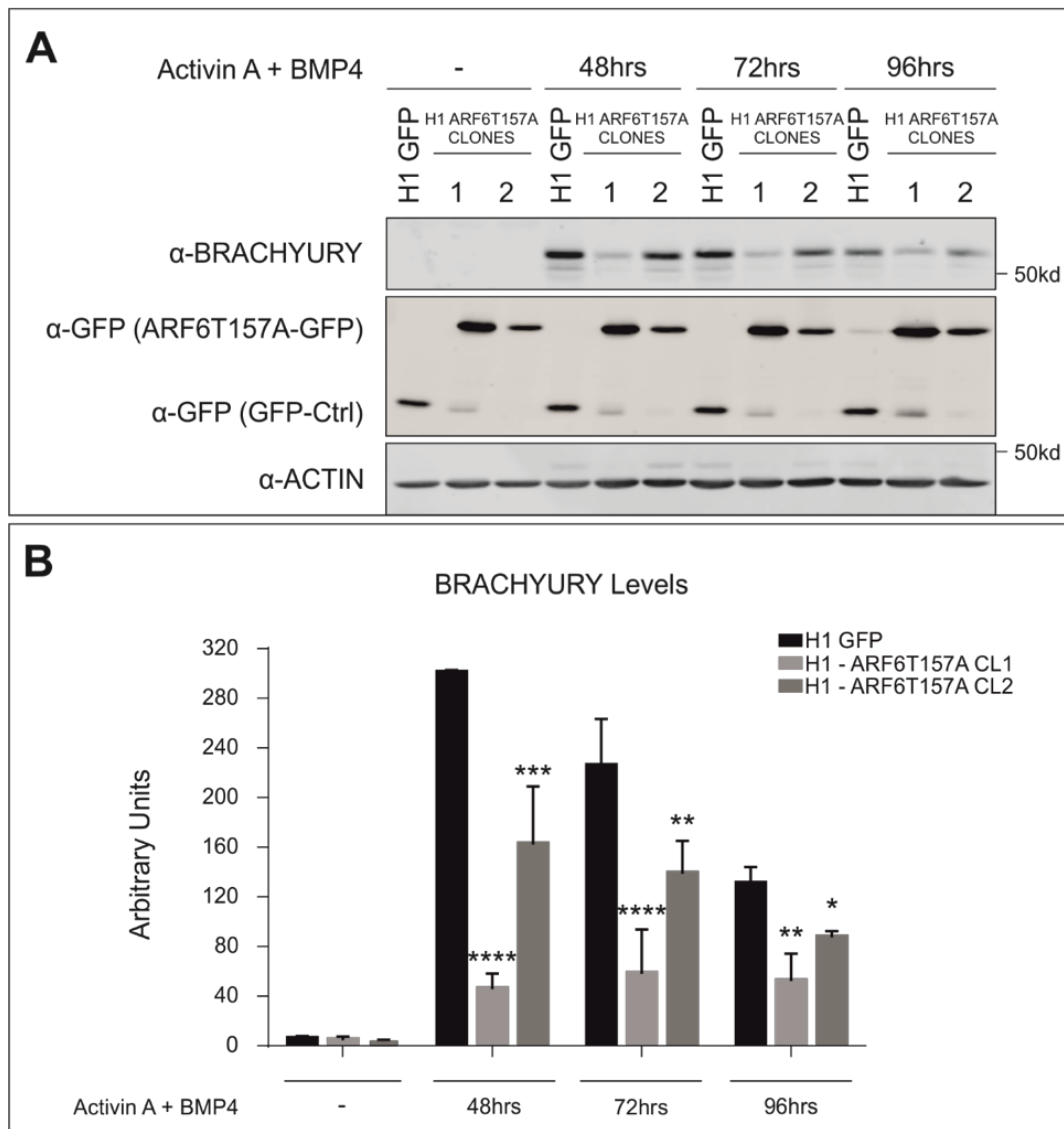
Figure 3.1: *Effect of ARF6 Activation on the Timing of BRACHYURY Expression upon Mesoderm Induction*. (A) Two H1 stable cell lines overexpressing the fast cycling form of ARF6 (ARF6T157A-GFP) were cultured to approximately 50% confluency. Differentiation to mesoderm was initiated by substituting mTeSR1 with a medium containing Activin A (50ng/mL) and BMP4 (50ng/mL). After 48, 72 and 96 hours cells were lysed using 1% SDS, subjected to SDS-PAGE and immunoblotted with an α-BRACHYURY antibody to investigate the effect of ARF6 activation in the expression levels of the mesodermal marker in a time dependent manner. (B) Changes in the expression levels of BRACHYURY in the presence of the fast cycling ARF6 mutant were assessed by densitometry using the Image Studio Lite software. Statistical significance was calculated in GraphPad Prism using the non-parametric Mann-Whitney test (N=3) (The above experiments were performed by Dr. Angelos Papadopoulos).

Figure 3.2: *Effect of ARF6 Knock-out on the Timing of BRACHYURY Expression upon Mesoderm Induction*. (A) Three H1 ARF6KO cell lines were cultured to approximately 50% confluency. Differentiation to mesoderm was initiated by substituting mTeSR1 with a medium containing Activin A (50ng/mL) and BMP4 (50ng/mL). After 48, 72 and 96 hours cells were lysed using 1% SDS, subjected to SDS-PAGE and immunoblotted with an α-BRACHYURY antibody to investigate the effect of ARF6 knock-out in the expression levels of the mesodermal marker in a time dependent manner. (B) Changes in the expression levels of BRACHYURY in the absence of ARF6 were assessed by densitometry using the Image Studio Lite software. Statistical significance was calculated in GraphPad Prism using the non-parametric Mann- Whitney test (N=3) (The above experiments were performed by Dr. Angelos Papadopoulos).

To ensure that the system was working properly in our hands we repeated the above experiment. We used the H1 ARF6 knock-out cell line (clone 5) and wild-type H1 wt cells cultured in mTeSR™Plus medium until they reached approximately 50% confluence. Cells were induced with BMP4 (50ng/mL) for 24 and 48 and 72 hours and lysates were analysed by western blotting with the outcome of differentiation being scored based on the expression levels of the early mesodermal marker BRACHYURY. The levels of BRACHYURY were normalised to endogenous h-GAPDH **Figure 3.3 (A)** (see alsp Supplementary Fig. 1). The results of the densitometry analysis demonstrated that BRACHYURY levels were increased in ARF6KO cells compared to H1 wt cells at both 24 (from 7 to 27 arbitrary units) and 48 hours (from 100 to 163 arbitrary units) following induction by BMP4 **Figure 3.3 (B)**. These results are in agreement with those obtained by Dr Angelos Papadopoulos, **Figure 3.2**.
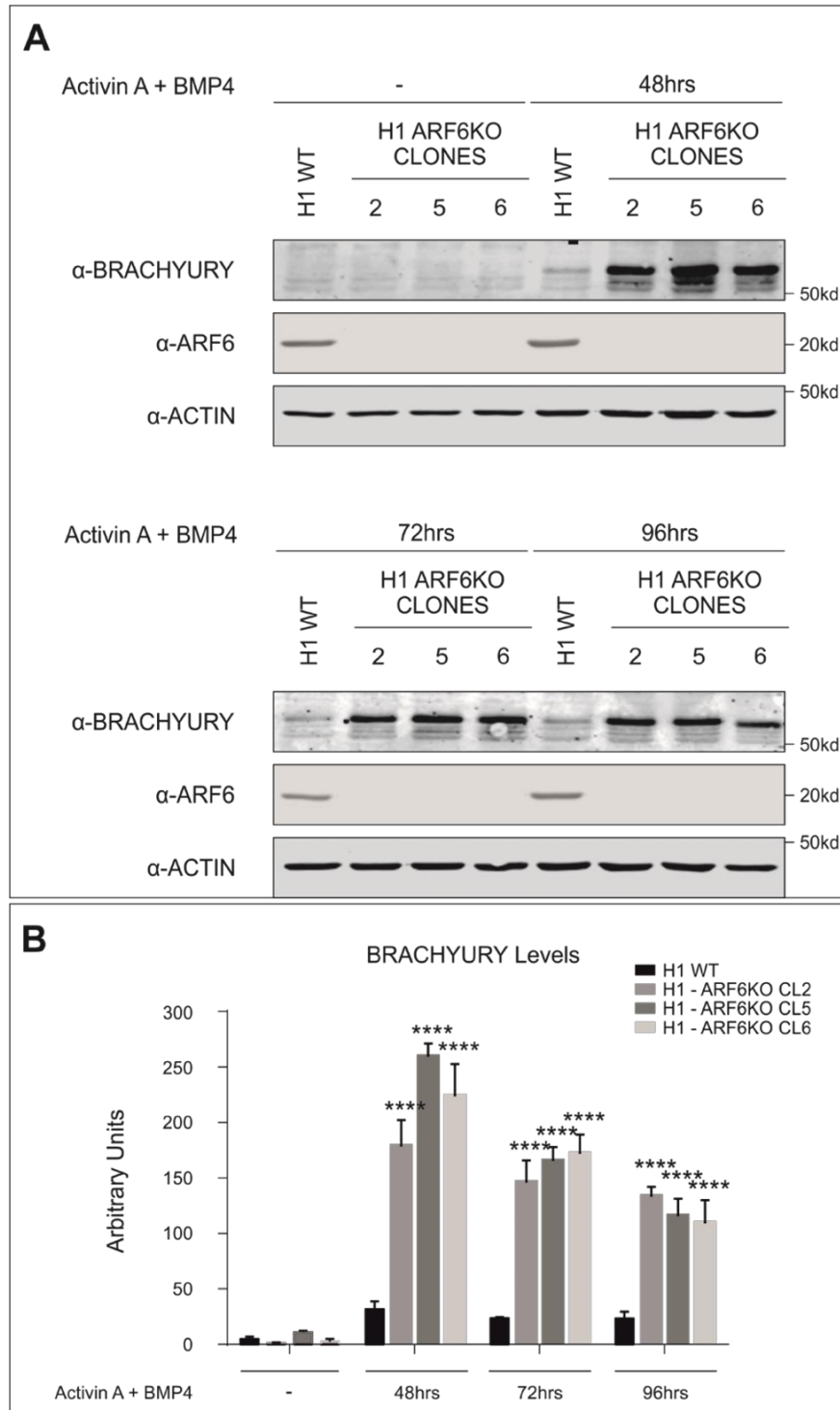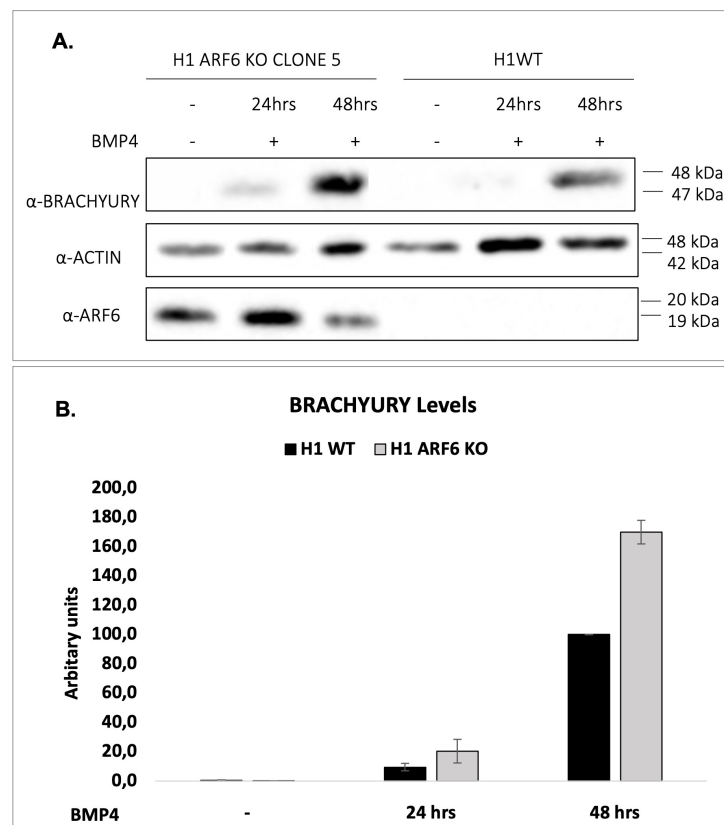

Figure 3.3: *Effect of ARF6 Knock-out on the Timing of BRACHYURY Expression upon Mesoderm Induction* A) H1 wt and H1 ARF6KO cells were cultured to approximately 50% confluency. Differentiation to mesoderm was initiated by substituting mTeSR™Plus with mTeSR™Plus containing BMP4 (50ng/mL). After 24 and 48 hours cells were lysed using 1% SDS, subjected to SDS-PAGE and immunoblotted with an α-BRACHYURY antibody to investigate the effect of ARF6 knock-out in the expression levels of the mesodermal marker in a time dependent manner. (B) Changes in the expression levels of BRACHYURY in the absence of the ARF6 were assessed by densitometry using the QuantityOne software. STDEV was calculated in excel using two independent experiments (N=2).

3.1.2. Mesodermal/ mesendodermal/ extra-embryonic endodermal/ extra-embryonic ectodermal markers are all increased in ARF6 KO hESCs upon induction with BMP4

Having shown, in agreement with the results of AP, that ARF6 KO increases the expression of BRACHYURY when compared to H1 wt cells upon induction with BMP4, we set out to investigate if this is specific for BRACHYURY or is rather a general effect on all BMP induced genes. To achieve this, H1 WT and H1 ARF6 KO cells were cultured in six-well plates and stimulated when 50% confluent with BMP4 (50ng/ml). RNA was extracted following induction with BMP4 at days 1, 2, 4 and 7 and used to check the levels of expression of several transcripts associated with differentiation (14). The transcripts tested can be categorised into three groups; the first group consists of PS and mesodermal genes (Mixl1, Wnt3 and GSC) and there was observed an upregulation of all genes in the ARF6 KO cell line, **Figure 3.4.A**. The second group contains Extraembryonic Endodermal transcripts (Gata6, Afp2), **Figure 3.4.B** and the third group consists of CDX2, a TE transcript, **Figure 3.4.C**. In H1 wt cells BMP4 induced the expression of the above transcripts in agreement with previous publications which suggest that BMP4 can induce both mesodermal and extra-embryonic markers in hESCs (11,14). In addition, we clearly show that BMP4 induction leads to an enhanced induction in the expression of the above transcripts in ARF6 KO compared to H1 wt cells, **Figure 3.4**. Therefore, we conclude that ARF6 KO increases the expression of BRACHYURY upon induction with BMP4 compared to H1 wt cells, and this is not specific for BRACHYURY but instead seems to be a general effect downstream of BMP4.
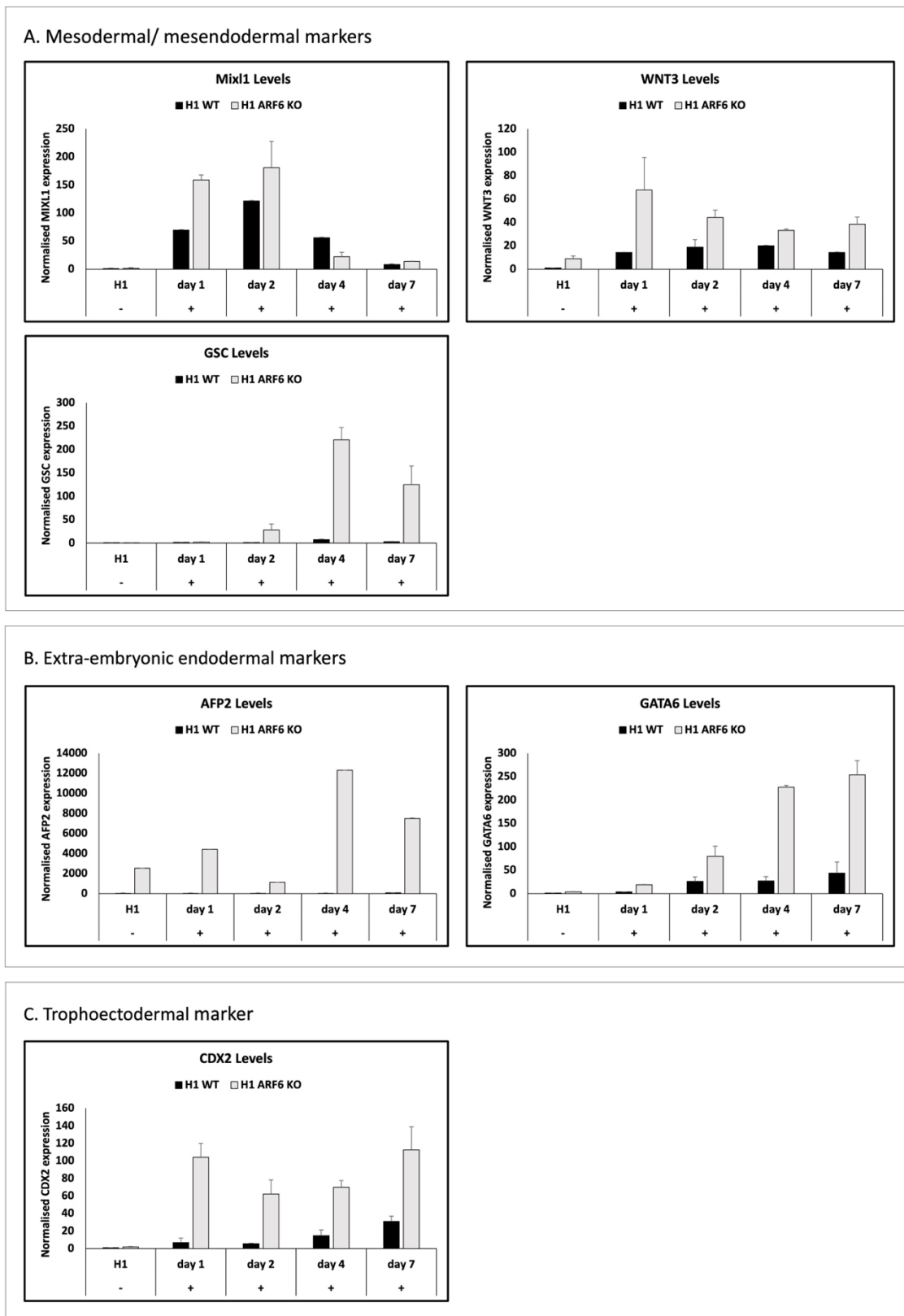
Figure 3.4: *Effect of ARF6 Knock-out on mesodermal/ mesendodermal/ extra-embryonic endodermal/ extra-embryonic ectodermal markers upon induction with BMP4*. H1WT cells and ARF6 KO cells were cells were cultured in six-well tissue culture plates with mTeSR™Plus to approximately 50% confluency. Then, they were induced with mTeSR™Plus containing BMP4 (50ng/ml) for 7 days. RNA was extracted and qRT-PCRs were performed in an AriaMx Real-Time PCR System. Data were analysed using AriaMx software and CT values were normalized against GAPDH (N=2).

3.2. ARF6 KO increases the expression of PAX6 neuroectodermal marker

In the above section we showed that ARF6 KO leads to an enhanced expression of BMP4 regulated transcripts compared to H1 wt cells. In order to address whether this effect was specific for BMP4, we differentiated ARF6 KO cells and H1 wt cells to neuroectoderm and analysed their response by visualising the level of PAX6, a classic neuroectodermal marker.

To differentiate the PSCs to neuroectoderm, we followed a published protocol which first generates embryoid bodies (EBs) and then on day 7 attaches the bodies to laminin coated dishes (for protocol see **Figure 3.5.A**. Both H1 wt and Arf6 KO cells formed EBs, however in the case of ARF6KO we noticed less and a little bit smaller embryoid bodies **Figure 3.5.B**. Following attachment of the EBs to laminin coated wells, the EBs differentiate to a population of neuroepithelial cells at day 10 which can be visualised by expression of neuroectoderm transcription factor PAX6 (176). We carried out confocal microscopy to detect PAX6 at day 10. As can be seen Pax6 is expressed and seemed similar in H1 wt and ARF6 KO, **Figure 3.6.B** – however it was difficult to quantitate efficiently the percentages of positive cells expressing the neuroectodermal marker PAX6, therefore we carried out western blot analysis to quantitate PAX6 levels, as shown in **Figure 3.7**. We then addressed whether the differentiation pattern was altered in the ARF6 KO cells.
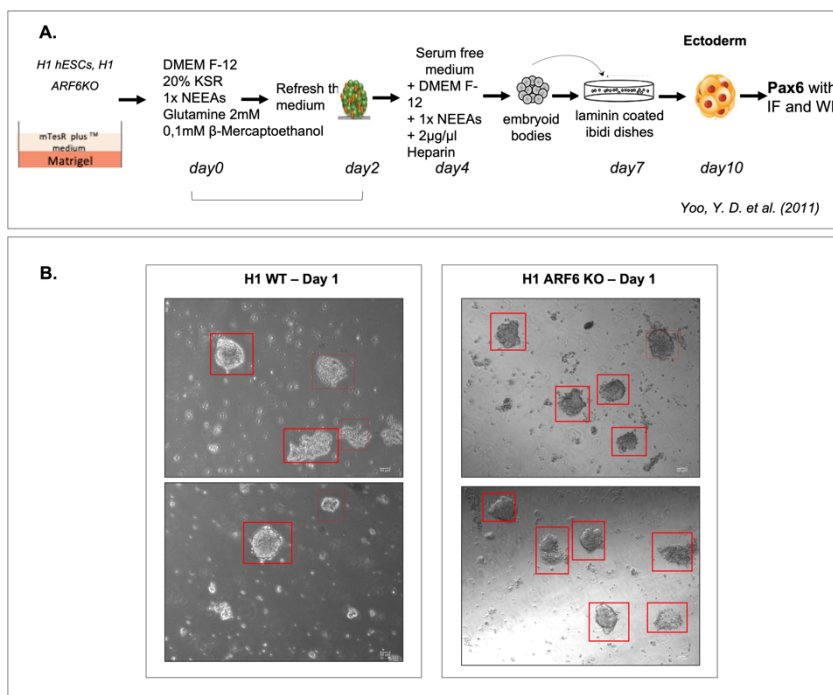
Figure 3.5: *Differentiation protocol to neuroectoderm*. For the neuroectodermal differentiation, H1 WT and H1 ARF6 KO cell lines were seeded on non adherent plates in a medium consisting of DMEM F-12, 20% KSR, 1X NEEAs, Glutamine (2mM), 0.1 mM β-mercaptoethanol. Suspension conditions enabled the folding of the colonies and the subsequent formation embryoid bodies. On the second day, medium was changed and on the 4th day the cell aggregates were transferred to a serum free medium containing DMEM F-12, 1X NEEAs, 2µg/µl Heparin. The embryoid bodies remained in suspension for 7 days post day 10 of differentiation.

A. *Differentiation protocol to neuroectoderm*

H1 hESCs, H1 ARF6KO

mTesR plus ™ medium

Matrigel

DMEM F-12
20% KSR
1x NEEAs
Glutamine 2mM
0,1mM β-Mercaptoethanol

Refresh the medium

Serum free medium
+ DMEM F-12
+ 1x NEEAs
+ 2µg/µl Heparin

embryoid bodies

laminin coated ibidi dishes

Ectoderm

Pax6 with IF and WB

day0   *day2*   *day4*   *day7*   *day10*

Yoo, Y. D. et al. (2011)

B.

Differentiation H1 wild type to neuroectoderm at day 10

Pax6 — Draq5 — Merge (20 µm)

C.

Differentiation H1 ARF6 KO to neuroectoderm at day 10

Pax6 — Draq5 — Merge (20 µm)

65

Figure 3.6: *Expression of neuroectodermal marker PAX6 in Wild type H1 cells and and H1 ARF6 KO cells*. The H1 Wild type cells (B) and the H1 ARF6 Knock-out cells (C) were cultured to approximately 80% confluency in six-well tissue culture plates coated with matrigel and mTeSR™Plus medium. Briefly, H1 colonies were detached with 1 mg/ml dispase and dissociated into small clumps. Neuroectodermal differentiation was initiated by growing the H1 clumps in suspension in non-adherent plates with the ESC growth medium consisting of Dulbecco's modified eagles medium (DMEM/F12), 20% Knockout replacement serum (KOSR), 0.1mM Non-Essential aminoacids, 2mM glutamine and 100µM β-mercaptoethanol to form embryoid bodies for 4 days. On day 4 of differentiation, the embryoid bodies were transferred to a serum-free minimal (SFM) medium consisting of DMEM/F12, 0.1mM Non Essential Aminoacids and 2 µg/ml heparin, and grown in suspension. After 3 days in suspension, on day 7, they were attached to laminin-coated ibidi dishes for immunostaining. On day-10 cells were harvested and fixed with PFA 3,7% and immunostained with primary antibody against PAX6 and Alexa Fluor® 594, TRITC labelled secondary antibody. PAX6 positive cells are shown in red panel, nuclei staining with Draq5 is shown in blue panel. Merge is presented in purple panel. All Images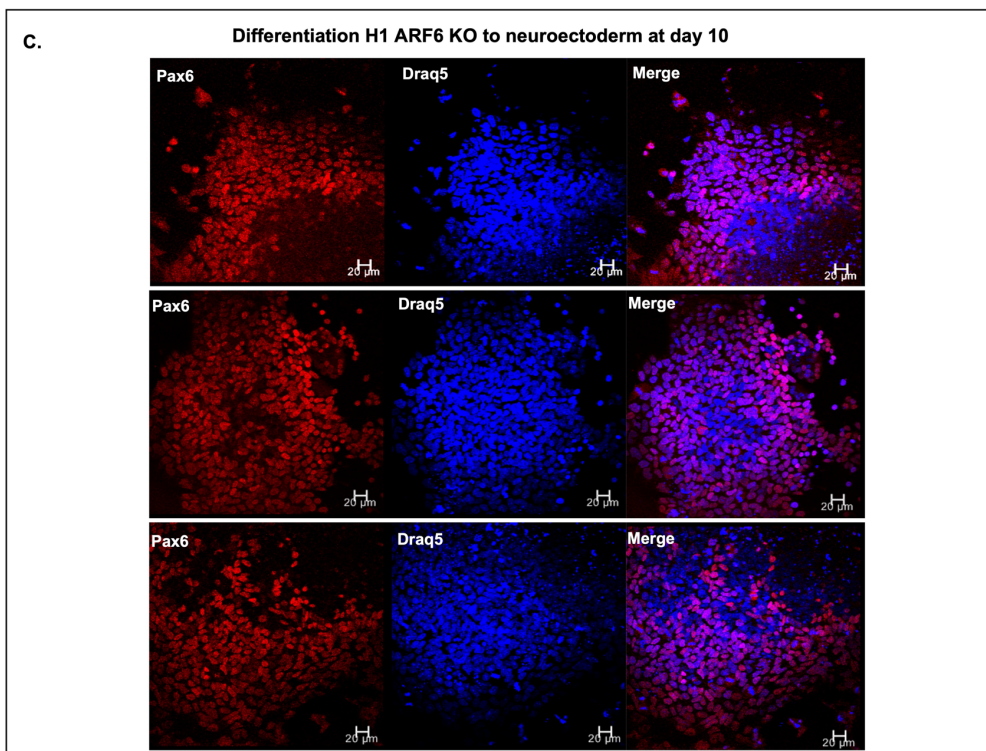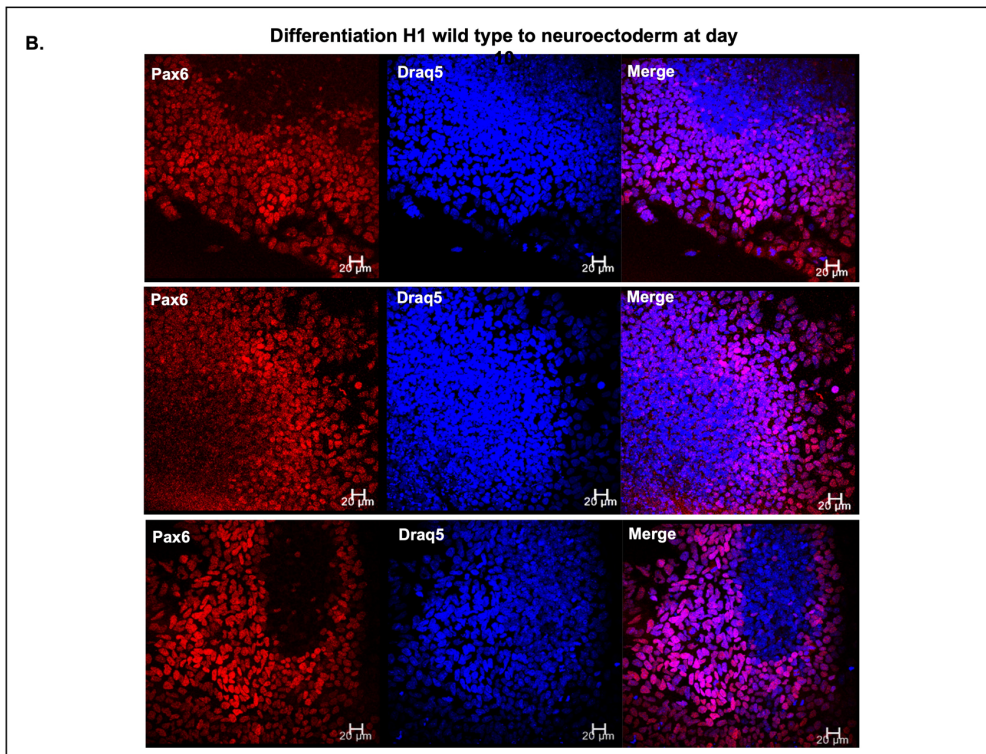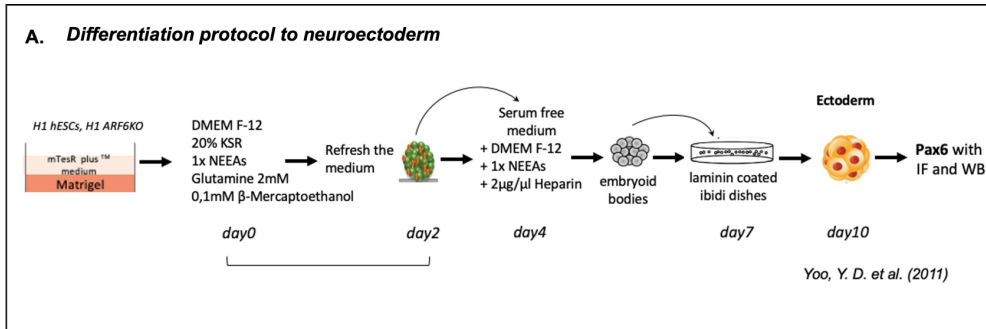 were obtained using a Leica SP8 Confocal Microscope and a 40X/1.30 NA objective. Scale bar size is 20µm. Images are maximum projections (N=3).

The levels of PAX6 were normalised to actin **Figure 3.7.A**. In control H1 cells upon differentiation to neuroectoderm, PAX6 expression was induced 1,96-fold, when in ARF6 KO cells the induction upon differentiation was 4,2-fold, **Figure 3.7.B**. At the end of differentiation to neuroectoderm, at day 10 comparing the ARF6 KO cells with the H1 wt cells were induced 2,14-fold. Therefore, the ARF6 KO leads to an enhanced expression of the characteristic neuroectodermal marker, PAX6 compared to H1 wt cells.
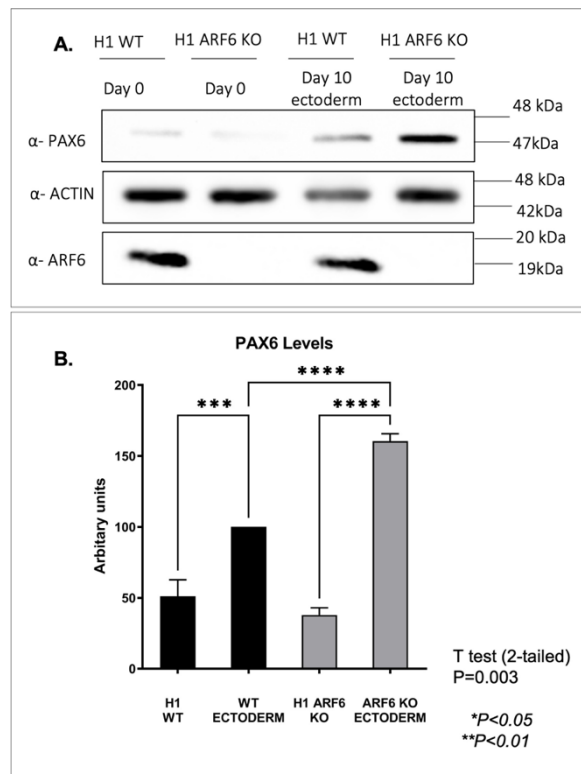
Figure 3.7: *Effect of ARF6 Knock-out on the PAX6 expression upon neuroectodermal induction*. H1 ARF6KO cells and H1 WT cells undifferentiated (day 0) and differentiated at day 10 were lysed using 1% SDS, subjected to SDS-PAGE and immunoblotted with an α-PAX6 antibody to investigate the effect of ARF6 knock-out in the expression levels of the neuroectodermal marker. (B) Changes in the expression levels of PAX6 in the absence of the ARF6 were assessed by densitometry using the QuantityOne software. Statistical significance was calculated in GraphPad Prism using the non-parametric One-Sample Test (N=3)

3.2.1. ARF6 FC has no effect on the expression of PAX6 neuroectodermal marker

In section 4.2. we demonstrated that ARF6 KO cell line increased the expression of PAX6 neuroectodermal marker under a chemically defined protocol of differentiation for 10 days compared to H1 wt cells. We further investigated the role of ARF6 in neuroectodermal differentiation using the fast cycling ARF6T157A and GFP control lines.

Confocal microscopy revealed PAX6 positive cells in both cell lines, indicative of neuroectodermal differentiation **Figure 3.9**. We also carried out western blot analysis of PAX6 expression levels normalized to actin to allow quantitation of the differentiation, as shown in **Figure 3.8**.
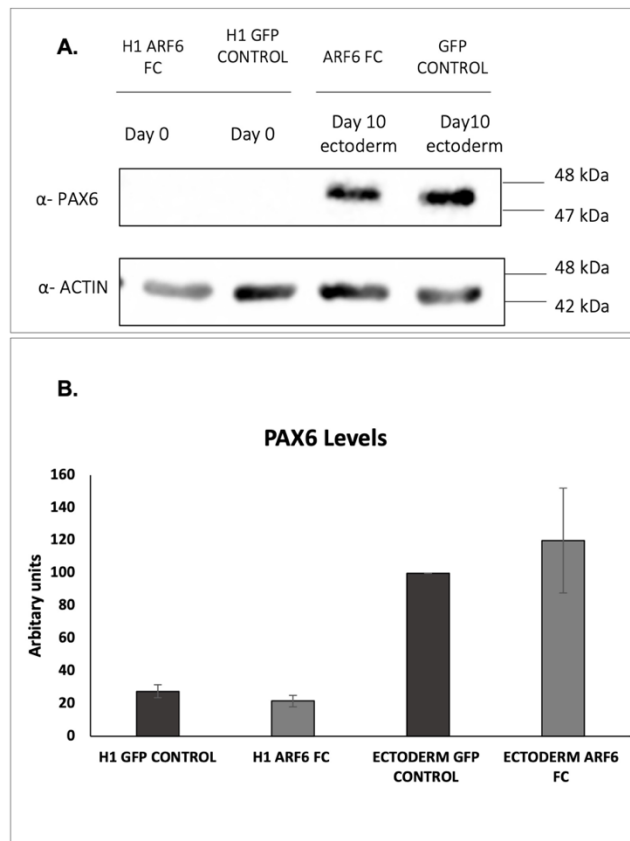
Figure 3.8: *Effect of ARF6 Activation on the PAX6 expression upon neuroectodermal induction*. A) H1 ARF6 FC cells (ARF6T157A-GFP) and H1 GFP control cells undifferentiated (day 0) and differentiated at day 10 were lysed using 1% SDS, subjected to SDS-PAGE and immunoblotted with an α-PAX6 antibody to investigate the effect of ARF6 fast cycling on the expression levels of the neuroectodermal marker. (B) Changes in the expression levels of PAX6 in the activated form of the ARF6 were assessed by densitometry using the QuantityOne software. STDV was calculated in excel using two independent experiments (N=2).

Densitometry demonstrated that PAX6 expression was induced 10,7 -fold in the GFP control cell line and 19 -fold in ARF6T157A cell line. **Figure 3.8 (B)**.

A. *Differentiation protocol to neuroectoderm*

H1 hESCs, H1 ARF6KO

mTesR plus ™ medium

Matrigel

→ DMEM F-12
20% KSR
1x NEEAs
Glutamine 2mM
0,1mM β-Mercaptoethanol

→ Refresh the medium

→ [embryoid bodies] → Serum free medium
+ DMEM F-12
+ 1x NEEAs
+ 2µg/µl Heparin

→ embryoid bodies → laminin coated ibidi dishes

→ **Ectoderm** → **Pax6** with IF and WB

day0   *day2*   *day4*   *day7*   *day10*

Yoo, Y. D. et al. (2011)

B.

GFP-control cells differentiated to neuroectoderm at day 10

C.

ARF6T157A-GFP cells differentiated to neuroectoderm at day 10

Figure 3.9: *Expression of neuroectodermal marker PAX6 in GFP control cells and H1-ARF6T157A-GFP cells.* The H1 stable cell line overexpressing GFP (A) and H1 stable cell line overexpressing the fast cycling form of ARF6 (ARF6T157A-GFP) (B) were cultured to approximately 80% confluency in six-well tissue culture plates coated with 69ormaliz and mTeSR™Plus medium. Briefly, H1 colonies were detached with 1 mg/ml dispase and dissociated into small clumps. Neuroectodermal differentiation was initiated by growing the H1 clumps in suspension in non-adherent plates with the ESC growth medium consisting of Dulbecco's modified eagles medium (DMEM/F12), 20% Knockout replacement serum (KOSR), 0.1mM Non-Essential Aminoacids, 2mM glutamine and 100μM β-mercapthoethanol to form embryoid bodies for 4 days. On day 4 of differentiation, the embryoid bodies were transferred to a serum-free minimal (SFM) medium consisting of DMEM/F12, 0.1mM Non Essential Aminoacids and 2 μg/ml heparin, and grown in suspension. After 3 days in suspension, on day 7, they were attached to laminin-coated ibidi dishes for immunostaining. On day-10 cells were harvested and fixed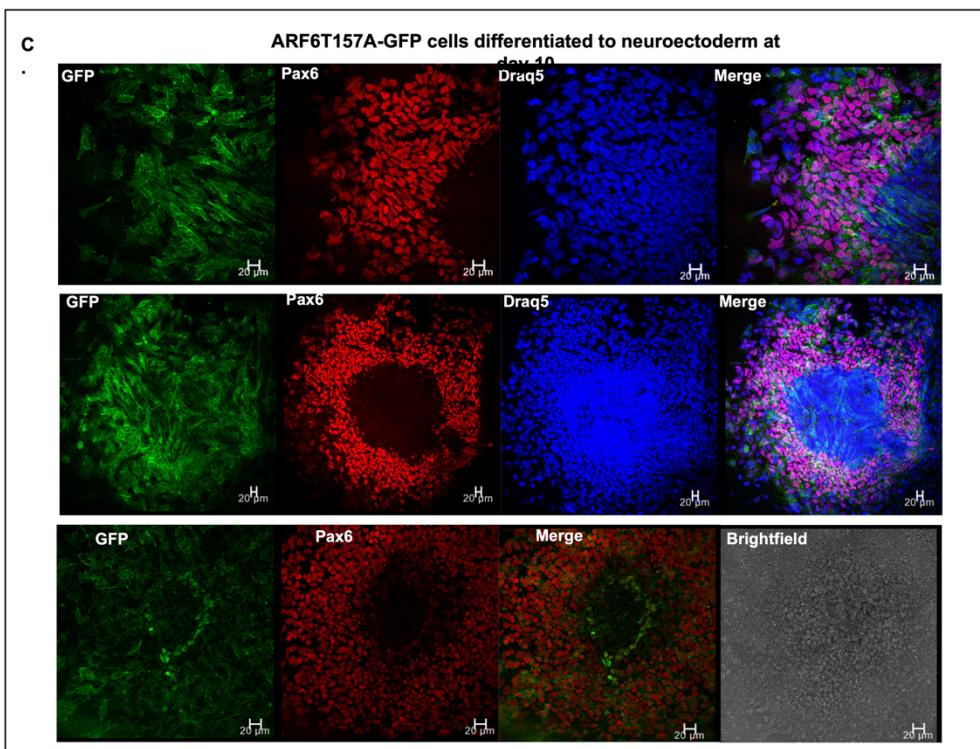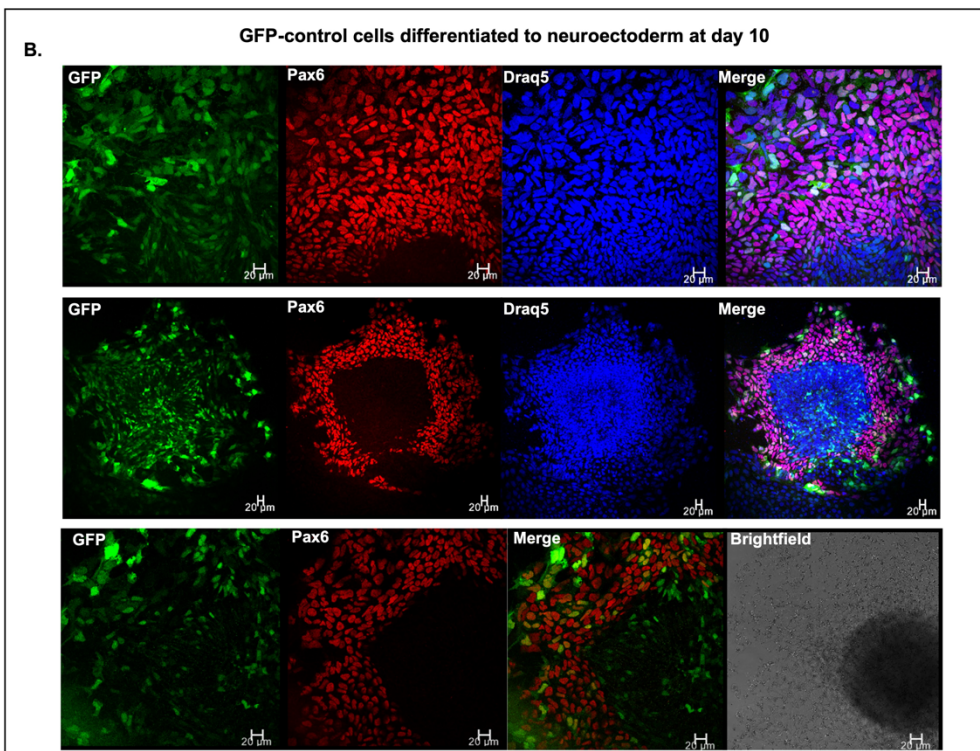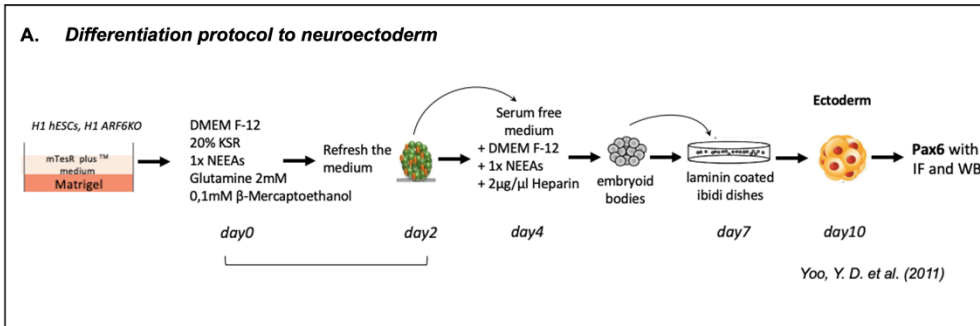 with PFA 3,7% and immunostained with primary antibody against PAX6 and Alexa Fluor® 594, TRITCH labelled secondary antibody. GFP positive cells are shown in green panel. PAX6 positive cells are shown in red panel, nuclei staining with Draq5 is shown in blue panel. Merge is presented in purple panel. All Images were obtained using a Leica SP8 Confocal Microscope and a 40X/1.30 NA objective. Scale bar size is 20μm. Images ae maximum projections (N=3).

In conclusion, activation of ARF6 using the ARF6T157A mutant, results in PAX6 expression upon neuroectodermal differentiation. The fold induction of PAX6 in the ARF6T157A mutant cell line was not statistically significantly different to that in GFP control H1 cell line. Therefore, ARF6T157A expression does not seem to affect the expression of PAX6 upon neuroectodermal differentiation. This experiment needs to repeat.

3.3. Endoderm differentiation is inhibited by ARF6

Previous experiments from our lab, conducted by Dr. Angelos Papadopoulos demonstrated that ARF6 KO reduced the activin A mediated SMAD2/3 phosphorylation in H1 cells. In order to address the impact of the phosphorylation of the R-SMADs in the absence of the GTPase, he used three independent H1 ARF6 knock-out clones, along with wild-type H1 control cells. Subsequently, the cells were serum starved for 4hrs in plain medium and induced with Activin A (50ng/mL) for 40min. The cell lysates were then analysed by western blotting using antibodies recognising the phosphorylated forms of SMAD2 and SMAD3 proteins. The total levels of SMAD2 and SMAD3 proteins remained the same after induction as revealed by probing with an antibody against total SMAD2/3. ACTIN served as a loading control **Figure 3.10 (A)**.

Densitometry analysis revealed that SMAD2 phosphorylation was reduced by 1.85-fold in ARF6KO clone 2, 1.4-fold in ARF6KO clone 5 and 1.2-fold in ARF6KO clone 6 **Figure 3.10 (B)**. In addition, SMAD3 phosphorylation was also reduced in all the clones by 3.5-fold, 3.1-fold and 3.4-fold, respectively **Figure 3.10 (C)**.

Taken together, these results indicate that knock-out of ARF6 in hES cells results in reduced phosphorylation levels of SMAD2 and SMAD3 upon activation with activin A.
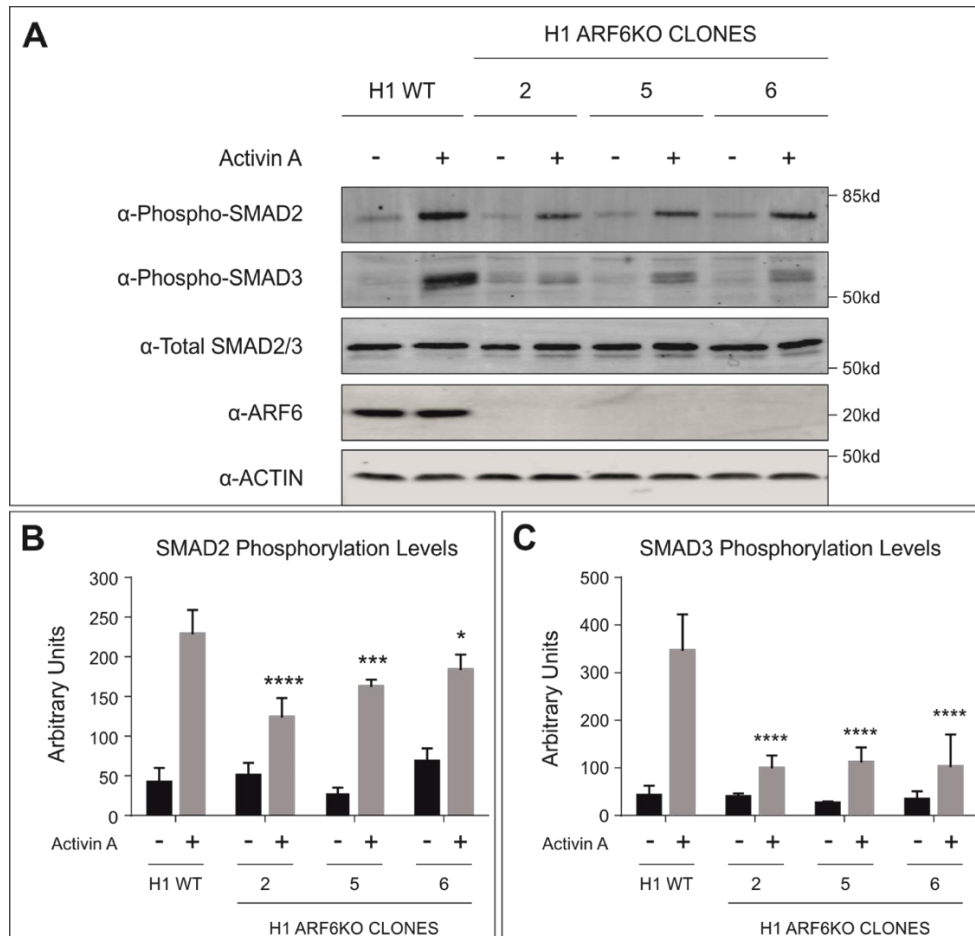
Figure 3.10: *ARF6 KO reduces the activin A mediated SMAD2/3 phosphorylation in H1 cells.* (A) Three H1 ARF6KO cell lines were cultured to approximately 50% confluency and subjected to 2hrs of growth factor starvation in minimal medium followed by induction with 50ng/ml Activin A. Cells were lysed using 1% SDS, subjected to SDS-PAGE and immunoblotted with α-pSMAD2 and α-pSMAD3 antibodies to check the effect of ARF6 knock-out in the Activin A mediated SMAD2/3 phosphorylation. Wild type H1 cells were used as a control. Changes in the phosphorylation levels of (B) SMAD2 and (C) SMAD3 in the absence of ARF6 were assessed by densitometry using the Image Studio Lite software. Statistical significance was calculated in GraphPad Prism using the non-parametric Mann-Whitney test (N=6) (The above experiments were performed by Dr. Angelos Papadopoulos).

Taking into consideration that ARF6 is implicated in the activin A induced phosphorylation of SMAD2/3 in H1 cells, that activin A is important for endoderm induction and the fact that the ablation of ARF6 is detrimental during liver formation in mice, we addressed the role of ARF6 during endoderm differentiation.

We set out to investigate if there is an effect in the absence of ARF6 during differentiation to definitive endoderm. To achieve this, H1 WT and H1 ARF6 KO cells were cultured in six-well plates and when 80% confluent were placed in RPMI medium containing 1% Glutamax, 0.5%

FBS, supplemented with Activin A (100ng/ml). Three days postinduction, the medium was refreshed using the same RPMI-based medium with 1% GlutaMax, 100 ng/ml activin A and 2% FBS. RNA was extracted following induction with Activin at days 5 and used to check the levels of expression of two characteristic endodermal markers, SOX17 and FOXA2. In H1 WT cells differentiated towards definitive endoderm, the characteristic endodermal markers, SOX17 and FOXA2 were induced, compared to undifferentiated pluripotent H1 WT and H1 ARF6 KO cells, as expected, **Figure 3.11**. However, in ARF6 KO cells, the levels of SOX17 and FOXA2 induced using the endodermal differentiation protocol were much lower than in the H1 wt cell line. The reduction in both SOX17 and FOXA2 markers is between 60 and 70%. We would now like to address whether the cell number or expression per cell is affected. In addition, this result will also be tested with other markers of endoderm induction, will be addressed in the ARF6 fast cycling hESC line. Due to the fact that endodermal markers are reduced we would also like to address whether downstream differentiation to hepatocytes is altered, as one might expect. In conclusion, our results suggest that ARF6 is required for expression of SOX17 and FOXA2 endodermal markers.
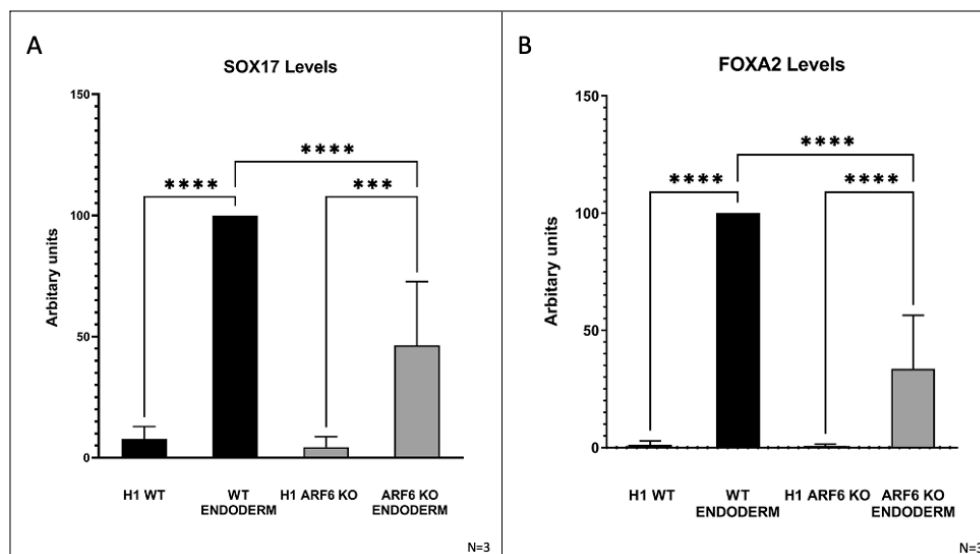
Figure 3.11: *ARF6 KO decreases the expression of SOX17 and FOXA2 endodermal markers*. H1 WT cells and ARF6 KO cells were cultured in six- well tissue culture plates with mTeSR™Plus to approximately 80% confluency. mTeSRbPlus was replaced with RPMI 1640 medium containing 1% GlutaMax, 0.5% defined FBS supplemented with activin A (100ng/ml). 3 days later, the medium was replaced with RPMI 1640 medium with 1% GlutaMax, 100ng/ml Activin A and 2% FBS. On day 5 of differentiation, RNA was extracted and qRT-PCRs for the characteristic endodermal markers SOX17 (A) and FOXA2 (B) were performed in an AriaMx Real-Time PCR System. Data were analysed using AriaMx software and CT values were normalized against GAPDH (N=3).

Chapter 4

Discussion

Previous unpublished results from our lab (by Dr Angelos Papadopoulos) have established that ARF6 is directly implicated in TGF- β and Activin A signalling. hESCs were generated either expressing a fast-cycling mutant of ARF6 or CRISPR-KO lines lacking the ARF6 protein. Using these 2 cell lines the experiments of AP led to the following conclusions: (1) Activin A or BMP4 induction in the presence of fast-cycling ARF6 leads to increased SMAD2/3 and SMAD1/5/9 phosphorylation, respectively. (2) Activin A or BMP4 induction in the absence of ARF6 leads to decreased SMAD2/3 and SMAD1/5/9 phosphorylation, respectively. (3) BRACHYURY expression is decreased during mesoderm formation in the presence of fast-cycling ARF6. (4) BRACHYURY expression is increased during mesoderm formation in the absence of ARF6, more cells are Brachyury positive suggesting an increased number of differentiating cells rather than enhanced expression per cell. (5) Activin A or BMP4 induction leads to ARF6 inactivation.

Mesodermal induction in ARF6 KO hESCs

The above findings opened many questions which we have addressed in the work presented in this Master's Thesis. The first question we asked was whether the effect of ARF6 was specific for Brachyury in mesoderm differentiation or indeed could ARF6 affect other markers of this differentiation lineage. Short-term BMP4 treatment is known to induce mesodermal progenitors in hESCs (195) including WNT3 and MIXL1. Therefore, we monitored the expression of both genes in hESCs with and without ARF6 following BMP4 induction. The expression levels of both WNT3 and MIXL1 were increased in ARF6 KO hESCs following BMP4 induction. This is similar to our observations in the case of Brachyury, therefore we conclude that ARF6KO cells have enhanced expression of mesodermal markers following BMP4 induction. As the mesodermal markers tested are induced by BMP4, and BMP4 signals through SMAD1/5/9, we had expected that the phosphorylation level of SMAD1/5/9 in ARF6KO cells would be enhanced compared to control hESCs, but this is not the case. Therefore, the mechanism involved remains under investigation and may involve WNT signalling.

BMP4 induction in hESCs is known to induce mesoderm, as stated above. However, mesendodermal cells have not been found (195). Mesendoderm is a rare population of cells present in the embryo only at gastrulation. This bipotent population gives rise to the mesoderm and the definitive endoderm and all mature cell types derived from these germ layers. GSC is a marker of mesendoderm and endoderm and is normally not induced by BMP4, however, ARF6 KO hESCs express GSC following BMP4 induction, while hESCs containing ARF6 do not. This finding will now be further investigated in the case of FOXA2, a marker of mesendoderm and endoderm, also not normally induced by BMP4. This indicates that in ARF6 KO cells BMP4 may be able to induce mesendoderm, however this finding needs to be supported by other lineage markers.

BMP4 induction for longer time periods induces the expression of extra-embryonic genes. These are characterised by CDX2, an early trophoectoderm marker (extra embryonic ectoderm) and early extra-embryonic endoderm marker GATA6. In addition, the expression of trophoblast markers hCG alpha and beta or the late extra-embryonic endoderm marker AFP2 were also induced at later time points. In the absence of ARF6 CDX2, GATA6 and AFP2 were all induced and their induction by BMP4 was strongly enhanced compared to hESCs harbouring ARF6.

Taking all the above results together, we can conclude that ARF6 KO hESCs respond to BMP4 induction and show an increased expression of mesodermal and extra-embryonic gene expression markers. Additionally, there may also be induction of mesendodermal gene expression (GSC), not normally seen following BMP4 induction under the experimental conditions used.

Ectodermal induction in ARF6 KO hESCs

We next asked whether the enhanced gene expression, in ARF6 KO hESCs, we witnessed in mesoderm induction was also present in other lineages, or was specific for mesoderm following BMP4 induction. Therefore, we differentiated ARF6 KO, ARF6 fast cycling and control hESCs to neuroectoderm and investigated the expression of PAX6, a neuroectodermal marker. From our results, we conclude that ARF6 KO enhances the induction of PAX6, by western blot analyses, and in agreement with our findings in mesodermal differentiation, it seems that

ARF6KO also results in enhanced differentiation to the ectodermal lineage. We are currently investigating whether more cells are PAX6 positive in ARF6KO hESCs or whether the expression of PAX6 per cell is enhanced. The effect of ARF6 fast cycling mutant in this system had no effect, we expected it to have the opposite effect to that of the ARF6KO line, as in the case of mesoderm induction. The reason we used the fast cycling ARF6 mutant and ARF6KO in all experiments was really to have an internal control for specificity. ARF6 was knocked out by CRISPR and one worries about off target effects. To control for that one can rescue the phenotype in the ARF6KO line by transfecting in ARF6 or generate an activated ARF6 cell line where the results can be validated (opposite effect). We chose the second option, reasoning that it would be difficult to obtain a rescued line with the same level of ARF6 as the endogenous. Therefore, in the case of ectodermal differentiation we will also repeat the experiment in a second independent ARF6KO hESC line.

Endoderm induction in ARF6 KO hESCs

Finally, we also addressed the role of ARF6 in differentiation to definite endoderm following a protocol requiring high levels of activin A (13). This differentiation protocol first yields definite endoderm which can then be further differentiated to hepatocytes or other endodermal derivatives. In contrast to the effect of ARF6KO in mesoderm and ectoderm, in the endodermal lineage ARF6KO proved inhibitory. The ARF6KO hESCs did not induce expression of SOX17 and FOXA2 endodermal markers to the level seen in hESCs harbouring ARF6 which showed robust induction, as expected (13). For endodermal differentiation, activin/Nodal signalling induces EOMES expression, which in turn cooperates directly with SMAD2/3 during in vitro DE differentiation in hESCs (196). Inhibition of Activin/Nodal signalling using an ALK4 inhibitor, SB431542, which in turn blocks SMAD2/3 phosphorylation, abolishes the expression of endodermal markers (196). We tested whether ARF6KO hESCs also causes decreased SMAD2/3 phosphorylation following activin A induction and indeed we found significant reduction in the level of pSMAD2/3. Therefore, it is possible that the reduced endodermal differentiation we observe is due to decreased activin A signalling in ARF6KO hESCs. We are currently investigating at which level ARF6 inhibits SMAD2/3 phosphorylation following activin A induction by addressing ligand uptake and receptor trafficking. Future plans include further

differentiation of the definite endodermal cells to hepatocytes to investigate the phenotype of the resulting cells.

Recently, Stepicheva and coworkers addressed the role of ARF6 during sea urchin morphogenesis. Among the defects observed perturbations in endodermal structures were observed, however endodermal specification was unaltered and the authors concluded that Arf6 may alter cadherin levels at the plasma membrane of endodermal cells that potentially impacts gastrulation and the morphology of the embryonic gut (197). Thus, it is likely that Arf6 impacts cells that undergo coordinated movement to form embryonic structures in the developing embryo. Their results differ from ours in that we do indeed see downregulation of endodermal markers in the absence of ARF6. It is difficult however to compare both systems. In vivo the differentiation to endoderm cannot be fully recapitulated in vitro – the in vitro hESC system allows one to address the induction of endodermal gene expression under controlled growth conditions, it does not take into consideration all the factors that come into play in the in vivo environment. Nevertheless, our results are exciting in the light of the findings that KO of ARF6 in mice is embryonic lethal and the results suggest that ARF6 is essential for liver development (7). In agreement, our results suggest that the early stages of endodermal differentiation are inhibited in the absence of ARF6 and our model can serve as a platform to address the molecular mechanisms involved. In addition, if definite endoderm specification is inhibited one might expect problems in other endodermal tissues including lung, pancreas, thyroid, and intestines. Suzuki and coworkers did not report alterations but it is likely that there are also changes in these cell types in the KO mice.

The mechanism of action of ARF6 in the 3 lineages, mesoderm, ectoderm and endoderm, is unlikely to be the same. ARF6 is involved in many processes but those likely to play a role in early differentiation are (1) growth factor receptor endocytosis and signalling output, including activin A and BMP and down stream pSMAD2/3 and 1/5/9 respectively (2) wnt signalling and/or (3) actin cytoskeletal effects. Regarding receptor endocytosis, ARF6 is known to play a role in the clathrin dependent and independent endocytosis, however trafficking pathways in pluripotent and differentiating cells differ from those in the mature differentiated cell types (198) and ARF6 has not been addressed under these conditions. In the case of WNT signalling, ARF6 has been shown to play a key role in differentiated cells

affecting E-cadherin recycling and altering adherens junctions as well as β-catenin abundance downstream of the Wnt signalling pathway (199,200). We have compared E-Cadherin levels in the ARF6KO hESCs and control hESCs and there is no difference in total E-cadherin, also the protein distribution on the plasma membrane seems comparable between both lines. However, we need to carefully address the E-cadherin distribution and downstream WNT signalling upon differentiation.

In conclusion, our results underline a key role for ARF6 in endoderm formation, perhaps related to the lower levels of pSMAD2/3 following activin A induction. In addition, ARF6 may control the level of mesoderm and ectodermal patterning programs, in both cases ARF6KO resulted in increased differentiation to both lineages. The mechanism behind this is currently under investigation.

References

1.   Schweitzer JK, Sedgwick AE, D'Souza-Schorey C. ARF6-mediated endocytic recycling impacts cell movement, cell division and lipid homeostasis. Semin Cell Dev Biol. 2011;22(1):39–47.

2.   D'Souza-Schorey C, Chavrier P. ARF proteins: Roles in membrane traffic and beyond. Nat Rev Mol Cell Biol. 2006 May;7(5):347–58.

3.   Aikawa Y, Martin T. ARF6 regulates a plasma membrane pool of phosphatidylinositol(4,5)bisphosphate required for regulated exocytosis. J Cell Biol. 2003 Sep 1;162:647–59.

4.   Balasubramanian N, Scott DW, Castle JD, Casanova JE, Schwartz MA. Arf6 and microtubules in adhesion-dependent trafficking of lipid rafts. Nat Cell Biol. 2007 Dec;9(12):1381–91.

5.   Schweitzer JK, D'Souza-Schorey C. Localization and Activation of the ARF6 GTPase during Cleavage Furrow Ingression and Cytokinesis*. Journal of Biological Chemistry [Internet]. 2002;277(30):27210–6. Available from: https://www.sciencedirect.com/science/article/pii/S0021925818600687

6.   Naslavsky N, Weigert R, Donaldson JG. Characterization of a nonclathrin endocytic pathway: Membrane cargo and lipid requirements. Mol Biol Cell. 2004 Aug;15(8):3542–52.

7.   Suzuki T, Kanai Y, Hara T, Sasaki J, Sasaki T, Kohara M, et al. Crucial Role of the Small GTPase ARF6 in Hepatic Cord Formation during Liver Development. Mol Cell Biol. 2006;26(16):6149.

8.   Vallier L, Alexander M, Pedersen RA. Activin/Nodal and FGF pathways cooperate to maintain pluripotency of human embryonic stem cells. J Cell Sci. 2005 Oct;118(Pt 19):4495–509.

9.   James D, Levine AJ, Besser D, Hemmati-Brivanlou A. TGFβ/activin/nodal signaling is necessary for the maintenance of pluripotency in human embryonic stem cells. Development. 2005 Mar;132(6):1273–82.

10. Nakao A, Imamura T, Souchelnytskyi S, Kawabata M, Ishisaki A, Oeda E, et al. TGF-beta receptor-mediated signalling through Smad2, Smad3 and Smad4. EMBO J. 1997 Sep;16(17):5353–62.

11. Xu RH, Chen X, Li DS, Li R, Addicks GC, Glennon C, et al. BMP4 initiates human embryonic stem cell differentiation to trophoblast. Nat Biotechnol [Internet]. 2002 Jun 13;20:1261+. Available from: https://link.gale.com/apps/doc/A621867819/HRCA?u=googlescholar&sid=googleScholar&xid=86ee6ed4

12. Yoo YD, Huang CT, Zhang X, Lavaute TM, Zhang SC. Fibroblast growth factor regulates human neuroectoderm specification through ERK1/2-PARP-1 pathway. Stem Cells. 2011;29(12):1975–82.

13. Agarwal S, Holton KL, Lanza R. Efficient Differentiation of Functional Hepatocytes from Human Embryonic Stem Cells. Stem Cells. 2008;26(5):1117–27.

14. Zhang P, Li J, Tan Z, Wang C, Liu T, Chen L, et al. Short-term BMP-4 treatment initiates mesoderm induction in human embryonic stem cells. Blood. 2008;111(4):1933–41.

15. Vallier L, Mendjan S, Brown S, Ching Z, Teo A, Smithers LE, et al. Activin/Nodal signalling maintains pluripotency by controlling Nanog expression. Development. 2009;136(8):1339–49.

16. Chavrier P, Goud B. The role of ARF and Rab GTPases in membrane transport. Curr Opin Cell Biol [Internet]. 1999;11(4):466–75. Available from: http://www.sciencedirect.com/science/article/pii/S0955067499800672

17. Gillingham AK, Munro S. The Small G Proteins of the Arf Family and Their Regulators. Annu Rev Cell Dev Biol. 2007;23:579–611.

18. D'Souza-Schorey C, Chavrier P. ARF proteins: Roles in membrane traffic and beyond. Nat Rev Mol Cell Biol. 2006;7(5):347–58.

19. Kahn RA, Gilman AG. The protein cofactor necessary for ADP-ribosylation of G(s) by cholera toxin is itself a GTP binding protein. Journal of Biological Chemistry. 1986;261(17):7906–7911.

20. Kahn RA, Gilman AG. Purification of a protein cofactor required for ADP-ribosylation of the stimulatory regulatory component of adenylate cyclase by cholera toxin. J Biol Chem. 1984 May;259(10):6228–34.

21. Moss J, Vaughan M. Structure and function of ARF proteins. Activators of cholera toxin and critical components of intracellular vesicular transport processes. Journal of Biological Chemistry. 1995;270(21):12327–30.

22. Cockcroft S, Thomas GMH, Fensome A, Geny B, Cunningham E, Gout I, et al. Phospholipase D: A downstream effector of ARF in granulocytes. Science (1979). 1994;263(5146):523–6.

23. Brown HA, Gutowski S, Moomaw CR, Slaughter C, Sternwels PC. ADP-ribosylation factor, a small GTP-dependent regulatory protein, stimulates phospholipase D activity. Cell. 1993;75(6):1137–44.

24. Ktistakis NT, Brown HA, Waters MG, Sternweis PC, Roth MG. Evidence that phospholipase D mediates ADP ribosylation factor-dependent formation of Golgi coated vesicles. Journal of Cell Biology. 1996;134(2):295.

25. Massenburg D, Han JS, Liyanage M, Patton WA, Rhee SG, Moss J, et al. Activation of rat brain phospholipase D by ADP-ribosylation factors 1, 5, and 6: Separation of ADP-ribosylation factor-dependent and oleate-dependent enzymes. Proc Natl Acad Sci U S A. 1994;91(24):11718–22.

26.   Hammond SM, Altshuller YM, Sung TC, Rudge SA, Rose K, Engebrecht JA, et al. Human ADP-ribosylation factor-activated phosphatidylcholine-specific phospholipase D defines a new and highly conserved gene family. Journal of Biological Chemistry. 1995;270(50):29640–3.

27.   Donaldson JG, Jackson CL. ARF family G proteins and their regulators: Roles in membrane transport, development and disease. Nat Rev Mol Cell Biol. 2011;12(6):362–75.

28.   Tsuchiya M, Price SR, Tsai SC, Moss J, Vaughan M. Molecular identification of ADP-ribosylation factor mRNAs and their expression in mammalian cells. Journal of Biological Chemistry. 1991;266(5):2772–7.

29.   Bonifacino JS, Glick BS. The Mechanisms of Vesicle Budding and Fusion. Cell. 2004;116(2):153–66.

30.   Gillingham AK, Munro S. The small G proteins of the Arf family and their regulators. Annu Rev Cell Dev Biol. 2007;23:579–611.

31.   Balasubramanian N, Scott DW, Castle JD, Casanova JE, Schwartz MA. Arf6 and microtubules in adhesion-dependent trafficking of lipid rafts. Nat Cell Biol. 2007;9(12):1381–91.

32.   Moss J, Vaughan M. Structure and function of ARF proteins. Activators of cholera toxin and critical components of intracellular vesicular transport processes. Journal of Biological Chemistry [Internet]. 1995 May 26 [cited 2023 Jan 4];270(21):12327–30. Available from: http://www.jbc.org/article/S0021925817496761/fulltext

33.   Acker T Van, Tavernier J, Peelman F. The small GTPase Arf6: An overview of its mechanisms of action and of its role in host- pathogen interactions and innate immunity. Int J Mol Sci. 2019;20(9).

34. Cherfils J, Zeghouf M. Regulation of small GTPases by GEFs, GAPs, and GDIs. Physiol Rev. 2013;93(1):269–309.

35. Chen EH, Pryce BA, Tzeng JA, Gonzalez GA, Olson EN. Control of myoblast fusion by a guanine nucleotide exchange factor, loner, and its effector ARF6. Cell. 2003;114(6):751–62.

36. Önel S, Bolke L, Klämbt C. The Drosophila ARF6-GEF schizo controls commissure formation by regulating slit. Development. 2004;131(11):2587–94.

37. Hongu T, Funakoshi Y, Fukuhara S, Suzuki T, Sakimoto S, Takakura N, et al. Arf6 regulates tumour angiogenesis and growth through HGF-induced endothelial β1 integrin recycling. Nat Commun. 2015;6(1):1–12.

38. Pasqualato S, Ménétrey J, Franco M, Cherfils J. The structural GDP/GTP cycle of human Arf6. EMBO Rep. 2001 Mar;2(3):234–8.

39. Ménétrey J, Macia E, Pasqualato S, Franco M, Cherfils J. Structure of Arf6-GDP suggests a basis for guanine nucleotide exchange factors specificity. Nat Struct Biol. 2000;7(6):466–9.

40. Antonny B, Beraud-Dufour S, Chardin P, Chabre M. N-terminal hydrophobic residues of the G-protein ADP-ribosylation factor-1 insert into membrane phospholipids upon GDP to GTP exchange. Biochemistry. 1997;36(15):4675–84.

41. Pasqualato S, Renault L, Cherfils J. Arf, Arl, Arp and Sar proteins: A family of GTP-binding proteins with a structural device for "front-back" communication. EMBO Rep. 2002;3(11):1035.

42. D'Souza-Schorey C, Li G, Colombo MI, Stahl PD. A regulatory role for ARF6 in receptor-mediated endocytosis. Science (1979). 1995;267(5201):1175–8.

43. Santy LC. Characterization of a fast cycling ADP-ribosylation factor 6 mutant. Journal of Biological Chemistry. 2002;277(43):40185–8.

44. Hongu T, Kanaho Y. Activation machinery of the small GTPase Arf6. Adv Biol Regul. 2014;54(1):59–66.

45. Cherfils J, Zeghouf M. Regulation of small GTPases by GEFs, GAPs, and GDIs. Physiol Rev. 2013;93(1):269–309.

46. Casanova JE. Regulation of Arf activation: The Sec7 family of guanine nucleotide exchange factors. Traffic. 2007;8(11):1476–85.

47. Laroche G, Giguère PM, Dupré E, Dupuis G, Parent JL. The N-terminal coiled-coil domain of the cytohesin/ARNO family of guanine nucleotide exchange factors interacts with Galphaq. Mol Cell Biochem. 2007 Dec;306(1–2):141–52.

48. Cox R, Mason-Gamer RJ, Jackson CL, Segev N. Phylogenetic Analysis of Sec7-Domain-containing Arf Nucleotide Exchangers. Mol Biol Cell. 2004;15(4):1487.

49. Paris S, Béraud-Dufour S, Robineau S, Bigay J, Antonny B, Chabre M, et al. Role of protein-phospholipid interactions in the activation of ARF1 by the guanine nucleotide exchange factor Arno. Journal of Biological Chemistry. 1997;272(35):22221–6.

50. Jackson TR, Kearns BG, Theibert AB. Cytohesins and centaurins: Mediators of PI 3-kinase-regulated Arf signaling. Trends Biochem Sci. 2000;25(10):489–95.

51. Klarlund JK, Guilherme A, Holik JJ, Virbasius J v., Chawla A, Czech MP. Signaling by phosphoinositide-3,4,5-trisphosphate through proteins containing pleckstrin and sec7 homology domains. Science (1979). 1997;275(5308):1927–30.

52. Li HS, Shome K, Rojas R, Rizzo MA, Vasudevan C, Fluharty E, et al. The guanine nucleotide exchange factor ARNO mediates the activation of ARF and phospholipase D by insulin. BMC Cell Biol. 2003;4(1):1–10.

53. Goldberg J. Structural and functional analysis of the ARF1-aRFGAP complex reveals a role for coatomer in GTP hydrolysis. Cell. 1999;96(6):893–902.

54. Inoue H, Randazzo PA. Arf GAPs and their interacting proteins. Traffic. 2007;8(11):1465–75.

55. Randazzo PA, Hirsch DS. Arf GAPs: Multifunctional proteins that regulate membrane traffic and actin remodelling. Cell Signal. 2004;16(4):401–13.

56. Spang A, Shiba Y, Randazzo PA. Arf GAPs: Gatekeepers of vesicle generation. FEBS Lett. 2010;584(12):2646–51.

57. Vitali T, Girald-Berlingeri S, Randazzo PA, Chen PW. Arf GAPs: A family of proteins with disparate functions that converge on a common structure, the integrin adhesion complex. Small GTPases. 2019;10(4):280.

58. Nie Z, Randazzo PA. Arf GAPs and membrane traffic. J Cell Sci. 2006;119(7):1203–11.

59. Bai M, Gad H, Turacchio G, Cocucci E, Yang JS, Li J, et al. ARFGAP1 promotes AP-2-dependent endocytosis. Nat Cell Biol. 2011;13(5):559–67.

60. Venkateswarlu K, Brandom KG, Lawrence JL. Centaurin-α1 Is an in Vivo Phosphatidylinositol 3,4,5-Trisphosphate-dependent GTPase-activating Protein for ARF6 That Is Involved in Actin Cytoskeleton Organization. Journal of Biological Chemistry. 2004;279(8):6205–8.

61. Shu Q, Lennemann NJ, Sarkar SN, Sadovsky Y, Coyne CB. ADAP2 Is an Interferon Stimulated Gene That Restricts RNA Virus Entry. PLoS Pathog. 2015;11(9):e1005150.

62. Vitale N, Patton WA, Moss J, Vaughan M, Lefkowitz RJ, Premont RT. GIT proteins, a novel family of phosphatidylinositol 3,4,5- trisphosphate-stimulated GTPase-activating proteins for ARF6. Journal of Biological Chemistry. 2000;275(18):13901–6.

63. Casalou C, Ferreira A, Barral DC. The Role of ARF Family Proteins and Their Regulators and Effectors in Cancer Progression: A Therapeutic Perspective. Front Cell Dev Biol. 2020;8:217.

64. Yoo SM, Antonyak MA, Cerione RA. The adaptor protein and Arf GTPase-activating protein Cat-1/Git-1 is required for cellular transformation. J Biol Chem. 2012 Sep;287(37):31462–70.

65. Huang WC, Chan SH, Jang TH, Chang JW, Ko YC, Yen TC, et al. MiRNA-491-5p and GIT1 serve as modulators and biomarkers for oral squamous cell carcinoma invasion and metastasis. Cancer Res. 2014;275(18):13901–6.

66. Chan SH, Huang WC, Chang JW, Chang KJ, Kuo WH, Wang MY, et al. MicroRNA-149 targets GIT1 to suppress integrin signaling and breast cancer metastasis. Oncogene. 2014;33(36):4496.

67. Peng H, Dara L, Li TWH, Zheng Y, Yang H, Tomasi ML, et al. MAT2B-GIT1 interplay activates MEK1/ERK 1 and 2 to induce growth in human liver and colon cancer. Hepatology. 2013 Jun;57(6):2299–313.

68. Premont RT, Claing A, Vitale N, Freeman JLR, Pitcher JA, Patton WA, et al. β2-Adrenergic receptor regulation by GIT1, a G protein-coupled receptor kinase-associated ADP ribosylation factor GTPase-activating protein. Proc Natl Acad Sci U S A. 1998;95(24):14082–7.

69. Chen PW, Jian X, Yoon HY, Randazzo PA. ARAP2 signals through arf6 and rac1 to control focal adhesion morphology. Journal of Biological Chemistry. 2013;288(8):5849.

70. Krugmann S, Andrews S, Stephens L, Hawkins PT. ARAP3 is essential for formation of lamellipodia after growth factor stimulation. J Cell Sci. 2006;119(3):425–32.

71. Tamaddon-Jahromi S, Kanamarlapudi V. ADP-Ribosylation Factor-6 (ARF6). In: Encyclopedia of Signaling Molecules. 2018. p. 230–8.

72. Schweitzer JK, Sedgwick AE, D'Souza-Schorey C. ARF6-mediated endocytic recycling impacts cell movement, cell division and lipid homeostasis. Semin Cell Dev Biol. 2011;22(1):39.

73. Palacios F, Schweitzer JK, Boshans RL, D'Souza-Schorey C. ARF6-GTP recruits Nm23-H1 to facilitate dynamin-mediated endocytosis during adherens junctions disassembly. Nat Cell Biol. 2002;4(12):929–36.

74. Pellon-Cardenas O, Clancy J, Uwimpuhwe H, D'Souza-Schorey C. ARF6-Regulated Endocytosis of Growth Factor Receptors Links Cadherin-Based Adhesion to Canonical Wnt Signaling in Epithelia. Mol Cell Biol. 2013;33(15):2963–75.

75. Hyman T, Shmuel M, Altschuler Y. Actin is required for endocytosis at the apical surface of Madin-Darby canine kidney cells where ARF6 and clathrin regulate the actin cytoskeleton. Mol Biol Cell. 2006;17(1):427.

76. Franco M, Peters PJ, Boretto J, van Donselaar E, Neri A, D'Souza-Schorey C, et al. EFA6, a sec7 domain-containing exchange factor for ARF6, coordinates membrane recycling and actin cytoskeleton organization. EMBO Journal. 1999;18(6):1480–91.

77. Wenk MR, de Camilli P. Protein-lipid interactions and phosphoinositide metabolism in membrane traffic: Insights from vesicle recycling in nerve terminals. Proc Natl Acad Sci U S A. 2004;101(22):8262.

78. Naslavsky N, Weigert R, Donaldson JG. Characterization of a nonclathrin endocytic pathway: Membrane cargo and lipid requirements. Mol Biol Cell. 2004;15(8):3542.

79. Donaldson JG. Multiple Roles for Arf6: Sorting, Structuring, and Signaling at the Plasma Membrane. Journal of Biological Chemistry. 2003;278(43):41573–6.

80. Brown FD, Rozelle AL, Yin HL, Balla T, Donaldson JG. Phosphatidylinositol 4,5-bisphosphate and Arf6-regulated membrane traffic. Journal of Cell Biology. 2001;

81. Robertson SE, Setty SRG, Sitaram A, Marks MS, Lewis RE, Chou MM. Extracellular signal-regulated kinase regulates clathrin-independent endosomal trafficking. Mol Biol Cell. 2006;17(2):645–57.

82. Jovanovic OA, Brown FD, Donaldson JG. An effector domain mutant of Arf6 implicates phospholipase D in endosomal membrane recycling. Mol Biol Cell. 2006;17(1):327.

83. Zimmermann P, Zhang Z, Degeest G, Mortier E, Leenaerts I, Coomans C, et al. Syndecan recyling is controlled by syntenin-PIP2 interaction and Arf6. Dev Cell. 2005;9(3):377–88.

84. DOBZHANSKY T. BIOLOGY, MOLECULAR AND ORGANISMIC. Am Zool. 1964 Nov;4:443–52.

85. Kolios G, Moodley Y. Introduction to stem cells and regenerative medicine. Respiration. 2012;85(1):3–10.

86. Chakraborty C, Agoramoorthy G. Stem cells in the light of evolution. Indian Journal of Medical Research. 2012;135(6):813–9.

87. Chagastelles PC, Nardi NB. Biology of stem cells: An overview. Kidney Int Suppl (2011). 2011;1(3):63–7.

88. Ramalho-Santos M, Willenbring H. On the origin of the term "stem cell". Cell Stem Cell. 2007 Jun;1(1):35–8.

89. Weger M, Diotel N, Dorsemans AC, Dickmeis T, Weger BD. Stem cells and the circadian clock. Dev Biol [Internet]. 2017;431(2):111–23. Available from: http://dx.doi.org/10.1016/j.ydbio.2017.09.012

90. Condic ML. Totipotency: What it is and what it is not. Stem Cells Dev. 2014;23(8):796–812.

91.   Kfoury Y, Scadden DT. Mesenchymal cell contributions to the stem cell niche. Cell Stem Cell [Internet]. 2015;16(3):239–53. Available from: http://dx.doi.org/10.1016/j.stem.2015.02.019

92.   Augello A, Kurth TB, de Bari C. Mesenchymal stem cells: a perspective from in vitro cultures to in vivo migration and niches. Eur Cell Mater. 2010 Sep;20:121–33.

93.   Wobus AM, Boheler KR. Embryonic stem cells: Prospects for developmental biology and cell therapy. Physiol Rev. 2005;85(2):635–78.

94.   Ratajczak MZ, Zuba-Surma E, Kucia M, Poniewierska A, Suszynska M, Ratajczak J. Pluripotent and multipotent stem cells in adult tissues. Adv Med Sci. 2012 Jun;57(1):1–17.

95.   Pietras EM, Warr MR, Passegué E. Cell cycle regulation in hematopoietic stem cells. Journal of Cell Biology. 2011;195(5):709–20.

96.   Bentzinger CF, Wang YX, von Maltzahn J, Rudnicki MA. The emerging biology of muscle stem cells: Implications for cell-based therapies. BioEssays. 2013;35(3):231–41.

97.   Ilic D, Polak JM. Stem cells in regenerative medicine: Introduction: Br Med Bull. 2011;98(1):117–26.

98.   Montagnani S, Rueger MA, Hosoda T, Nurzynska D. Adult Stem Cells in Tissue Maintenance and Regeneration. Stem Cells Int. 2016;2016.

99.   Wong CC, Loewke KE, Bossert NL, Behr B, de Jonge CJ, Baer TM, et al. Non-invasive imaging of human embryos before embryonic genome activation predicts development to the blastocyst stage. Nat Biotechnol. 2010 Oct;28(10):1115–21.

100. Chen Q, Shi J, Tao Y, Zernicka-Goetz M. Tracing the origin of heterogeneity and symmetry breaking in the early mammalian embryo. Nat Commun [Internet]. 2018;9(1):1819. Available from: https://doi.org/10.1038/s41467-018-04155-2

101. Strumpf D, Mao CA, Yamanaka Y, Ralston A, Chawengsaksophak K, Beck F, et al. Cdx2 is required for correct cell fate specification and differentiation of trophectoderm in the mouse blastocyst. Development. 2005 May;132(9):2093–102.

102. Semb H. Human embryonic stem cells: Origin, properties and applications. Vol. 113, Apmis. 2005. p. 743–50.

103. Thomson JA. Embryonic stem cell lines derived from human blastocysts. Science (1979). 1998;282(5391):1145–7.

104. Schoenwolf GC, Bleyl SB, Brauer PR, Francis-West PH. Larsen's Human Embriology. Larsen's Human Embryology. 2015. 548 p.

105. Finkel T, Bolli R, Gepstein L. Derivation and Potential Applications of Human Embryonic Stem Cells. Circ Res [Internet]. 2002 Nov 15 [cited 2022 Dec 15];91(10):866–76. Available from: https://www.ahajournals.org/doi/abs/10.1161/01.RES.0000041435.95082.84

106. Warmflash A, Sorre B, Etoc F, Siggia ED, Brivanlou AH. A method to recapitulate early embryonic spatial patterning in human embryonic stem cells. Nature Methods 2014 11:8 [Internet]. 2014 Jun 29 [cited 2022 Dec 15];11(8):847–54. Available from: https://www.nature.com/articles/nmeth.3016

107. Martin GR. Isolation of a pluripotent cell line from early mouse embryos cultured in medium conditioned by teratocarcinoma stem cells. Proc Natl Acad Sci U S A. 1981;78(12 II):7634–8.

108. Chambers I, Smith A. Self-renewal of teratocarcinoma and embryonic stem cells. Oncogene. 2004 Sep;23(43):7150–60.

109. Trounson A. The production and directed differentiation of human embryonic stem cells. Endocr Rev. 2006 Apr;27(2):208–19.

110. Dumevska B, Schaft J, Schmidt U. Chapter 36 - Derivation of Human Embryonic Stem Cells from Blastocysts. In: Loring JF, Peterson SEBTHSCM (Second E, editors. Boston: Academic Press; 2012. p. 557–76. Available from: https://www.sciencedirect.com/science/article/pii/B9780123854735000369

111. Nichols J, Smith A. Naive and Primed Pluripotent States. Cell Stem Cell [Internet]. 2009;4(6):487–92. Available from: http://dx.doi.org/10.1016/j.stem.2009.05.015

112. Fang Wang, Hui-Juan Kong, Quan-Cheng Kan, Ju-Yan Liang 1 Fang Zhao, Ai-Hong Bai, Peng-Fen Li and YPS. Analysis of Blastocyst Culture of Discarded Embryos and its Significance for Establishing Human Embryonic Stem Cell Lines Fang. J Cell Biochem [Internet]. 2012;113(12):3835–42. Available from: https://pubmed.ncbi.nlm.nih.gov/22821471/

113. Takashima Y, Guo G, Loos R, Nichols J, Ficz G, Krueger F, et al. Resetting transcription factor control circuitry toward ground-state pluripotency in human. Cell. 2014 Sep;158(6):1254–69.

114. Matsui Y, Zsebo K, Hogan BLM. Derivation of pluripotential embryonic stem cells from murine primordial germ cells in culture. Cell [Internet]. 1992 Sep 4;70(5):841–7. Available from: https://doi.org/10.1016/0092-8674(92)90317-6

115. Davidson KC, Mason EA, Pera MF. The pluripotent state in mouse and human. Development (Cambridge). 2015;142(18):3090–9.

116. Gafni O, Weinberger L, Mansour AA, Manor YS, Chomsky E, Ben-Yosef D, et al. Derivation of novel human ground state naive pluripotent stem cells. Nature [Internet]. 2013;504(7479):282–6. Available from: http://dx.doi.org/10.1038/nature12745

117. Messmer T, von Meyenn F, Savino A, Santos F, Mohammed H, Lun ATL, et al. Transcriptional Heterogeneity in Naive and Primed Human Pluripotent Stem Cells at Single-Cell Resolution. Cell Rep. 2019 Jan;26(4):815-824.e4.

118. Choumerianou DM, Dimitriou H, Kalmanti M. Stem cells: Promises versus limitations. Tissue Eng Part B Rev. 2008;14(1):53–60.

119. Spradling A, Drummond-Barbosa D, Kai T. Stem cells find their niche. Nature. 2001 Nov;414(6859):98–104.

120. Nurzynska D, di Meglio F, Romano V, Miraglia R, Sacco AM, Latino F, et al. Cardiac primitive cells become committed to a cardiac fate in adult human heart with chronic ischemic disease but fail to acquire mature phenotype: genetic and phenotypic study. Basic Res Cardiol. 2013 Jan;108(1):320.

121. Hosoda T, Rota M, Kajstura J, Leri A, Anversa P. Role of stem cells in cardiovascular biology. J Thromb Haemost. 2011 Jul;9 Suppl 1:151–61.

122. Watt FM, Hogan BL. Out of Eden: stem cells and their niches. Science. 2000 Feb;287(5457):1427–30.

123. Ferraro F, Celso C lo, Scadden D. Adult stem cels and their niches. Adv Exp Med Biol. 2010;695:155–68.

124. Khan FA, Almohazey D, Alomari M, Almofty SA. Isolation, Culture, and Functional Characterization of Human Embryonic Stem Cells: Current Trends and Challenges. Stem Cells Int. 2018;2018.

125. Chen L. A Balanced Network: Transcriptional Regulation in Pluripotent Stem Cells. J Stem Cell Res Ther. 2012;01(S10).

126. Nichols J, Zevnik B, Anastassiadis K, Niwa H, Klewe-Nebenius D, Chambers I, et al. Formation of pluripotent stem cells in the mammalian embryo depends on the POU transcription factor Oct4. Cell. 1998 Oct;95(3):379–91.

127. Niwa H, Miyazaki J ichi, Smith AG. Quantitative expression of Oct-3/4 defines differentiation, dedifferentiation or self-renewal of ES cells. Nat Genet [Internet]. 2000;24(4):372–6. Available from: https://doi.org/10.1038/74199

128. Chambers I, Colby D, Robertson M, Nichols J, Lee S, Tweedie S, et al. Functional expression cloning of Nanog, a pluripotency sustaining factor in embryonic stem cells. Cell. 2003 May;113(5):643–55.

129. Kuroda T, Tada M, Kubota H, Kimura H, Hatano S ya, Suemori H, et al. Octamer and Sox elements are required for transcriptional cis regulation of Nanog gene expression. Mol Cell Biol. 2005 Mar;25(6):2475–85.

130. Avilion AA, Nicolis SK, Pevny LH, Perez L, Vivian N, Lovell-Badge R. Multipotent cell lineages in early mouse development depend on SOX2 function. Genes Dev. 2003 Jan;17(1):126–40.

131. de Paepe C, Krivega M, Cauffman G, Geens M, van de Velde H. Totipotency and lineage segregation in the human embryo. Mol Hum Reprod. 2014;20(7):599–618.

132. Liu N, Lu M, Tian X, Han Z. Molecular mechanisms involved in self-renewal and pluripotency of embryonic stem cells. J Cell Physiol. 2007;211(2):279–86.

133. Boyer LA, Tong IL, Cole MF, Johnstone SE, Levine SS, Zucker JP, et al. Core transcriptional regulatory circuitry in human embryonic stem cells. Cell. 2005;122(6):947–56.

134. Hough SR, Clements I, Welch PJ, Wiederholt KA. Differentiation of mouse embryonic stem cells after RNA interference-mediated silencing of OCT4 and Nanog. Stem Cells. 2006 Jun;24(6):1467–75.

135. Pan GJ, Chang ZYI, Schöler HR, Pei D. Stem cell pluripotency and transcription factor Oct4. Cell Res. 2002;12(5–6):321–9.

136. Scholer HR. Octamania: the POU factors in murine development. Trends Genet. 1991 Oct;7(10):323–9.

137. Pesce M, Schöler HR. Oct-4: Control of totipotency and germline determination. Mol Reprod Dev [Internet]. 2000;55(4):452–7. Available from: https://doi.org/10.1002/(SICI)1098-2795(200004)55:4%3C452::AID-MRD14%3E3.0.CO

138. Palmieri SL, Peter W, Hess H, Scholer HR. Oct-4 transcription factor is differentially expressed in the mouse embryo during establishment of the first two extraembryonic cell lineages involved in implantation. Dev Biol. 1994 Nov;166(1):259–67.

139. Wang YJ, Kang B. OCT4 (Octamer-Binding Transcription Factor 4) BT - Encyclopedia of Signaling Molecules. In: Choi S, editor. Cham: Springer International Publishing; 2018. p. 3643–50. Available from: https://doi.org/10.1007/978-3-319-67199-4_101982

140. Niwa H. Molecular mechanism to maintain stem cell renewal of ES cells. Cell Struct Funct. 2001;26(3):137–48.

141. Liu P, Chen M, Liu Y, Qi LS, Ding S. CRISPR-Based Chromatin Remodeling of the Endogenous Oct4 or Sox2 Locus Enables Reprogramming to Pluripotency. Cell Stem Cell [Internet]. 2018;22(2):252-261.e4. Available from: https://doi.org/10.1016/j.stem.2017.12.001

142. Vigano MA, Staudt LM. Transcriptional activation by Oct-3: evidence for a specific role of the POU-specific domain in mediating functional interaction with Oct-1. Nucleic Acids Res. 1996 Jun;24(11):2112–8.

143. Pan GJ, Pei DQ. Identification of two distinct transactivation domains in the pluripotency sustaining factor nanog. Cell Res. 2003;13(6):499–502.

144. Gehring WJ, Qian YQ, Billeter M, Furukubo-Tokunaga K, Schier AF, Resendez-Perez D, et al. Homeodomain-DNA recognition. Cell. 1994;78(2):211–23.

145. Mitsui K, Tokuzawa Y, Itoh H, Segawa K, Murakami M, Takahashi K, et al. The homeoprotein Nanog is required for maintenance of pluripotency in mouse epiblast and ES cells. Cell. 2003 May;113(5):631–42.

146. Chazaud C, Yamanaka Y, Pawson T, Rossant J. Early Lineage Segregation between Epiblast and Primitive Endoderm in Mouse Blastocysts through the Grb2-MAPK Pathway. Dev Cell. 2006;10(5):615–24.

147. Abranches E, Guedes AMV, Moravec M, Maamar H, Svoboda P, Raj A, et al. Stochastic NANOG fluctuations allow mouse embryonic stem cells to explore pluripotency. Development (Cambridge). 2014;141(14):2770–9.

148. Zhang S. Sox2, a key factor in the regulation of pluripotency and neural differentiation. World J Stem Cells. 2014;6(3):305.

149. Botquin V, Hess H, Fuhrmann G, Anastassiadis C, Gross MK, Vriend G, et al. New POU dimer configuration mediates antagonistic control of an osteopontin preimplantation enhancer by Oct-4 and Sox-2. Genes Dev. 1998 Jul;12(13):2073–90.

150. Yuan H, Corbi N, Basilico C, Dailey L. Developmental-specific activity of the FGF-4 enhancer requires the synergistic action of Sox2 and Oct-3. Genes Dev. 1995 Nov;9(21):2635–45.

151. Nishimoto M, Fukushima A, Okuda A, Muramatsu M. The gene for the embryonic stem cell coactivator UTF1 carries a regulatory element which selectively interacts with a complex composed of Oct-3/4 and Sox-2. Mol Cell Biol. 1999 Aug;19(8):5453–65.

152. Reményi A, Lins K, Nissen LJ, Reinbold R, Schöler HR, Wilmanns M. Crystal structure of a POU/HMG/DNA ternary complex suggests differential assembly of Oct4 and Sox2 on two enhancers. Genes Dev. 2003;17(16):2048.

153. Gagliardi A, Mullin NP, Ying Tan Z, Colby D, Kousa AI, Halbritter F, et al. A direct physical interaction between Nanog and Sox2 regulates embryonic stem cell self-renewal. EMBO Journal. 2013;32(16):2231–47.

154. Campolo F, Gori M, Favaro R, Nicolis S, Pellegrini M, Botti F, et al. Essential role of Sox2 for the establishment and maintenance of the germ cell line. Stem Cells. 2013;31(7):1408–21.

155. Fong H, Hohenstein KA, Donovan PJ. Regulation of Self-Renewal and Pluripotency by Sox2 in Human Embryonic Stem Cells. Stem Cells. 2008;26(8):1931–8.

156. Rueger MA, Schroeter M. In vivo imaging of endogenous neural stem cells in the adult brain. World J Stem Cells. 2015 Jan;7(1):75–83.

157. Pauklin S, Vallier L. Activin/Nodal signalling in stem cells. Development. 2015 Feb;142(4):607–19.

158. Papanayotou C, Collignon J. Activin/Nodal signalling before implantation: setting the stage for embryo patterning. Philos Trans R Soc Lond B Biol Sci. 2014 Dec;369(1657).

159. Vallier L, Reynolds D, Pedersen RA. Nodal inhibits differentiation of human embryonic stem cells along the neuroectodermal default pathway. Dev Biol. 2004 Nov;275(2):403–21.

160. Beattie GM, Lopez AD, Bucay N, Hinton A, Firpo MT, King CC, et al. Activin A maintains pluripotency of human embryonic stem cells in the absence of feeder layers. Stem Cells. 2005 Apr;23(4):489–95.

161. Xiao L, Yuan X, Sharkis SJ. Activin A Maintains Self-Renewal and Regulates Fibroblast Growth Factor, Wnt, and Bone Morphogenic Protein Pathways in Human Embryonic Stem Cells. Stem Cells. 2006;24(6):1476–86.

162. James D, Levine AJ, Besser D, Hemmati-Brivanlou A. TGFbeta/activin/nodal signaling is necessary for the maintenance of pluripotency in human embryonic stem cells. Development. 2005 Mar;132(6):1273–82.

163. Singh AM, Reynolds D, Cliff T, Ohtsuka S, Mattheyses AL, Sun Y, et al. Signaling network crosstalk in human pluripotent cells: a Smad2/3-regulated switch that controls the balance between self-renewal and differentiation. Cell Stem Cell. 2012 Mar;10(3):312–26.

164. Xu RH, Sampsell-Barron TL, Gu F, Root S, Peck RM, Pan G, et al. NANOG is a direct target of TGFbeta/activin-mediated SMAD signaling in human ESCs. Cell Stem Cell. 2008 Aug;3(2):196–206.

165. Sakaki-Yumoto M, Liu J, Ramalho-Santos M, Yoshida N, Derynck R. Smad2 is essential for maintenance of the human and mouse primed pluripotent stem cell state. J Biol Chem. 2013 Jun;288(25):18546–60.

166. Urist MR. Bone morphogenetic protein: the molecularization of skeletal system development. J Bone Miner Res. 1997;12(2):343–6.

167. Rahman MS, Akhtar N, Jamil HM, Banik RS, Asaduzzaman SM. TGF-β/BMP signaling and other molecular events: regulation of osteoblastogenesis and bone formation. Bone Res [Internet]. 2015;3(1):15005. Available from: https://doi.org/10.1038/boneres.2015.5

168. Winnier G, Blessing M, Labosky PA, Hogan BL. Bone morphogenetic protein-4 is required for mesoderm formation and patterning in the mouse. Genes Dev. 1995 Sep;9(17):2105–16.

169. Groeneveld EHJ, Burger EH. Bone morphogenetic proteins in human bone regeneration. Eur J Endocrinol. 2000;142(1):9–21.

170. Wu, C-J, Lu HK. Smad signal pathway in BMP-2-induced osteogenesis — a mini review. J Dent Sci. 2008;3(1):13–21.

171. Lin GL, Hankenson KD. Integration of BMP, Wnt, and notch signaling pathways in osteoblast differentiation. J Cell Biochem. 2011;112(12):3491–501.

172. Muenster U, Korupolu R, Rastogi R, Read J, Fischer WH. Antagonism of Activin by Activin Chimeras. Vitam Horm. 2011;85:105–28.

173. Bonor J, Adams EL, Bragdon B, Moseychuk O, Czymmek KJ, Nohe A. Initiation of BMP2 signaling in domains on the plasma membrane. J Cell Physiol. 2012;227(7):2880–8.

174. Budi EH, Duan D, Derynck R. Transforming Growth Factor-β Receptors and Smads: Regulatory Complexity and Functional Versatility. Trends Cell Biol. 2017;27(9):658–72.

175. Yu P, Pan G, Yu J, Thomson JA. FGF2 Sustains NANOG and Switches the Outcome of BMP4 Induced Human.pdf. 2011;8(3):326–34.

176. Morikawa M, Koinuma D, Tsutsumi S, Vasilaki E, Kanki Y, Heldin CH, et al. ChIP-seq reveals cell type-specific binding patterns of BMP-specific Smads and a novel binding motif. Nucleic Acids Res. 2011;39(20):8712–27.

177. Morikawa M, Koinuma D, Mizutani A, Kawasaki N, Holmborn K, Sundqvist A, et al. BMP Sustains Embryonic Stem Cell Self-Renewal through Distinct Functions of Different Krüppel-like Factors. Stem Cell Reports. 2016 Jan;6(1):64–73.

178. Kurek D, Neagu A, Tastemel M, Tüysüz N, Lehmann J, van de Werken HJG, et al. Endogenous WNT signals mediate BMP-induced and spontaneous differentiation of epiblast stem cells and human embryonic stem cells. Stem Cell Reports. 2015 Jan;4(1):114–28.

179. Richter A, Valdimarsdottir L, Hrafnkelsdottir HE, Runarsson JF, Omarsdottir AR, Ward-van Oostwaard D, et al. BMP4 promotes EMT and mesodermal commitment in human embryonic stem cells via SLUG and MSX2. Stem Cells. 2014 Mar;32(3):636–48.

180. Bieberich E, Wang G. Molecular Mechanisms Underlying Pluripotency. In: Pluripotent Stem Cells. 2013. p. 153–78.

181. Xu C, Inokuma MS, Denham J, Golds K, Kundu P, Gold JD, et al. Feeder-free growth of undifferentiated human embryonic stem cells. Nat Biotechnol. 2001;19(10):971–4.

182. Armstrong L, Hughes O, Yung S, Hyslop L, Stewart R, Wappler I, et al. The role of PI3K/AKT, MAPK/ERK and NFκβ signalling in the maintenance of human embryonic stem cell pluripotency and viability highlighted by transcriptional profiling and functional analysis. Hum Mol Genet. 2006 Apr 27;15(11):1894–913.

183. Kang HB, Kim JS, Kwon HJ, Nam KH, Youn HS, Sok DE, et al. Basic Fibroblast Growth Factor Activates ERK and Induces c-Fos in Human Embryonic Stem Cell Line MizhES1. Stem Cells Dev. 2005 Aug 1;14(4):395–401.

184. Ornitz DM, Itoh N. The Fibroblast Growth Factor signaling pathway. Wiley Interdiscip Rev Dev Biol. 2015;4(3):215–66.

185. Logan CY, Nusse R. The Wnt signaling pathway in development and disease. Annu Rev Cell Dev Biol. 2004;20:781–810.

186. Bejsovec A. Wnt pathway activation: new relations and locations. Cell. 2005 Jan;120(1):11–4.

187. Stamos JL, Weis WI. The β-catenin destruction complex. Cold Spring Harb Perspect Biol. 2013;5(1):a007898.

188. Kühl SJ, Kühl M. On the role of Wnt/β-catenin signaling in stem cells. Biochim Biophys Acta Gen Subj. 2013;1830(2):2297–306.

189. Sato N, Meijer L, Skaltsounis L, Greengard P, Brivanlou AH. Maintenance of pluripotency in human and mouse embryonic stem cells through activation of Wnt signaling by a pharmacological GSK-3-specific inhibitor. Nat Med. 2004;10(1):55–63.

190. James D, Levine AJ, Besser D, Hemmati-Brivanlou A. TGFβ/activin/nodal signaling is necessary for the maintenance of pluripotency in human embryonic stem cells. Development. 2005;132(6):1273–82.

191. Sumi T, Tsuneyoshi N, Nakatsuji N, Suemori H. Defining early lineage specification of human embryonic stem cells by the orchestrated balance canonical Wnt/β-catenin, activin/Nodal and BMP signaling. Development. 2008;135(17):2969–79.

192. Villa-Diaz LG, Pacut C, Slawny NA, Ding J, O'Shea KS, Smith GD. Analysis of the factors that limit the ability of feeder cells to maintain the undifferentiated state of human embryonic stem cells. Stem Cells Dev. 2009;18(4):641–51.

193. Ding VMY, Ling L, Natarajan S, Yap MGS, Cool SM, Choo ABH. FGF-2 modulates Wnt signaling in undifferentiated hESC and iPS cells through activated PI3-K/GSK3β signaling. J Cell Physiol. 2010;225(2):417–28.

194. Davidson KC, Adams AM, Goodson JM, McDonald CE, Potter JC, Berndt JD, et al. Wnt/β-catenin signaling promotes differentiation, not self-renewal, of human embryonic stem cells and is repressed by Oct4. Proc Natl Acad Sci U S A. 2012 Mar;109(12):4485–90.

195. Zhang P, Li J, Tan Z, Wang C, Liu T, Chen L, et al. Short-term BMP-4 treatment initiates mesoderm induction in human embryonic stem cells. Blood [Internet]. 2008 Feb 15;111(4):1933–41. Available from: https://doi.org/10.1182/blood-2007-02-074120

196. Teo AKK, Arnold SJ, Trotter MWB, Brown S, Ang LT, Chng Z, et al. Pluripotency factors regulate definitive endoderm specification through eomesodermin.

Genes Dev [Internet]. 2011 Feb 1 [cited 2022 Dec 13];25(3):238–50. Available from: https://pubmed.ncbi.nlm.nih.gov/21245162/

197. Stepicheva NA, Dumas M, Kobi P, Donaldson JG, Song JL. The small GTPase Arf6 regulates sea urchin morphogenesis. Differentiation [Internet]. 2017 May 1 [cited 2022 Dec 13];95:31–43. Available from: https://pubmed.ncbi.nlm.nih.gov/28188999/

198. Kostopoulou N, Bellou S, Bagli E, Markou M, Kostaras E, Hyvönen M, et al. Embryonic stem cells are devoid of macropinocytosis, a trafficking pathway for activin A in differentiated cells. J Cell Sci [Internet]. 2021 Jul 1 [cited 2022 Dec 13];134(13). Available from: https://pubmed.ncbi.nlm.nih.gov/34313314/

199. Grossmann AH, Yoo JH, Clancy J, Sorensen LK, Sedgwick A, Tong Z, et al. The small GTPase ARF6 stimulates β-catenin transcriptional activity during WNT5A-mediated melanoma invasion and metastasis. Sci Signal [Internet]. 2013 Mar 5 [cited 2022 Dec 13];6(265). Available from: https://pubmed.ncbi.nlm.nih.gov/23462101/

200. Pellon-Cardenas O, Clancy J, Uwimpuhwe H, D'Souza-Schorey C. ARF6-regulated endocytosis of growth factor receptors links cadherin-based adhesion to canonical Wnt signaling in epithelia. Mol Cell Biol [Internet]. 2013 Aug [cited 2022 Dec 13];33(15):2963–75. Available from: https://pubmed.ncbi.nlm.nih.gov/23716594/

201. Yu P, Pan G, Yu J, Thomson JA. FGF2 sustains NANOG and switches the outcome of BMP4-induced human embryonic stem cell differentiation. Cell Stem Cell. 2011 Mar;8(3):326–34.

202. Yamauchi Y, Miura Y, Kanaho Y. Machineries regulating the activity of the small GTPase Arf6 in cancer cells are potential targets for developing innovative anti-cancer drugs. Adv Biol Regul [Internet]. 2017;63:115–21. Available from: https://www.sciencedirect.com/science/article/pii/S2212492616300604

203. Warmflash A, Arduini BL, Brivanlou AH. The molecular circuitry underlying pluripotency in embryonic stem cells. Wiley Interdiscip Rev Syst Biol Med. 2012;4(5):443–56.

204. Richards M, Tan SP, Tan JH, Chan WK, Bongso A. The transcriptome profile of human embryonic stem cells as defined by SAGE. Stem Cells. 2004;22(1):51–64.

205. Rahkonen N, Yliopisto T. REGULATION OF SELF-RENEWAL AND DETECTION OF KARYOTYPIC CHANGES OF PLURIPOTENT HUMAN by. 2013.
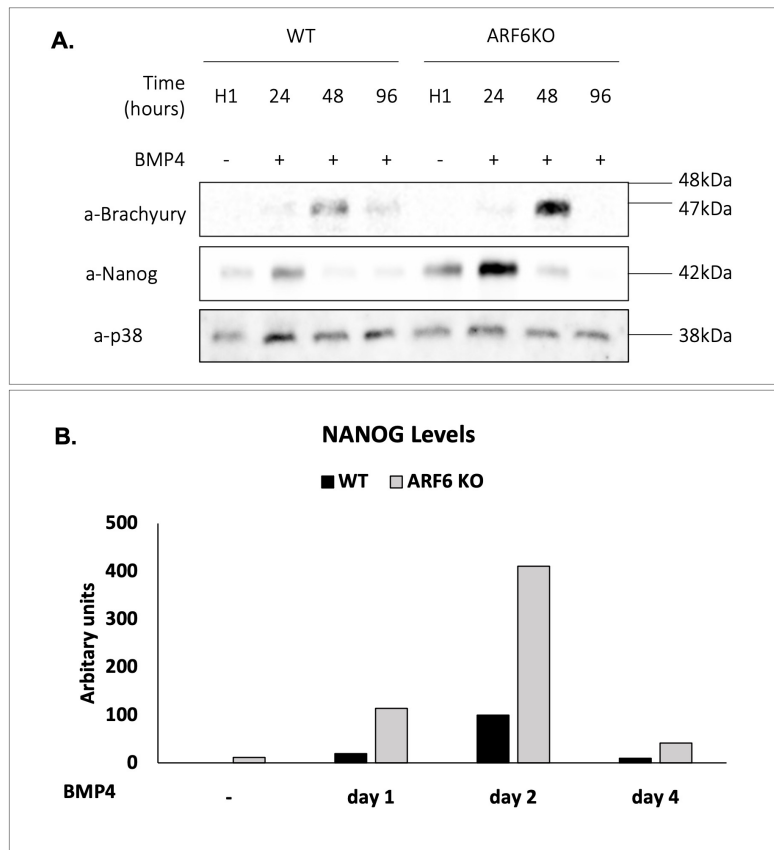
Supplementary Figures

I.   ARF6 KO increases the expression of BRACHYURY upon induction with BMP4
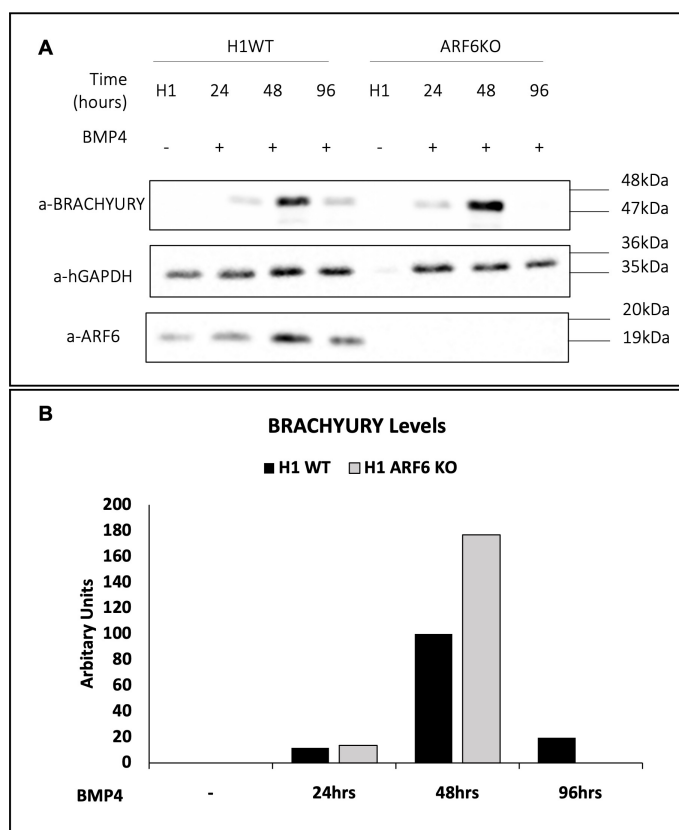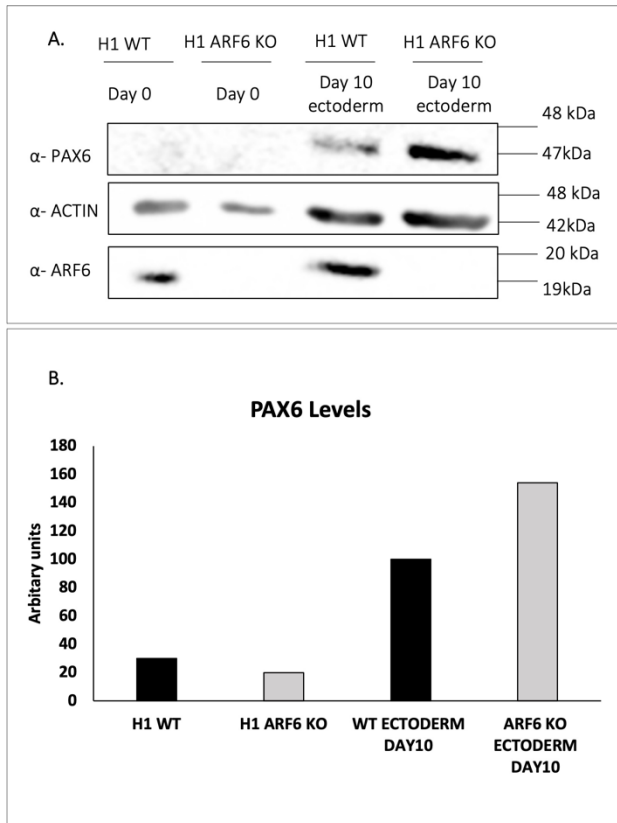

Supplementary Figure 1: *Effect of ARF6 Knock-out on the Timing of BRACHYURY Expression upon Mesoderm Induction* A) H1 wt and H1 ARF6KO cells were cultured to approximately 50% confluency. Differentiation to mesoderm was initiated by substituting mTeSR™Plus with mTeSR™Plus containing BMP4 (50ng/mL). After 24, 48 and 96 hours cells were lysed using 1% SDS, subjected to SDS-PAGE and immunoblotted with an α-BRACHYURY antibody to investigate the effect of ARF6 knock-out in the expression levels of the mesodermal marker in a time dependent manner. (B) Changes in the expression levels of BRACHYURY in the absence of the ARF6 were assessed by densitometry using the QuantityOne software (N=2).

It is known that in the presence of bFGF and FGF2 NANOG expression increases post induction and then by 48 hrs is decreased, in the ARF6KO cells we see enhanced induction of NANOG at 24 hrs which is in agreement with also enhanced induction of Brachyury (201).
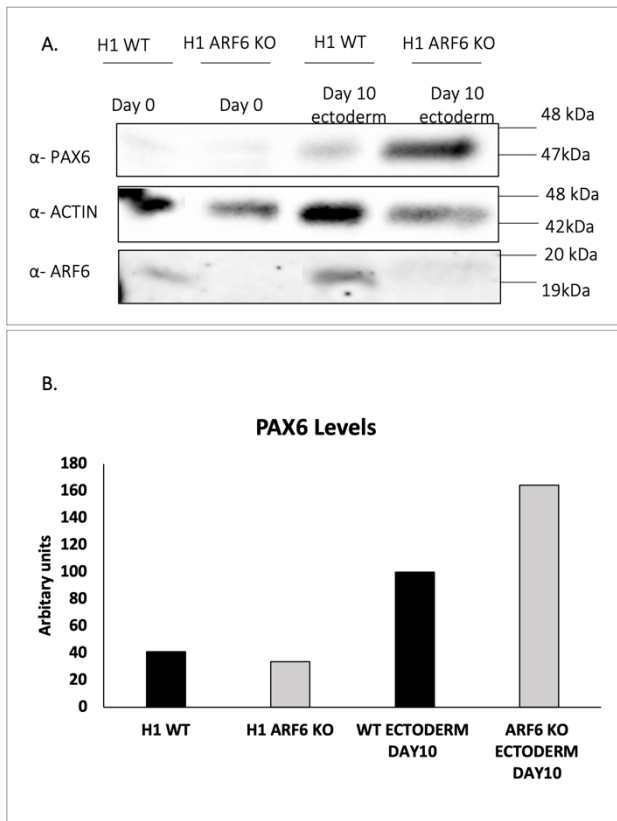
Supplementary Figure 2: *Effect of ARF6 Knock-out on the Timing of NANOG Expression upon Mesoderm Induction* A) H1 wt and H1 ARF6KO cells were cultured to approximately 50% confluency. Differentiation to mesoderm was initiated by substituting mTeSR™Plus with mTeSR™Plus containing BMP4 (50ng/mL). After 24, 48 and 96 hours cells were lysed using 1% SDS, subjected to SDS-PAGE and immunoblotted with an α-NANOG antibody to investigate the effect of ARF6 knock-out in the expression levels of the marker of pluripoency in a time dependent manner. (B) Changes in the expression levels of NANOG in the absence of the ARF6 were assessed by densitometry using the QuantityOne software (N=1).

## II.   ARF6 KO increases the expression of PAX6 neuroectodermal marker

Supplementary Figure 3: *Effect of ARF6 Knock-out on the PAX6 expression upon neuroectodermal induction.* H1 ARF6KO cells and H1 WT cells undifferentiated (day 0) and differentiated at day 10 were lysed using 1% SDS, subjected to SDS-PAGE and immunoblotted with an α-PAX6 antibody to investigate the effect of ARF6 knock-out in the expression levels of the neuroectodermal marker. (B) Changes in the expression levels of PAX6 in the absence of the ARF6 were assessed by densitometry using the QuantityOne software. (N=3).

Supplementary Figure 4: *Effect of ARF6 Knock-out on the PAX6 expression upon neuroectodermal induction.* A) H1 ARF6KO cells and H1 WT cells undifferentiated (day 0) and differentiated at day 10 were lysed using 1% SDS, subjected to SDS-PAGE and immunoblotted with an α-PAX6 antibody to investigate the effect of ARF6 knock-out in the expression levels of the neuroectodermal marker. (B) Changes in the expression levels of PAX6 in the absence of the ARF6 were assessed by densitometry using the QuantityOne software. (N=3).

III.   ARF6 FC has no effect on the expression of PAX6 neuroectodermal marker
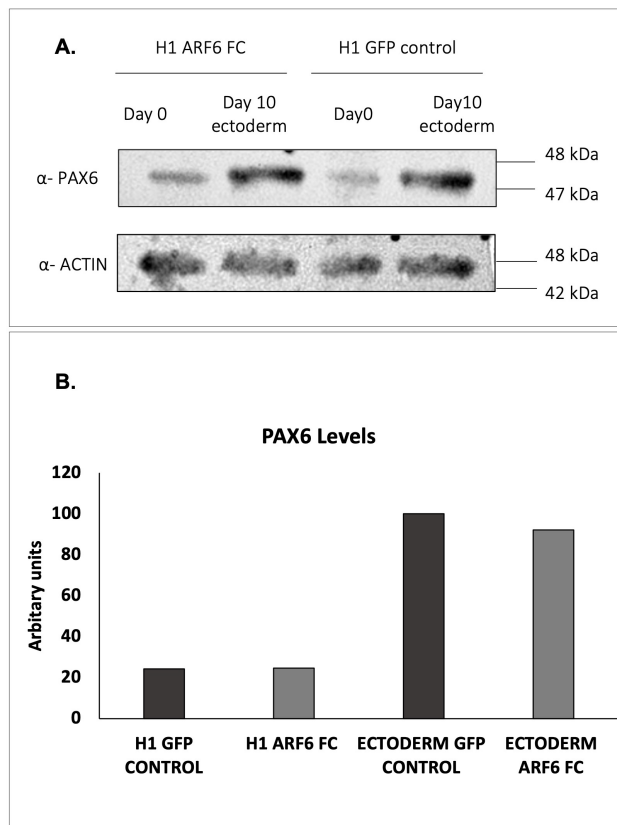
Supplementary Figure 5: *Effect of ARF6 Activation on the PAX6 expression upon ectodermal induction*. A) H1 ARF6 FC cells (ARF6T157A-GFP) and H1 GFP control cells undifferentiated (day 0) and differentiated at day 10 were lysed using 1% SDS, subjected to SDS-PAGE and immunoblotted with an α-PAX6 antibody to investigate the effect of ARF6 fast cycling onn the expression levels of the neuroectodermal marker. (B) Changes in the expression levels of PAX6 in the activated form of the ARF6 were assessed by densitometry using the QuantityOne software. (N=2).